

博士論文（要約）

Paracrine interactions in mouse testis

（マウス精巣におけるパラクライン制御機構）

Department of Veterinary Anatomy

Graduate School of Agricultural and Life Sciences

The University of Tokyo

平成 28 年度入学

獣医学専攻 博士課程 内田あや

指導教員 金井克晃

Table of Contents

List of Symbols, Abbreviations and Nomenclature	4
1. GENERAL INTRODUCTION.....	8
1.1 Mammalian Testis	9
1.2 Spermatogonial Stem Cell	13
1.3 Paracrine Regulation in the testis	14
1.4 Objectives and hypothesis	18
1.5 Figures	20
2. CHAPTER 1	21
“A bead transplantation assay to examine <i>in vivo</i> dynamics of germ cells stimulated by paracrine factors”	
2.1 Abstract	22
2.2 Introduction.....	22
2.3 Materials & Methods	23
2.4 Results.....	24
2.5 Discussion	28
2.6 Figures & Table	31
3. CHAPTER 2	38
“Paracrine signals mediate regionalization of the Sertoli Valve epithelia”	
3.1 Abstract	39
3.2 Introduction.....	39
3.3 Materials & Methods	40
3.4 Results.....	42

3.5 Discussion	46
3.6 Figures & Table	49
 4. CHAPTER 3	 58
 “Testicular valve formation and spermatogenesis modulated by SOX17-positive rete testis in mammals”	
4.1 Abstract	59
4.2 Introduction.....	59
4.3 Materials & Methods	60
4.4 Results.....	64
4.5 Discussion	69
4.6 Figures & Table	72
 5. GENERAL DISCUSSION	 90
 6. ACKNOWLEDGEMENT.....	 94
 7. REFERENCES.....	 96

List of Symbols, Abbreviations and Nomenclature

Symbol	Definition
3bHSD	3 β -Hydroxysteroid dehydrogenase
A_{aligned}	Type A aligned spermatogonia
A_{diff}	Differentiating spermatogonia
A_{paired}	Type A paired spermatogonia
A_{single}	Type A single spermatogonia
A_{undiff}	Undifferentiated spermatogonia
ace-TUB	Acetylated tubulin
ACTA2	Actin Alpha 2, Smooth Muscle
Actb1	Actin beta1
ADH	Alcohol dehydrogenases
AKT	Ak strain transforming
Aldh1a1	Aldehyde dehydrogenase 1 family, member A1
Aldh1a2	Aldehyde dehydrogenase 1 family, member A2
AMH	Anti-mullerian hormone
AMH-Treck	AMH-toxin receptor-mediated cell knockout
ANOVA	Analysis of variance
AR	Androgen receptor
αSMA	Alpha-smooth muscle actin
ATP	Adenosine triphosphate
BL	Basal lamina
BMP	Bone morphogenetic proteins
BSA	Bovine serum albumin
BTB	Blood-testis-barrier
c-KIT/KIT	Ctyrosine-protein kinase Kit
CA2	Carbonic Anhydrase 2
CCND1	Cyclin-D1
Cd68	Cluster of Differentiation 68
CDH1/ECAD	Cadherin-1 or E-cadherin
cDNA	Complementary DNA
cKO	Conditional knock out
Cldn	Claudin
CSF1	Colony stimulating factor 1
CXCL	Chemokine (C-X-C motif) ligand
Cyp26a1	Cytochrome P450 Family 26 Subfamily A Member 1
Cyp26b1	Cytochrome P450 Family 26 Subfamily B Member 1
DapB	4-hydroxy-tetrahydrodipicolinate reductase
DAPI	4',6-diamidino-2-phenylindole

DEG	Differentially expressed gene
Dhh	Desert Hedgehog Signaling Molecule
DiI	DiI18(3); 1,1'-dioctadecyl-3,3,3',3'-tetramethylindocarbocyanine
Dmrt1	Doublesex And Mab-3 Related Transcription Factor 1
DMSO	Dimethyl sulfoxide
DNA	Deoxyribonucleic acid
DT	Diphtheria toxin
ECM	Extra-cellular matrix
EDTA	Ethylenediaminetetraacetic acid
EF	Efferent duct
EGF	Epidermal growth factor
EGFP	Enhanced Green Fluorescent Protein
ER	Oestrogen receptor
ERK	Extracellular signal-regulated kinase
ES	Ectoplasmic specialization
FBS	Fetal bovine serum
FGF	Fibroblast growth factor
FGFR	Fibroblast growth factor receptor
GATA4	GATA-binding family 4
GDNF	Glial cell-line derived neurotrophic factor
GFRα1	Glial cell-line derived neurotrophic factor receptor alpha 1
GS	Germline stem
H&E	Hematoxylin & Eosin
HBSS	Hank's buffered salt solution
Hsd3b1	3 β -hydroxysteroid dehydrogenase-1
HSP70	70 kilodalton heat shock proteins
HSPG	Heparan sulfate proteoglycan
ID4	Inhibitor of DNA binding 4
IL	Interleukin
Kitl	KIT Ligand
KRT8	Keratin-8
LAMA1	Laminin Subunit Alpha 1
LIF	Leukemia inhibitory factor
LIN28A	Lin-28 homolog A
MAP2K1/2	Mitogen-activated protein 2 kinases 1/2
MAPK	RAS-mitogen-activated protein kinase
MEF	Mouse embryonic fibroblast
MEK	Serine/tyrosine/threonine kinase.
MKLP1	Mitotic kinesin-like protein
mRNA	messenger RNA
MVH/DDX4	Mouse vasa homolog /DEAD-Box Helicase 4

NELL2	Neural epidermal growth factor–like–like 2
NGN3	Neurogenin 3
Nr5a1	Nuclear Receptor Subfamily 5 Group A Member 1
Ocln	Occludin
OCT-4	Octamer-binding transcription factor 4
Odf1	Outer Dense Fiber Of Sperm Tails 1
P	Postnatal
p-AKT	phosphorylated AKT
p-STAT3	phosphorylated STAT3
Pax7	Paired Box 7
PAX8	Paired box gene 8
PBS	Phosphate buffered saline
Pdgfa	Platelet Derived Growth Factor Subunit A
Pecam1	Platelet And Endothelial Cell Adhesion Molecule 1
PFA	Paraformaldehyde
pHH3	Phosphohistone H3
PI3K	Phosphoinositide 3-kinase
PLZF	Promyelocytic leukaemia zinc finger
Ppib	Peptidylprolyl Isomerase B
Prm1	Protamine 1
pSV	Protruded SV
qRT-PCR	Quantitative Real-Time Reverse Transcription PCR
RA	Retinoic acid
RALDH	Retinaldehyde dehydrogenases
RARγ	Retinoic acid receptor γ
Rbp1	Retinol Binding Protein 1
Rhox5	Rhox homeobox family member 5
RNA	Ribonucleic acid
RSPO	R-spondin
RT	Rete testis
s.e.m.	Standard error of the mean
SALL4	Spalt Like Transcription Factor 4
SCF	Stem cell factor
SCP3	Synaptonemal complex protein 3
scRNAseq	Single cell RNA sequencing
SF1	Steroidogenic factor 1
SOX17	SRY-Box Transcription Factor 17
SOX9	SRY-Box Transcription Factor 9
Spc	Spermatocytes
Spt	Spermatids
SRY	Sex determining region on Y chromosome

SSC	Spermatogonial stem cell
ST	Seminiferous tubule
STAR	Steroidogenic Acute Regulatory Protein
STAT3	Signal transducers and activators of transcription 3
STF	Seminiferous tubular fluid
STRA8	Stimulated by retinoic acid 8
SV	Sertoli valve
Tcf21	Transcription Factor 21
TEM	Transmission electron microscopy
Tg	Transgenic
TGFβ	Transforming growth factor beta
TNB	Tris-NaCl-blocking buffer
TUNEL	Terminal deoxynucleotidyl transferase dUTP nick end labeling
UMAP	Uniform Manifold Approximation and Projection
VASA	DEAD-Box helicase 4
W/W^v	WBB6F1/Kit-KitW/KitW ^v /Slc
WNT	Wingless-INT
WT1	Wilms tumor 1
Zbtb16	Zinc Finger And BTB Domain Containing 16

1. General Introduction

1.1 Mammalian Testis

Anatomy of the testis

The testis is a male reproductive organ responsible for spermatogenesis and hormone production. A main structure of the testis is divided into the seminiferous tubule (ST) and the interstitial tissue, which is covered by the tunica albuginea, together with the rete testis (RT) at the anterior part. In the ST, the somatic cells called Sertoli cells support germ cells at different stages of differentiation. In the testicular interstitium, peritubular myoid cells and lymphatic endothelial cells reside in the peritubular interstitial space, while Leydig cells, macrophages and blood vessels are in the intratubular interstitial space (Fig.1-1A). Spermatogenesis is conducted in the ST in a cyclic manner that is called seminiferous epithelium cycle. The seminiferous epithelium cycle is divided into 12 stages in mice, and this stage cyclicality regulates not only spermatogenic activity, but also the behavior of spermatogenic stem cells (SSCs) in the ST. The period of one complete seminiferous epithelium cycle in the mouse is approximately 8.6 days, and the length of each stage of the seminiferous epithelial cycle is tightly regulated (Russell *et al.*, 1990). The terminal segment of the ST is connected to the RT, where the intra-testicular excretory duct connects the testis to the efferent duct (Hess *et al.*, 2021). The region connecting the ST and the RT is called Sertoli valve (SV), where Sertoli cell protrude into the lumen of RT to construct a valve-like structure (Aiyama *et al.*, 2015; Figueiredo *et al.*, 2021). Although the SV and RT structures are phylogenetically conserved structures across mammalian species, their physiological roles remain unknown.

In the testis, STs and interstitial parts are segregated by the basement membrane. The basement membrane consists of extra-cellular matrix (ECM) proteins including laminin, collagen IV, fibronectin and Heparan sulfate proteoglycan (HSPG) (Hadley and Dym, 1987; Lian *et al.*, 1992; Kleinman and Schnaper, 1993; Dym, 1994; Brucato *et al.*, 2001). The basement membrane functions as a reservoir for growth factors, and both Sertoli cells and peritubular myoid cells participate in the production of basement membrane proteins (Timpl, 1993). Seminiferous epithelia of the ST are divided into the basal compartment and the adluminal compartment by blood-testis-barrier (BTB). BTB is constituted exclusively by specialized junctions between adjacent Sertoli cells (Setchell, 2018). Unlike other blood-tissue junction in the body, BTB is composed of multiple junction types, namely specialized tight junction, gap junctions, and anchoring junctions that include a testis-specific actin-based adherens junction called ectoplasmic specialization (ES) and desmosome-like junctions (Li *et al.*, 2016; Wen *et al.*,

2018). BTB prevents the entry of immune cells from the interstitium into the seminiferous epithelia to protect the meiotic and haploid cells from autoimmune response (Li *et al.*, 2016). Therefore, mitotic germ cells ranged from spermatogonia to preleptotene spermatocytes reside in the basal compartment of the ST, whereas meiotic and post-meiotic germ cells such as primary to secondary spermatocytes, round spermatids, and elongated spermatids reside in the adluminal compartment of the ST to be protected from exposure of various paracrine factors and immune attack derived from the basal compartment (Mruk & Cheng, 2015). BTB undergoes extensive reconstruction during the seminiferous epithelial cycle of spermatogenesis to facilitate the transit of preleptotene spermatocytes from the basal compartment to the adluminal compartment of the seminiferous epithelia (Cheng and Mruk, 2012). BTB is composed of various tight junction proteins. For example, Claudin 11 is indispensable for the formation of tight junction and its barrier integrity, thus deletion of Claudin 11 makes the animal sterile (Gow *et al.*, 1999). Whereas Claudin 1, 3 and occludin regulate the translocation of preleptotene spermatocytes across the BTB (Chihara *et al.*, 2013; Mruk and Cheng, 2015). Among them, expression of Claudin3 is dependent on appearance of meiotic germ cells, hence its expression is depleted by germ cell ablation (Kanatsu-Shinohara *et al.*, 2020).

Spermatogenesis

In the mouse spermatogenesis, singly isolated spermatogonia (A_{single}) give rise to syncytia of two spermatogonia (A_{paired}) and spermatogonial chains (A_{aligned} 4, 8, 16, and occasionally 32). They subsequently differentiate into A1–A4, intermediate and B-type spermatogonia. The GFR α 1-positive population of spermatogonia up to A_{aligned} 8 are generally regarded as undifferentiated spermatogonia (A_{undiff}), whereas GFR α 1-negative/ cytosine-protein kinase Kit (c-KIT)-positive spermatogonia later than A_{aligned} 16 are referred as differentiating spermatogonia (A_{diff}) in normal healthy mouse testes (Subash & Kumar, 2020). B-type spermatogonia then differentiated into tetraploid primary spermatocyte to enter a first meiotic division (meiosis I) and generate diploid secondary spermatocyte. Secondary spermatocyte further undergoes a second meiotic division (meiosis II) to form haploid round spermatids. Round spermatids then go through drastic morphological change to become elongated spermatids and spermatozoa (Griswold, 2016). The fully-differentiated spermatozoa are finally released from the seminiferous epithelia into the luminal space through a process known as spermiation. This process of generating mature spermatozoa from round spermatids is called “spermiogenesis” that is divided into four different phases: Golgi phase to develop polarity, the cap phase to form acrosomal cap, formation of sperm tail, and the maturation stage to remove cytoplasm remnants of the spermatids (O'Donnell, 2014).

Since the released spermatozoa are immotile, their transportation in the testis is conducted by seminiferous tubular fluid (*i.e.*, luminal fluid) that unidirectionally flow towards the RT. However, the basic physiological principles that control luminal transport of spermatozoa in the ST remain poorly defined.

Luminal fluid flow in the testis

The lumen of ST is filled with the luminal fluid, of which production commences concomitantly with the BTB formation around P14-21 in mouse testes. Sertoli cells are responsible for the secretion of luminal fluid through its expression of ion transporters and aquaporins (Rato et al., 2010). In general, transportation of functional fluids in the body is mediated through pumping mechanism and fluid-structure interactions. In the testis, the contractile tubular movement is induced by peritubular myoid cells that pump the luminal fluid inside the ST (Diez-Torre et al., 2011; Fleck et al., 2020). The contraction of peritubular myoid cells is modulated by several stimuli such as extracellular adenosine triphosphate (ATP), endothelin, prostaglandins, oxytocin, transforming growth factor beta (TGF β) and nitric oxide cyclic GMP (Mackawa et al., 1996; Tripiciano et al., 1998; Fleck et al., 2020). The reduced contractile ability of peritubular myoid cells cause the reduced movement of the luminal fluid flow in the ST (Uchida et al., 2020). Although the “pumping” mechanism of the luminal fluid has started to be uncovered, the mechanism to regulate the “direction” of luminal fluid flow remain a mystery.

The Sertoli valve (SV)

The testis harbors a valve-like structure called SV at the terminal segment of each ST (Aiyama et al., 2015; Figueroa et al., 2021). Based on its morphological traits, function of the SV has been speculated to prevent the reflux of spermatozoa and the luminal fluid back to the upstream ST (Lindner, 1982; Roosen-Runge, 1961; Tainosho et al., 2011). The SV is a widely conserved structure in the testis that have been reported in various mammalian species: mouse, hamster (Aiyama et al., 2015), rat (Figueroa et al., 2021), guinea pig (Fawcett & Dym, 1973), rabbit, goat, boar, ram (Osman & Plöen, 1978), bull (Wrobel et al., 1982), monkey (Dym, 1974) and human (Jonté and Holstein, 1987). The SV is constructed by ‘modified’ Sertoli cells with constitutively high expression of phosphorylated AKT (p-AKT) and phosphorylated STAT3 (Nagasawa et al., 2019; Imura-Kishi et al., 2021). Cytoplasmic processes of such Sertoli cells are filled with microtubular bundles distinguished by its expression of acetylated tubulin (ace-TUB) (Aiyama et al., 2015). Notably, the modified Sertoli cells at the SV lack tight junction

complexes and ES that is specific for BTB (Osman, 1978; Figuerdo et al., 2021). Therefore, this region is suggested to be vulnerable to the immune cell infiltration (Takahashi et al., 2006). The SV epithelia is underlined by multi-layered thick basement membrane that appeared to be wrinkled, in contrast to a single-layered flat basement membrane of the ST (Tainosho et al., 2011). Such basement membrane at the SV is enriched with HSPG in hamster testis (Aiyama et al., 2015), suggesting a unique growth factor milieu at the SV. Intriguingly, the SV epithelia serve as an anatomically defined niche for SSCs. While the SV epithelia constitutively maintain A_{undiff} , most of spermatogenic activity is suppressed within the SV region. Namely, differentiation of A_{undiff} into A_{diff} are suppressed, and the emergence of meiotic germ cells are repressed locally in the SV (Aiyama et al., 2015). Interestingly, Aiyama et al. (2015) also revealed that the modified Sertoli cells constructing the SV maintain its proliferative activity and highly express GDNF, a mitogen for SSCs (Meng et al., 2000). These data indicate that the SV serves a niche both for SSCs and Sertoli cells, potentially through its unique growth factor milieu. Since the modified Sertoli cells at the SV is non-cell-autonomously specialized adjacent to the RT (Imura-Kishi et al., 2021), certain induction mechanisms of the SV through the RT-derived signals were implicated (Imura-Kishi et al., 2021); however, its detailed mechanism remains unclear.

The rete testis (RT)

In the mouse testis, the RT is situated at the cranial pole of the testis and located just under the testicular capsule known as the tunica albuginea. The RT serves a channel for sperm transport from the ST to the efferent duct (Free et al., 1980). The epithelia of the RT consist of a single layer of cuboidal epithelial cells with microvilli and a primary cilium on the apical surface. The RT epithelial cells express markers for gonadal somatic cells such as steroidogenic factor 1 (SF1; also known Nr5a1), SRY-Box Transcription Factor 9 (SOX9), GATA Binding Protein 4 (GATA4) and Wilms tumor 1 (WT1) alike Sertoli cells (Omotehara et al., 2020; Kulibin & Malolina, 2020). Meanwhile, the RT epithelial cells are distinguished by its unique marker expression of Paired box gene 8 (PAX8), Cadherin-1 (CDH1) and Keratin-8 (KRT8) (Aiyama et al., 2015; Kulibin & Malolina, 2020). Unlike Sertoli cells, epithelial cells of the RT do not have BTB, thus the RT is not immune-privileged environment (Gong et al., 2020). Indeed, the previous study has demonstrated that lymphocytes occasionally infiltrate into the lumen of the RT (Naito et al., 2008). The RT epithelia has active endocytosis activity, thus they modify the luminal fluid contents by their ability of secretion and reabsorption. The composition of luminal fluid in the RT and the ST is different each other in terms of K, Na, Cl and a series of proteins (Tuck et al., 1970;

Setchell et al., 1998; Fisher, 2002). Although it is seemingly a passive passageway, the function of the RT could be rather versatile. However, most of the physiological function of the RT remains unclear.

1.2 Spermatogonial stem cells (SSCs)

SSCs are the stem cells at the origin of spermatogenesis. The existence of SSCs was first demonstrated in 1994 with the establishment of intratesticular germ cell transplantation technique (Brinster and Avarbock, 1994; Brinster and Zimmermann, 1994). SSCs transplanted into the empty ST of genetically infertile (*e.g.*, W/W^0) mice or cytotoxic reagent (*e.g.*, busulfan)-treated mice could recolonize the ST and regenerate spermatogenesis (Brinster and Zimmermann, 1994; Ogawa et al., 2000; Kanatsu-Shinohara et al., 2016; Nakamura et al., 2021). Alike the other tissue stem cells, SSCs are defined by their ability of self-renewal and differentiation. The balance of self-renewal and differentiation of SSCs is supported within a specialized microenvironment called SSC niche, of which regulatory mechanism has been a long-standing focus of interest (Morrison and Spradling, 2008). The SSC niche in the mammalian testis consists of testicular somatic cells and growth factor milieu. Unlike the general “closed” niches with definitive structure to constantly harbor a certain stem cell population, the SSC niche in the ST is an “open” or “transient” niche, which does not have a structurally specified location. Whereas *Drosophila* testis has a well-defined germline stem cell niche at its proximal segment (Persico et al., 2019), the SSCs in mammalian testis are widely scattered along the seminiferous tubule. As stated above, recent study has discovered a closed SSC niche at the SV, that appeared to be analogous to the germline stem cell niche in *Drosophila* (Aiyama et al., 2015). However, the regulatory mechanism of SSC niche at the SV largely remain to be uncovered.

The population of spermatogonia is categorized according to their heterogeneous gene expression (Yoshida, 2012). While whole population of A_{undiff} is marked by the expression of Promyelocytic leukemia zinc finger protein (PLZF) and spalt like transcription factor 4 (SALL4), a subpopulation of A_{undiff} express glial cell line-derived neurotrophic factor-family receptor- $\alpha 1$ (GFR $\alpha 1$), of which expression is restricted to A_{single} , A_{paired} and rarely $A_{aligned\ 4/8}$ (Morimoto *et al.*, 2013; Hara *et al.*, 2014; Lovelace et al., 2016). Such GFR $\alpha 1$ -positive fraction of A_{undiff} comprises most of the self-renewing pool of SSCs, which constantly give rise to the differentiation-primed GFR $\alpha 1$ -negative/PLZF-positive A_{diff} ; hence GFR $\alpha 1$ -positive spermatogonia is regarded as a indicator of SSC population (Hara *et al.*, 2014; Garbuzov et al., 2018). Differentiation-primed fraction of A_{undiff} can be distinguished as GFR $\alpha 1$ -negative/retinoic acid receptor γ (RAR γ)-positive spermatogonia (Hara et al., 2014; Ikami et al.,

2015; Carrieri et al., 2017). As elaborated in Fig.1-1C, various other markers have been reported to label spermatogonia at different stage of differentiation (Subash and Kumar, 2020; Ibtisham and Honaramooz, 2020).

In the “A_{single} model” proposed in 1971, A_{single} spermatogonia was regarded as a definitive SSC population, and spermatogonial syncytia was believed to irreversibly undergo differentiation (Huckins, 1971, Oakberg, 1971). However, a recent study with *in vivo* live imaging revealed that SSCs interconvert between A_{single} and syncytial states continually (Hara et al., 2014). Syncytial A_{undiff} undergo fragmentation by breaking down its own intercellular bridges, and they also interconvert self-renewal-biased and differentiation-primed states stochastically (Hara et al., 2014; Nakagawa et al., 2010, 2021). The self-renewal of GFR α 1-positive A_{undiff} is supported by glial cell line-derived neurotrophic factor (GDNF), which is a ligand for GFR α 1 (Meng et al., 2000). On the other hand, GFR α 1-negative/RAR γ -positive spermatogonia were shown to differentiate into the A_{diff} characterized by the expression of c-KIT, when exposed to Retinoic acid (RA) (Nakagawa et al., 2007, Nakagawa et al., 2010). Once A_{undiff} differentiates into A_{diff}, it loses the potential as SSCs and successively undergo meiotic differentiations (Ohbo et al., 2003). Since the transition of A_{undiff} into A_{diff} is mediated by RA, temporal block of RA synthesis leads to the improved fertility restoration of the infertile host upon intratesticular SSC transplantation (Nakamura et al., 2021).

1.3 Paracrine Regulation in the STs

Chemical signaling in multicellular organism is categorized into 4 different types: (i) paracrine, (ii) autocrine, (iii) endocrine and (iv) signaling across gap junction. In paracrine signaling, a cell produces a signaling molecules that act locally to affect the cells located nearby. Paracrine signals are often diffused through the ECM. In autocrine signaling, a cell secret signaling molecules that is consumed by the same cell. The ligands released in endocrine signaling are called hormones, which is produced by endocrine cells to target a distant cell through the bloodstream. Direct signaling across gap junctions is conducted between the plasma membranes of two neighboring cells. This is particularly for the electrical communication between cells. In the testis, paracrine signaling plays significant roles in the fate decision of the germ cells and the regulation of mitosis and meiosis. Hereafter I introduce several paracrine signaling molecules that has significant functions on SSC maintenance and spermatogenesis and will be discussed in this thesis.

Glial cell line-derived neurotrophic factor (GDNF)

GDNF is a family ligand of the TGF β superfamily that is critical for the development of the kidneys, brain, and enteral nervous system (Kingsley, 1994). Together with the expression of its receptor (*i.e.*, GFR α 1), GDNF support the self-renewal of the SSCs both *in vitro* and *in vivo* (Meng *et al.*, 2000; Kanatsu-Shinohara *et al.*, 2003, 2005). The discovery of GDNF has greatly promoted our understanding of SSC niche in mammals. Decrease of GDNF *in vivo* result in the reduced germ cells in the testis (Meng *et al.*, 2001), while GDNF pan-overexpression result in the aberrant proliferation and accumulation of A_{undiff} (Meng *et al.*, 2000). GDNF also allowed the propagation of SSCs *in vitro*, which led to the establishment of germline stem (GS) cells culture system (Kanatsu-Shinohara *et al.*, 2003). The expression of GDNF is cyclically regulated in the seminiferous epithelia dependent on its seminiferous epithelium cycle, and its expression become high in stages I-VI (Sato *et al.*, 2011; Sharma and Braun, 2018). Although it has been well recognized that Sertoli cells secrete GDNF (Meng *et al.*, 2000), recent study uncovered that peritubular myoid cells also secrete GDNF to support A_{undiff} pool in the testis (Chen *et al.*, 2016). The expression of GDNF is stimulated by follicle-stimulating hormone (FSH) in Sertoli cells (Tadokoro *et al.*, 2002), whereas by Testosterone in peritubular myoid cells (Chen *et al.*, 2014). Interestingly, SV region constitutively express GDNF at high levels (Aiyama *et al.*, 2015). This might partially explain the reason why the SSC niche is maintained at the SV.

Fibroblast growth factor (FGF)

FGF family ligands play crucial roles in a series of biological process such as cell proliferation, tissue regeneration and development. It is well known that FGFs act in either paracrine or endocrine manner. Among twenty three FGF family members, paracrine FGFs include 15 family ligands (FGF1–6, 7–10, 16–18, 20 and 22) and act on nearby cells as locally secreted signals via diffusion (Itoh *et al.*, 2016; Xie *et al.*, 2020). These FGF members have heparan sulfate-binding site and bind to heparan sulfate proteoglycans (HSPGs), as well as to their cognate receptors (FGFRs) (Xie *et al.*, 2020). Heparan sulfate is necessary for the stable interactions of paracrine FGFs with FGFRs, while it independently interacts with FGFs and FGFRs (Itoh *et al.*, 2016; Xie *et al.*, 2020). Since HSPGs are ubiquitously accumulated in the basement membrane of the STs in mammalian testis (Brucato *et al.*, 2001; Aiyama *et al.*, 2015), FGF signaling in the STs has been speculated to support the spermatogonia reside in the basal compartment. The FGF-FGFR-heparan sulfate complex in turn activates several intracellular signaling pathways such as phosphoinositide 3-kinase (PI3K)-AKT, signal transducer and activator of transcription (STAT), and

RAS-mitogen-activated protein kinase (MAPK) signaling cascades (Goetz and Mohammadi, 2013; Ornitz and Itoh, 2015). In mammalian testis, several paracrine FGFs were shown to support the self-renewal of SSCs, and the density of SSCs *in vivo* is reported to depend on its local dose of FGFs (Kitadate et al., 2019). Among the FGF ligands, FGF2 has been traditionally utilized in the culture system of GS cells to promote its self-renewal (Kanatsu-Shinohara et al., 2003, 2005). FGF2 is known to induce phosphorylation of AKT and MAPK in GS cells *in vitro* (Ishii et al., 2012). Being distinct from GDNF, FGF2 was shown to support the differentiation-prone population of spermatogonia positive for RAR γ 1 and GFR α 1 *in vivo* (Takashima et al., 2015; Masaki et al., 2018). FGF5, FGF8 and FGF9 were also demonstrated to induce the proliferation of SSCs through AKT, ERK1/2 and p38 MAPK signaling (Hasegawa and Saga, 2014; Tian et al., 2019; Kitadate et al., 2019; Yang et al., 2021). However, exact localization of most of the FGF ligands in the testis remains unclear. Moreover, FGF actions on testicular somatic cells has paid relatively little attention compared to germ cells.

Retinoic acid (RA)

RA is an active metabolite of vitamin A, that plays significant roles in cell growth, differentiation, and organ development (Kam et al., 2012). The crucial role of RA in germ cell differentiation in the testis was first recognized due to the study showing that Vitamin A deficient diet make the animal sterile with an arrest of spermatogenesis at A_{undiff} (Wolbach et al., 1925; Thompson et al., 1966). The concentration of RA in the seminiferous epithelia is regulated based on the seminiferous epithelium cycle stages; the RA levels are maintained low during the stages II–VI, while high during the stages VII–XII and I (Endo et al., 2015, 2017). The RA support the germ cell differentiation, while modulating the formation of BTB in the testis (Chihara et al., 2013). Elevation of RA signals at seminiferous epithelial stages VII–VIII cause the following spermatogenic events in the ST; (i) differentiation of A_{undiff} into A_{diff}, (ii) initiation of meiosis (i.e., differentiation of A_{diff} into primary spermatocytes), and (iii) spermiation of elongated spermatids (Endo *et al.*, 2019; Gewiss et al., 2021). RA is received by a receptor called retinoic acid receptor gamma1 (RAR γ 1) in spermatogonia (Gely-Pernot et al., 2015), hence A_{undiff} expressing RAR γ 1 is considered as a differentiation-primed spermatogonial population (Fig.1-1C). The RA exposure to A_{diff} induce its expression of stimulated by retinoic acid gene 8 (STRA8) and MEIOSIN, which collaborate each other to regulate the mitosis to meiosis fate transition of germ cells in the testis (Endo et al., 2015; Ishiguro et al., 2020; Oatley and Griswold, 2020).

RA in the testis is synthesized *in situ* via two-step metabolic process. First, vitamin A is oxidized by alcohol dehydrogenases (ADH) into retinaldehyde. This step is mediated by the expressions of ADH3

and ADH1 in Sertoli cells, and ADH4 in late spermatids (Deltour et al., 1997; Molotkov et al., 2002). The resulting retinaldehyde is then oxidized by retinaldehyde dehydrogenases (ALDH) and transformed into RA. This step is catalyzed by RALDH1 and RALDH2 encoded by *Aldh1a1* and *Aldh1a2*, respectively (Zhai et al., 2001; Lopez-Fernandez et al., 1997). While *Aldh1a1* is expressed in Sertoli cells, *Aldh1a2* is expressed in spermatogonia, spermatids, and spermatocytes (Wang et al., 1996; Arnold et al., 2015). RALDH2 is regarded as the primary source of RA in mammalian spermatogenesis because germ cells depletion drastically drops the RA levels in the testis (Chen et al., 2018). The degradation of RA is catalyzed by Cytochrome P450 (CYP26) Enzymes that include CYP26A1, B1 and C1 (Hogarth et al., 2015). Among those, *Cyp26a1* and *Cyp26b1* are expressed in testis and play key roles in RA degradation to coordinate spermatogenesis (Bowles et al., 2006; Hogarth et al., 2015).

Wingless-INT (WNT)

WNT signaling is one of the highly conserved pathways in cell-to-cell paracrine interactions to modulate development and tissue homeostasis (Cadigan, 2008). WNT ligands binds to a Frizzled family receptor and induce signal transduction through canonical pathway that involves β -catenin or non-canonical pathway that is independent of β -catenin (Rao et al., 2010). Several WNT signals were previously shown to regulate the proliferation of A_{undiff} (Golestaneh et al., 2009; Takase and Nusse, 2016), yet the function of individual WNT ligand on spermatogonia *in vivo* mostly remained unclear due to its complexity of the signaling cascade and complementarity among various WNT family members (Chen *et al.*, 2016b). Several previous studies claimed that canonical WNT family ligands, WNT4 and WNT6, are expressed in Sertoli cells (Boyer *et al.*, 2012; Takase and Nusse, 2016). While WNT6 was indicated to support the proliferation of A_{undiff} (Takase and Nusse, 2016), WNT4 was reported to inhibit the self-renewal of A_{undiff} and promote their cell death *in vitro* (Boyer *et al.*, 2012). However, *in situ* hybridization data on WNT4 did not show its expression in Sertoli cells in the convoluted seminiferous tubules (Takase and Nusse, 2016), which contradict with the results shown in Boyer *et al.* (2012).

WNT5a is a non-canonical WNT ligand which blocks β -catenin-dependent signaling. *Wnt5a* was reported to be expressed in Leydig cells of zebrafish testes (Safian *et al.*, 2018), together with peritubular myoid cells and Leydig cells in mouse testis (Takase and Nusse, 2016). WNT5a administration *in vitro* was reported to promote survival of GS cells *in vitro* (Yeh *et al.*, 2011). Likewise *in vitro*, *Wnt3a* and *Wnt10b* were demonstrated to induce cell proliferation of cultured germ cells (Yeh *et al.*, 2013; Golestaneh et al., 2009). However, above-stated studies were conducted mostly *in vitro*, thus the direct function of most WNT ligands *in vivo* remained unclear. R-spondin (Rspo) is an activator of WNT/ β -catenin signaling

pathway, and there are four members of RSPO family proteins in vertebrates (*i.e.*, RSPO1, 2, 3, 4). In the testis, the expression of *Rspo4* was reported in the basement membrane, which is speculated to modulate A_{undiff} in the basal compartment of STs in collaboration with canonical WNT ligands produced by Sertoli cells (Takase and Nusse, 2016). Since RSPO and WNT signals play a pivotal role in gonadal sex determination, their roles in embryonic gonads have been studied extensively (Chassot et al., 2014). However, little attention had been devoted to the roles of WNT signaling in the postnatal testis in mammals.

The others

Aside from the above-mentioned paracrine ligands, there are a series of cytokines and growth factors that contribute to the testicular homeostasis. For instance, activin A, stem cell factor (SCF), Bone morphogenetic proteins (BMP) 4 and BMP8A promote the differentiation of SSCs, while colony stimulating factor 1 (CSF1) and epidermal growth factor (EGF) support the self-renewal of SSCs (Pellegrini et al., 2003; Abe et al., 2008; Oatley et al., 2009; Wu et al., 2017). In the STs, distribution of SSCs is biased to the region close to the vasculature (Yoshida et al., 2007), lymphatic endothelial cells (Kitadate et al., 2019), macrophages (DeFalco et al., 2016) and testicular endothelial cells (Bhang et al., 2018). This may be due to several local paracrine signals that are secreted by these somatic cells, and the SSC dynamics *in vivo* is speculated to depend on the local concentration of mitogens in the transient site of the STs as a “open” SSC niche (Kitadate et al., 2019). Although the regulatory mechanism of this ‘open’ SSC niche in the STs has been extensively studied, the regulatory mechanism of the ‘closed’ SSC niche at the SV has remained a mystery.

1.4 Objectives and hypothesis of this study

In summary, GDNF and FGFs support the self-renewal of A_{undiff} , while RA signals induce the A_{undiff} -to- A_{diff} transition in the basal compartment of STs. However, effects of these paracrine factors on the dynamics of A_{undiff} *in vivo* remains unclear. This is mainly due to the lack of *in vivo* assay system of the paracrine factors in mammalian testes. Moreover, in the proximal part testis region, the paracrine and/or autocrine actions of several signaling factors may modulate the formation and maintenance of the SV niche. However, the direct evidence to confirm such paracrine interactions are missing. In order to elucidate the paracrine actions in RT-SV-ST, I set three subjects in my PhD study as follow:

- 1: Develop an assay to examine the function of paracrine signals on A_{undiff} in the testis *in vivo*
- 2: Reveal the regulatory mechanism of the SV epithelia through paracrine signals.
- 3: Explore the roles of the RT and SV in testicular homeostasis.

In brief, I first developed a novel bead transplantation assay to assess the *in vivo* function of paracrine factors on A_{undiff} in Chapter 1. By applying the bead transplantation assay to GDNF, I demonstrated its function as a mitogen for A_{undiff} and validated the assay. By using the assay developed in Chapter 1, I next aimed to dissect the regulatory mechanism of the SV formation. Based on the microarray data showing the region-specific expression of *Fgf* family members including *Fgf9* at the RT, I transplanted FGF9-soaked bead and demonstrated the function of FGF9 to induce SV-specific AKT phosphorylation in the Sertoli cells near the FGF9-beads. Noting the SV region-specific expression of a RA-degrading enzyme, *Cyp26a1*, I transplanted RA-soaked beads around the SV and revealed that high dose of RA at the SV partially caused the differentiation of its local A_{undiff} and disrupted the valve structure at the SV region. These data suggest the contribution of the paracrine interactions of FGFs and RA in formation and maintenance of the SV region. In Chapter 3, after identifying the region-specific expression of *Sox17* in the RT epithelia, I demonstrated the disruption of the valve-like structure at the SV by using mutant mice with RT-specific *Sox17* depletion (*Sox17*-cKO). Single cell RNA sequencing (scRNAseq) analysis of *Sox17*-cKO testes revealed the downregulation of several genes encoding a growth factor in the RT epithelia, suggesting possible involvement of several growth factors downstream of *Sox17* action in RT epithelia. The valve disruption of *Sox17*-cKO testes resulted in the backflow of the luminal fluid in the STs, leading to the spermiogenesis defects in the upstream ST. Meanwhile, *Sox17* over-expression in Sertoli cells resulted in the hyperplasia of the valve-like structure at the SV. These data indicate potential paracrine regulation of the SV by the RT epithelial cells, as a downstream action of *Sox17*. Taken together, I concluded that the SOX17-positive RT epithelia modulate the SV specification/formation in a novel paracrine system downstream of *Sox17* action, which is essential for proper spermiogenesis in upstream STs *in vivo*.

1.5 Figures

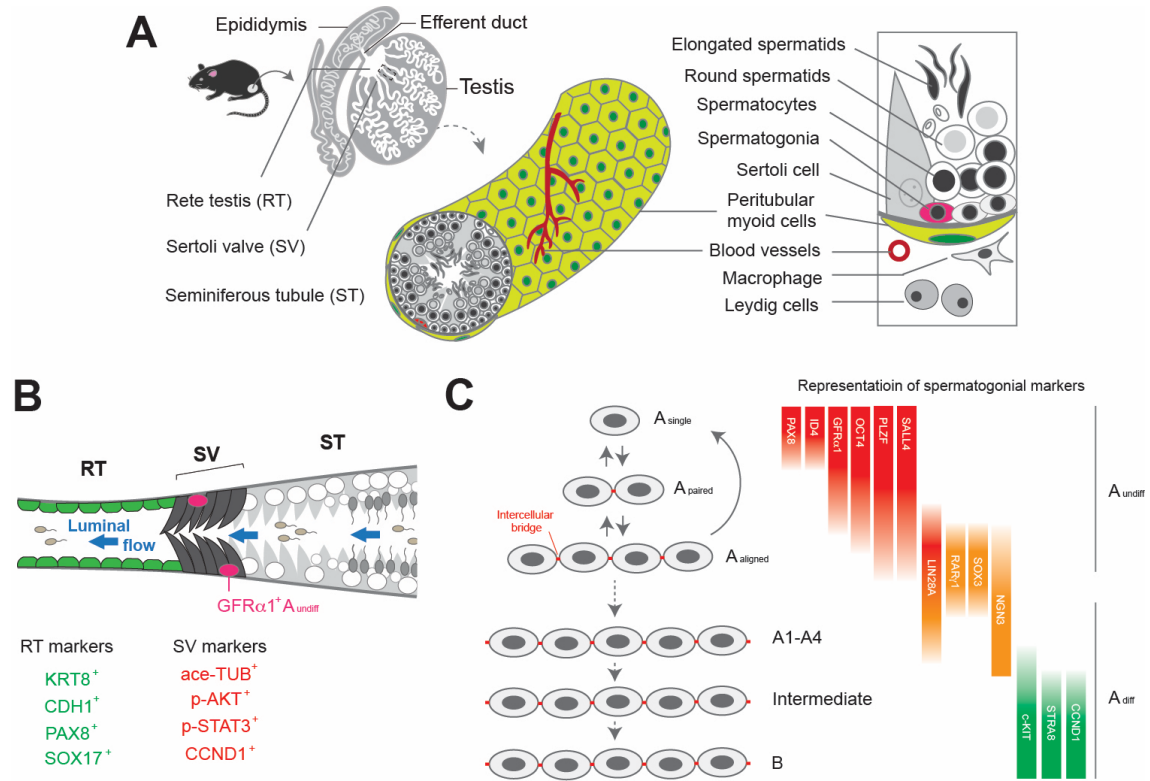


Fig.1-1 Anatomy of the mouse testis and spermatogonial differentiation.

(A) Schematic illustration of the anatomy of mouse testis. Spermatogenesis take place in the tubule structure called seminiferous tubule (ST) in mouse testis. The ST and testicular interstitium is segregated by the basement membrane outlining the ST. (B) Schematic illustration of the connection of the rete testis (RT), Sertoli valve (SV) and the ST and the list of markers for the RT and SV epithelial cells. Sperm produced in the ST is unidirectionally transported through a valve-like structure at the SV, and then flow into the RT. (C) Comparative developmental patterns and expression profile of spermatogonial markers at each differentiation stage in mouse testis. GFR α 1-positive spermatogonia is regarded to represent spermatogonial stem cell population, while c-KIT-positive spermatogonia is regarded as differentiating spermatogonia (A_{diff}) in this study. Spermatogonia differentiate while connecting via intercellular bridge. RT, Rete testis; SV, Sertoli valve; ST: seminiferous tubule. A_{single} , singly isolated spermatogonia; A_{paired} , paired spermatogonia; $A_{aligned}$, Aligned Spermatogonia; A_{diff} , differentiating spermatogonia. A_{undiff} , undifferentiated spermatogonia.

2. CHAPTER 1

“A bead transplantation assay to examine *in vivo* dynamics of germ cells stimulated by paracrine factors”

2.1 Abstract

The balance of self-renewal and differentiation of SSCs is orchestrated by a series of growth factors *in vivo*. However, the function of each secreted factors on the dynamics of SSCs *in vivo* largely remains unclear. Here I developed a simple method for transplanting recombinant protein-soaked microbeads into the testicular interstitium in mouse. By using this method, I first demonstrated the functional roles of GDNF as a mitogen for SSCs. The bead-derived GDNF signals induced the stratified aggregate formation of GFR α 1-positive A_{undiff} by day 3 post-transplantation. Each aggregate consisted of tightly compacted A_{single} and marginal A_{paired} to A_{aligned} GFR α 1-positive spermatogonia and was surrounded by A_{aligned} GFR α 1-negative spermatogonia at more advanced stages. These data not only provide *in vivo* evidence for the inductive roles of GDNF in forming a rapid aggregation of GFR α 1-positive spermatogonia but also indicate the usefulness of this *in vivo* assay system of various growth factors for the stem/progenitor spermatogonia in mammalian spermatogenesis. By utilizing this assay, I further demonstrated the effect of WNT ligands on the dynamics of spermatogonia *in vivo*.

2.2 Introduction

Testicular homeostasis is coordinated by paracrine interactions in the testicular cells, and the maintenance of SSCs is orchestrated by a series of growth factors (Yoshida, 2018). However, functions of growth factors on SSC dynamics have largely remained unclear *in vivo*. Genetic ablation of a gene encoding a growth factor has been a most popular strategy to get an insight into functions of the growth factor *in vivo*. However, it is often difficult to separate the first effects directly caused by the knockout from the secondary effect such as tissue degeneration. In addition, a considerable number of growth factors has a functional redundancy, which often makes phenotype of the knockout mice undetectable. Establishment of GS cells has extended our understanding of growth factor functions on SSCs *in vitro* (Kanatsu-Shinohara *et al.*, 2003, 2005). However, it had remained a challenge to elucidate the spatiotemporal spermatogonial dynamics influenced by individual growth factors *in vivo* due to the lack of adequate experimental model system. Therefore, I first set a goal of this study to establish an experimental assay to examine the function of growth factors in mouse testis *in vivo*. By using this assay, I then aimed to uncover the spatiotemporal dynamics of germ cells exposed to the growth factors.

Hereafter, I developed a transplantation assay of growth factor-soaked microbead into the testicular interstitium. By applying this assay to GDNF, I demonstrated the accumulation of A_{undiff} in the seminiferous tubules close to the transplanted GDNF-soaked beads. It not only validated the function of GDNF to support the self-renewal of SSCs, but also uncovered the the proliferation dynamics, differentiation pattern and kinetics of GFR α 1-positive spermatogonia in response to GDNF signals *in vivo* for the first time. We further extend the bead transplantation assay to uncover function of growth factors, of which roles on dynamics of spermatogonia remain unclear *in vivo*.

2.3 Materials & Methods

Animals

Wild-type (8-week-old, ICR strain; SLC, Inc.) and GFR α 1-GFPknock-in male mice (Uesaka *et al.*, 2007) were used in this study. All animal experiments were performed in strict accordance with the Guidelines for Animal Use and Experimentation at the University of Tokyo (Approval IDs: P13-762, P14-025, P15-075, P15-078, P16-083).

Bead preparation and transplantation

Affi-Gel blue beads (approximately 100 μ m in diameter; Bio Rad) were soaked in a solution of recombinant GDNF (0.1 mg/ml; Calbiochem), WNT4 (0.1 mg/ml; R&D systems), WNT5a (0.1 mg/ml; R&D systems) or BSA (bovine serum albumin; 0.1 mg/ml; Sigma-Aldrich) for 1 hour at room temperature. To mark the tubular wall adjacent to the transplanted beads, beads were immersed in DiI (0.83 mg/ml; Thermo Fisher Scientific) solution for 15 min. For transplantation, the adult testes were gently extracted from the abdominal cavity under anesthesia, and then the GDNF- or BSA (negative control)-soaked beads were transplanted into the testicular interstitium (approximately eight beads [one or two beads per site] were separated with appropriate intervals) via vitrified micro-capillary under a dissecting microscope. For *in vivo* time-course analysis using GFR α 1-EGFP-knock-in testes, the beads were transplanted into the subsurface region (underneath the tunica albuginea) of the testes. Under anesthesia, the GFP fluorescence images, including GFR α 1 (GFP)-positive spermatogonia around the transplanted beads, were photographed after transplantation (*i.e.*, days 0, 3, and 5 post-transplantation) using an Olympus stereomicroscope (SZX16 plus U-LH100HG) with a Bex fluorescence adaptor (SFA-RB; Bex Co., Ltd).

Histology and immunohistochemistry

Testes were fixed in 4% paraformaldehyde (PFA) for 8 hours at 4°C, dehydrated, embedded in paraffin, and then sectioned (4 mm in thickness). The deparaffinized sections were incubated overnight at 4°C with the primary antibodies listed in Table 2.1. For whole-mount analysis, testes were fixed in 4% PFA at 4°C overnight, removed from the tunica albuginea, and dispersed in cold PBS. ST fragments were isolated manually, permeabilized with a gradient series of methanol, and incubated overnight at 4°C with the primary antibodies listed in Table 2.1. Immunoreactions were visualized by using Alexafluor-488/555/594/680-conjugated secondary antibodies (Abcam) or biotin-conjugated secondary antibodies with the Elite ABC Kit (Vector Laboratories). The stained samples were analyzed using an Olympus fluorescence microscope (BX51N-34-FL2) and a Leica TCSSP8 confocal laser microscope (Leica Microsystems GmbH).

Cell proliferation and statistical analysis

For the anti-pHH3/GFR α 1 double-stained whole mount segments, pHH3-positive indices in each GFR α 1-positive spermatogonia were estimated separately in the GFR α 1-positive A_{aligned}-like aggregates located close to the transplanted beads and in the GFR α 1-positive cells of normal seminiferous tubules located far from the transplanted beads in the same testis. Quantitative data are represented as means \pm s.e.m. Comparisons were made by using two-sided unpaired Student's *t*-test. In this study, A *P*-value < 0.05 was considered significant.

2.4 Results

Transplantation of GDNF-soaked beads and potential diffusion of GDNF from the beads *in vivo*

Affi-Gel blue beads are commonly used microbeads for protein purification (Bio-Rad). It had been often used *in vitro* to test the function of a growth factor on cells or tissue (Higashiyama *et al.*, 2017), yet there was no application reported *in vivo* in mammalian testis. By modifying the intra-testicular transplantation system developed by Brinster *et al.* (Brinster & Zimmermann, 1994), I first developed a transplantation assay of Affi-Gel blue bead into the testicular interstitium via vitrified microcapillary (Fig. 2-1A). The rationale of developing this method is to uncover function of a secreted factor *in vivo*. To begin with, we aimed to validate the bead transplantation assay by demonstrating the ability of GDNF to support the self-renewal of SSCs (Meng *et al.*, 2000).

I transplanted GDNF-soaked microbeads into testicular interstitium of mouse at 8 weeks of age (Fig. 2-1A) to examine the dynamics of spermatogonia exposed to GDNF signals. First, to analyze the diffusion and attenuation pattern of GDNF derived from the transplanted beads, I examined the immunoreactive GDNF signals in the testicular tissues around the transplanted beads (Fig. 2-1A–C). As a result, GDNF immunoreactivity were detected in the beads and seminiferous epithelia located close to the GDNF-soaked beads at day 1 post-transplantation. This suggests that GDNF derived from the bead can be diffused into seminiferous epithelia of the adjacent seminiferous tubule. The GDNF signals in the seminiferous epithelia had diminished to undetectable levels by day 3 post-transplantation (“1d” and “3d” in Fig. 2-1C), while GDNF immunoreactivity was still maintained within the beads. GDNF immunoreactivity in the transplanted beads were the highest at day 1 post-transplantation (“1d” in Fig. 2-1C), and they clearly decreased over time (“3d” and “1m” in Fig. 2-1C). Of note, faint GDNF immunoreactivity was still detected in the beads at 1-month post-transplantation compared with BSA-soaked control beads at day 1 post-transplantation (“1m” and “BSA” in Fig. 2-1C). These results suggest that GDNF-soaked beads transplanted into the testicular interstitium release GDNF to affect the ST located close to the bead upon transplantation, while the amount of GDNF released from the bead decrease over time.

Formation of A_{undiff} aggregates close to the transplanted GDNF-soaked beads

GDNF secreted from Sertoli cells located in the seminiferous epithelia is known to promote self-renewal of SSCs *in vivo* (Meng *et al.*, 2000). Meanwhile, it had remained unknown whether testicular interstitium-derived GDNF can affect spermatogonia in the seminiferous tubules. Although recent study suggested that *Gdnf* expression in peritubular myoid cells in the testicular interstitium also support the spermatogonia by using *Myh11Cre: Gdnf^{fllox/flox}* mice (Chen *et al.*, 2016a), it had remained controversial due to the lack of specific marker for peritubular myoid cells to specifically deplete *Gdnf* expression. In addition, there was no direct evidence that interstitial GDNF can affect spermatogonia reside within seminiferous tubules *in vivo*. To examine the effect of interstitium-derived GDNF on spermatogonia located in the seminiferous tubules adjacent to the transplanted beads, I next analyzed the distribution patterns of spermatogonia around the transplanted GDNF-soaked beads by immunohistochemistry. Immunohistochemistry with anti-GFR α 1 antibody revealed the ectopic formation of stratified aggregates of GFR α 1-positive A_{undiff} close to the GDNF-soaked beads at 5 days post-transplantation (Fig. 2-2A; also see “A1” and “A2”). This is in sharp contrast to GFR α 1-positive spermatogonia located away from transplanted GDNF-soaked beads, which showed no appreciable formation of such aggregates (also see

“A3” [with an interval of one tubule from the bead] in Fig. 2-2). There were few GFR α 1-positive aggregated cells in the BSA-bead transplanted control testes (figure not shown). I also confirmed this result by performing immunohistochemistry with anti-PLZF antibody, which marks A_{undiff} at a wider range than GFR α 1 (Nakagawa *et al.*, 2010; Suzuki *et al.*, 2009). PLZF immunohistochemistry revealed 2 to 3 layers of PLZF-positive spermatogonia stratified in the basal compartment of the ST (Fig. 2-2B).

Spatiotemporal changes in the aggregate of GFR α 1-positive spermatogonia induced by transplanted GDNF-soaked beads

Next, to see the spatiotemporal dynamics of spermatogonia exposed to GDNF derived from the transplanted bead, I performed whole mount immunohistochemistry of the seminiferous tubules. The ST located next to the transplanted bead was distinguished by DiI (red fluorescence). As a result, GFR α 1-positive spermatogonia were found to form the aggregates in the seminiferous tubules marked with DiI at day 3 post-transplantation (left in Fig. 2-2C) (27 of 29 testes [93.1%]). On the other hand, no appreciable GFR α 1-positive aggregates were detected in the seminiferous tubules close to the transplanted control (BSA-soaked) beads (right in Fig. 2-2C) or in the seminiferous tubules located far from the GDNF-soaked beads (figure not shown). At day 3 post-transplantation, A_{aligned}-like aggregates with various cell numbers were observed in the seminiferous tubules close to the transplanted GDNF-soaked beads (Fig. 2-2D). Large aggregates consisting of more than 3 GFR α 1-positive cells were detected even at day 3 post-transplantation (rightmost plate in Fig. 2-2D). Because such aberrant aggregation resembles the abnormal accumulation of A_{undiff} in mouse testis over-express *Gdnf* (Meng *et al.*, 2000; Creemers *et al.*, 2002; Yomogida *et al.*, 2003), it is likely that bead-derived GDNF signals could affect the basal compartment of the seminiferous epithelia, leading to the aggregation of GFR α 1-positive spermatogonia at days 3 to 5 post-transplantation. To my surprise, small-sized aggregates of GFR α 1-positive cells were observed in the ST next to the transplanted bead at day 1 post-transplantation (Fig. 2-3A). GFR α 1-positive aggregates appear to gradually increase in size at days 3 to 5 post-transplantation, but no GFR α 1-positive cell aggregates were detected at 1 month post-transplantation (Fig. 2-3A). Quantitative analysis of each GFR α 1-positive A_{aligned}-like aggregates with more than four cells showed that the number of GFR α 1-positive cells gradually increased in each aggregate by day 5 post-transplantation (Fig. 2-3B).

To further confirm the rapid increase of A_{undiff} upon its exposure to GDNF, I next performed time-course tracking of GFR α 1-positive spermatogonia by using GFR α 1-GFP knock in mice. Spermatogonia marked by GFR α 1-GFP was tracked under a fluorescence stereomicroscope

at days 0, 3, and 5 post-transplantations (Fig. 2-3C, D). Soon after the transplantation, only a few GFR α 1-GFP-positive spermatogonia were seen within the seminiferous tubules around the GDNF-soaked beads. GFP-positive cells then appeared to increase in number and expand widely around the GDNF-soaked beads by day 5 post-transplantation (arrow in Fig. 2-3D, D1). This is in sharp contrast with the lack of appreciable increase of GFR α 1-GFP-positive cells in the area close to the BSA-soaked beads in the same testes (lower plates of Fig. 2-3D). Additionally, at day 5 post-transplantation, the GFP-positive signals around the GDNF-soaked beads were confirmed to be identical to the aggregates of GFP-positive spermatogonia (the same tubular region after fixation and removal of the tunica albuginea; Fig. 2-3D2). Taken together, these data suggest that GDNF delivered by the bead transplantation promoted the expansion of GFR α 1-positive A_{undiff} located nearby, but in a temporal manner.

Proliferation and differentiation of GFR α 1-positive spermatogonia in the aggregate

Next, I examined proliferation patterns of cells in the aggregate, in order to confirm that the aggregate of GFR α 1-positive spermatogonia was formed by the proliferation of GFR α 1-positive spermatogonia induced by GDNF signals, rather than by their chemoattractant actions. In this study, I used Cyclin-D1 (CCND1; which promotes passage through G1 phase) and phospho-Histone H3 (pHH3; marks condensed chromatin at G2/M transition) as a marker for cell proliferation in the aggregate. As a result, majority of GFR α 1-positive cells of small-sized aggregates were immunoreactive for CCND1. Considerable variations of CCND1 signal intensity were observed among the GFR α 1-positive cells in the middle-to-large-sized clusters (rightmost plate in Fig. 2-4A). Consistently, pHH3 immunoreactivity was observed more frequently in GFR α 1-positive spermatogonia constructing the aggregates compared with the GFR α 1-positive cells of the normal segments of the seminiferous tubules located far from GDNF-soaked beads (pHH3-positive ratio in GFR α 1-positive cells: $13.7 \pm 2.6\%$ in the aggregates vs. $2.4 \pm 1.4\%$ in the normal fragments, $p < 0.01$; Fig. 2-4B, C). pHH3-positive mitotic spermatogonia frequently appeared at the marginal region of the GFR α 1-positive cluster, suggesting a non-synchronously proliferating state of each cell within the GFR α 1-positive aggregate. Anti-PLZF staining visualized the GFR α 1-negative spermatogonia at the advanced stages near the GFR α 1-positive aggregate (Fig. 2-4D). Interestingly, PLZF-positive/GFR α 1-negative spermatogonia were often observed outside the marginal region of the GFR α 1-positive cluster (arrowheads in Fig. 2-4D). Such PLZF-positive/GFR α 1-negative spermatogonia appear to be closely in contact with GFR α 1-positive aggregate through one end of PLZF-positive chained cells. These data suggest the possibility that spermatogonia constructing the aggregate gradually undergo differentiation while expanding outwards the aggregate. To visualize the connection of

the spermatogonia (i.e., number of chained cells) within the aggregate, I next analyzed the distribution patterns of the intercellular bridges among the GFR α 1-positive aggregate by performing immunohistochemistry on mitotic kinesin-like protein (MKLP1), which is one of the intercellular bridge components (Iwamori *et al.*, 2011). In the aggregate, MKLP1-positive ring-like signals were frequently observed between GFR α 1-positive cells at the margin (Fig. 2-4E, F). In contrast, no appreciable ring-like signals were detected in the GFR α 1-positive cells in the tightly compacted region at the center of aggregate. These data suggest that the GFR α 1-positive aggregate consists of the tightly-compacted A_{single} cells at the core and marginal A_{paired} to A_{aligned} spermatogonia, which are concentrically surrounded by the GFR α 1-negative/PLZF-positive cells. Altogether, I demonstrated the ability of GDNF to induce proliferation of spermatogonia *in vivo* by applying the bead transplantation assay I developed and further revealed the dynamics of GFR α 1-positive spermatogonia exposed to GDNF signals *in vivo* (Fig. 2-5).

Application of the bead transplantation assay to growth factors of which *in vivo* function remain unclear

Finally, I applied the bead transplantation assay to growth factors, of which function *in vivo* remain unknown. I transplanted WNT4-soaked beads into testicular interstitium and examined the distribution pattern of GFR α 1-positive spermatogonia located close to the transplanted beads. As a result, A_{aligned} GFR α 1-positive spermatogonia were observed to extend their cytoplasmic process (Fig. 2-6A). Since such extended cytoplasmic process is characteristic to migrating spermatogonia (Hara *et al.*, 2014), this suggest that WNT4 might affect the chemotactic migration of local spermatogonia *in vivo*. On the other hand, transplantation of WNT5a-soaked beads induced local expansion of GFR α 1-positive spermatogonia close to the transplanted beads (Fig. 2-6B). This result is consistent with the previous report showing that WNT5a promoted the self-renewal of SSCs *in vitro* (Yeh *et al.*, 2011). However, these data remain preliminary, and further study is required to uncover the exact function of WNT4 and WNT5a on spermatogonial dynamics *in vivo*.

2.5 Discussion

It is well known that, GFR α 1-positive spermatogonia in mouse testes consist mainly of A_{single} and A_{paired} and rarely of A_{aligned}-4 (Nakagawa *et al.*, 2010; Suzuki *et al.*, 2009). On the contrary, the present study demonstrated that GDNF-soaked bead transplantation can induce the formation of the A_{aligned}-like

aggregates of GFR α 1-positive spermatogonia in the restricted region close to the GDNF-soaked beads transplanted in the testicular interstitium. This phenotype is consistent with the typical phenotype of the aberrant accumulation of A_{undiff} in testes over-expressing *Gdnf* (Meng *et al.*, 2000; Creemers *et al.*, 2002; Yomogida *et al.*, 2003). The similar A_{aligned}-like GFR α 1-positive aggregates were also frequently observed in the early colonization of the SSCs transplantation assay using the germ cell-depleted *W/W^v* mouse testes (Nagai *et al.*, 2012), in which GDNF is regionally expressed at considerably high levels (Sato *et al.*, 2011; Tadokoro *et al.*, 2002). Therefore, it is likely that interstitial GDNF signals can affect the dynamics of the GFR α 1-positive cells located in the basal compartment, leading to the formation of the GFR α 1-positive aggregates *in vivo*. This is also consistent with the recent finding showing the importance of GDNF signals derived from the peritubular myoid cells for the maintenance of A_{undiff} in the mouse testes (Chen *et al.*, 2016). *In vitro* experiments showed that GDNF is crucial for the proliferation and maintenance of GS cells, a cell line of SSCs (Kanatsu-Shinohara *et al.*, 2003, 2005, 2013). The formation of GFR α 1-positive cell clusters is reminiscent of that of proliferated GS cells under high-GDNF conditions *in vitro* (Kanatsu-Shinohara *et al.*, 2003, 2005, 2011; Kubota *et al.*, 2004; Araki *et al.*, 2010), in which GDNF promoted activated states like A_{aligned}-like cell aggregates in the GS cell colony *in vitro* (Morimoto *et al.*, 2009). A_{aligned}-like aggregation in this study may reflect the dynamic changes into the active states from the normal A_{single} to A_{paired} GFR α 1-positive cells stimulated by high-level GDNF signals.

The doubling time of mouse SSCs *in vivo* is estimated to be 7.9 days (Nagano *et al.*, 2003). The previous live-imaging experiment determined the rate of cell division of GFR α 1-positive spermatogonia to be approximately one cell division per 10 days under healthy conditions (Hara *et al.*, 2014). The present study revealed A_{aligned 8/16}-like aggregates emerged at day 1 post-transplantation while A_{aligned}-like aggregates with more than 32 cells were found by day 3 post-transplantation. This suggests the rapid formation of GFR α 1-positive cell aggregation by *in vivo* GDNF-soaked bead treatment, even if they were in a situation similar to that of the activated fast-growing GS cells *in vitro*, which doubling time is estimated to be approximately 2.7 days (Kanatsu-Shinohara *et al.*, 2012). As GDNF signals were previously shown to induce the chemotactic migration of mouse A_{undiff} *in vitro* (Huleihel *et al.*, 2013; Dovere *et al.*, 2013), such a rapid A_{aligned}-like formation may be partially explained by the assembling of several independent GFR α 1-positive cells in the seminiferous tubules near the beads. This is consistent with the *in vivo* time-course data, which show a rapid increase of GFP/GFR α 1-positive aggregates near the GDNF-soaked beads (Fig. 2-3D).

The present study revealed that the middle-to-large-sized GFR α 1-positive cluster consisted of the tightly compacted A_{single} and marginal A_{paired} to A_{aligned} spermatogonia, which were surrounded by the GFR α 1-negative chained cells at days 3 to 5 post transplantation. With regard to the normal temporal orders in both cell division (*i.e.*, from A_{single} to A_{aligned} spermatogonia) and differentiation states (*i.e.*, from GFR α 1-positive to -negative spermatogonia), it is possible that a GFR α 1-positive cell aggregate first appears as a core and then generates GFR α 1-positive A_{paired} to A_{aligned} cells, which results in the increase of the cluster size together with the appearance of GFR α 1-negative PLZF-positive spermatogonia around each GFR α 1-positive aggregate. This hypothesis is consistent with the data on the proliferative patterns of donor-derived GFR α 1-positive spermatogonia in *W/W^v* seminiferous tubules during early colonization in the SSC transplantation assay. After the first appearance of the A_{aligned4/8}-like GFR α 1-positive cells at day 7 post-transplantation, A_{aligned}-like GFR α 1- positive aggregates with more than 32 cells were formed at and after day 10 post-transplantation; they were subsequently surrounded by GFR α 1-negative spermatogonia (Nagai *et al.*, 2012). However, *in vivo* time-lapse analyses using GFR α 1-knock-in mice are required to clarify the exact dynamics of the GFR α 1-positive cells during the process of the A_{aligned}-like aggregations in this assay.

The present transplantation assay is so simple and easy technique that it could be applied to non-model animals in the future. This assay may be useful not only for *in vivo* analyses of various growth factors for SSCs. but also, potentially, for therapeutic purposes such as fertility preservation or restoration in subfertile and infertile males of various mammal species.

2.6 Figures & Tables

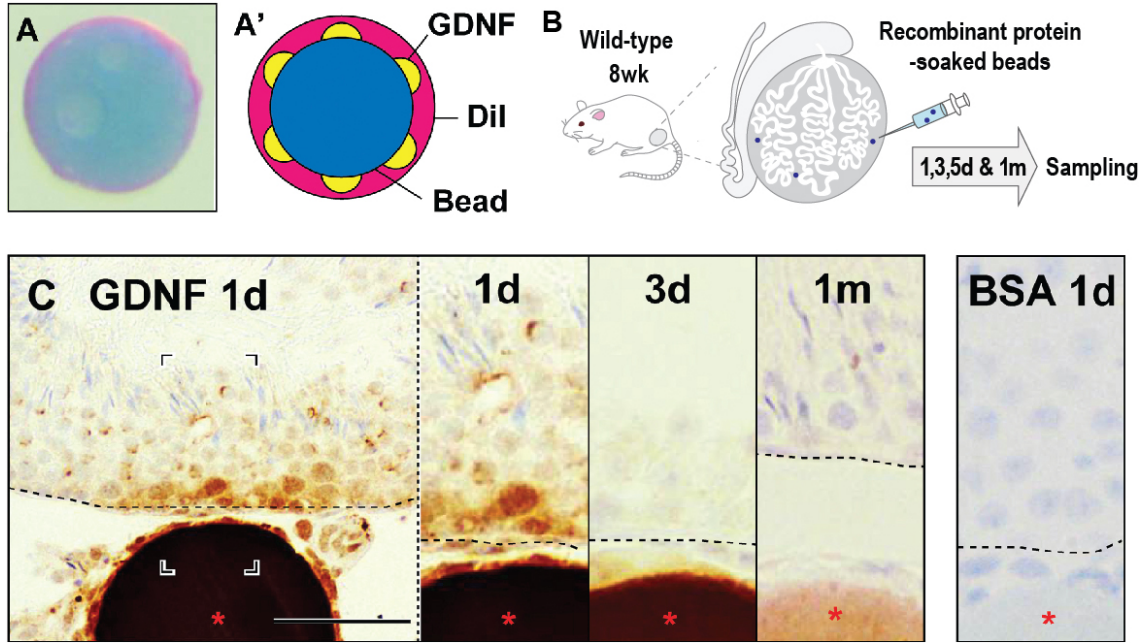


Fig. 2-1. *In vivo* transplantation of DiI-labeled/GDNF-soaked beads into the testicular interstitium.

(A) DiI-labeled GDNF-soaked beads. Plate A' presents the schematic diagram of A. (B) Schematic illustration of the bead transplantation into the testicular interstitium. (C) GDNF immunohistochemistry (brown) of mouse testes transplanted with GDNF or BSA-soaked beads at 1 day, 3 days, and 1-month post-transplantation ("1d", "3d", "1 m", respectively, in C). Panel 1d represents the region surrounded by a broken rectangle in C. Asterisk, transplanted beads. Broken line, outline of seminiferous tubule. Scale bar, 100 μ m.

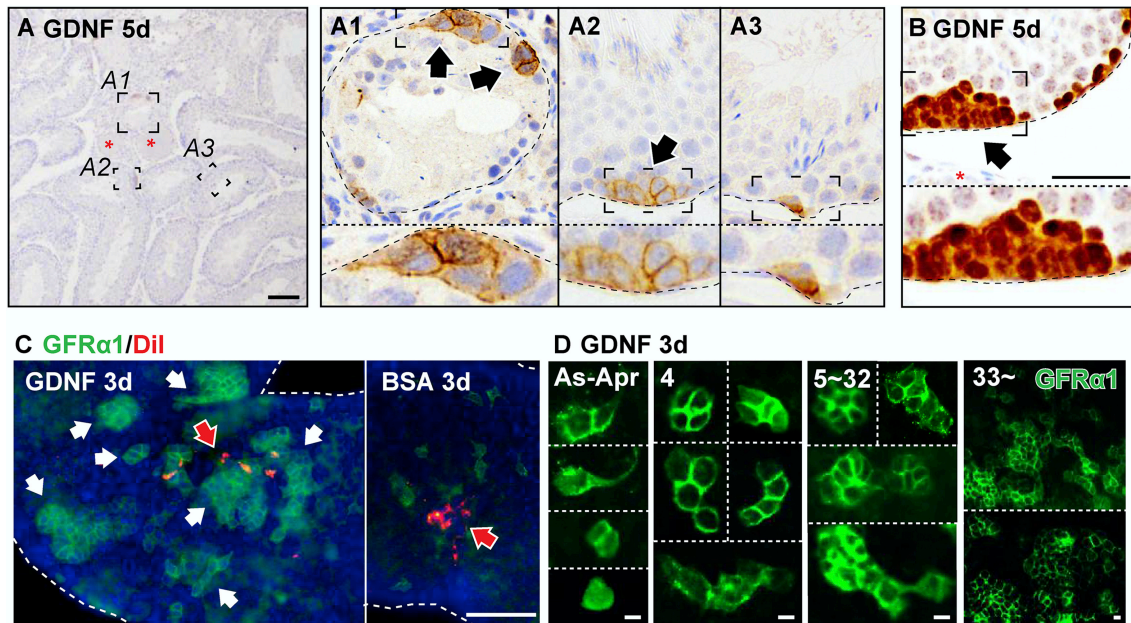


Fig. 2-2. Aggregates of GFR α 1-positive spermatogonia in the basal compartment of seminiferous tubules formed close to the GDNF-soaked beads. (A, B) GFR α 1 (brown in A) and PLZF (brown in B) immunohistochemistry of mouse testis transplanted with GDNF-soaked beads at day 5 post-transplantation. Plates A1 to A3 show the regions surrounded by broken rectangles in A at higher magnification. Plates A1 to A3 and B also include the insets indicated by broken rectangles. (C, D) Whole-mount GFR α 1 immunohistochemistry (green) of GDNF or BSA-soaked bead transplants at day 3 post-transplantation. In plate D, the number in the left upper corner indicates the number of GFR α 1-positive spermatogonia in each aggregate is indicated in the left upper corner of each . Asterisk, bead; broken line, outline of seminiferous tubule; black/white arrow, GFR α 1-positive aggregate; red arrow, DiI-marking (bead-attaching) site. As, A_{single}. Apr, A_{paired}. Bar, 100 μ m in A to C, 10 μ m in D.

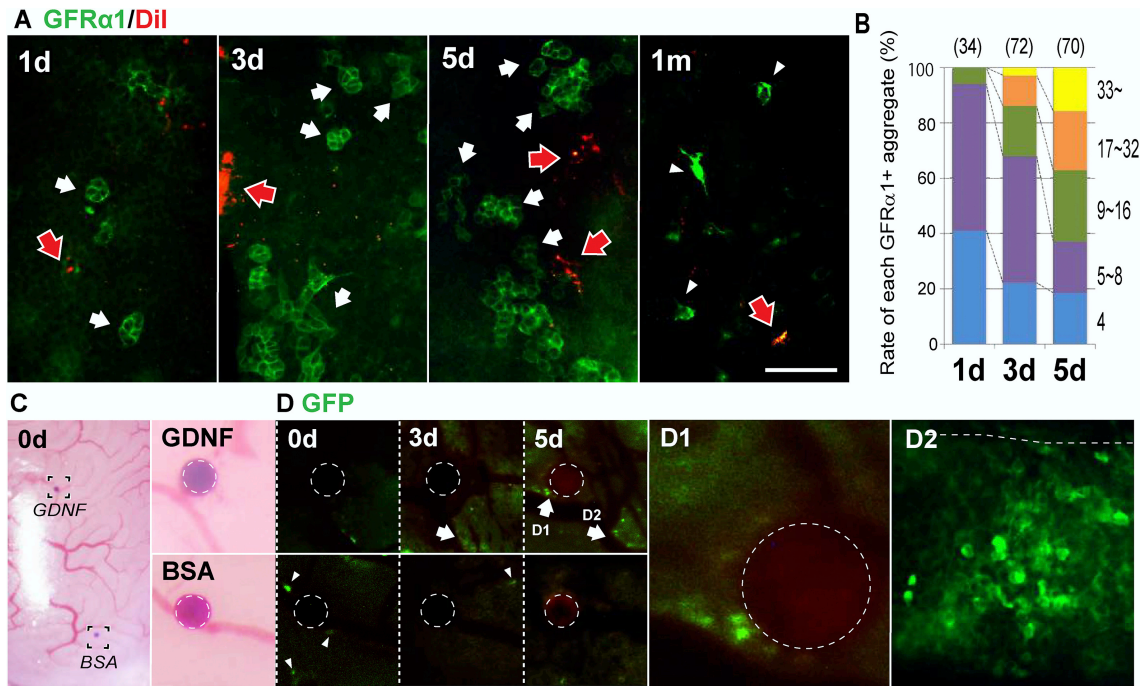


Fig. 2-3. Temporal changes of GFRα1-positive aggregates in the ST close to the transplanted GDNF-soaked beads. (A) Whole-mount anti-GFRα1 staining (green) of the seminiferous tubules near the transplanted GDNF-soaked beads at days 1, 3, and 5 and 1 month post-transplantation (“1d,” “3d,” “5d,” and “1 m” in A). (B) A bar graph showing changes in the appearance ratio of each Aaligned-like aggregate (4 [blue], 5 to 8 [purple], 9 to 16 [green], 17 to 32 [orange], or more than 33 [yellow] cells from bottom to top) at days 1, 3, and 5 post-transplantation. The number in parenthesis above each bar in B shows the total number of GFRα1-positive aggregates examined. (C, D) *In vivo* time-course analyses around the transplanted beads into GFRα1-EGFP-knock-in mouse testis (C, bright field; D, GFP). Plate C shows the bead-transplanted testis just after the transplantation (two right insets, the higher magnified images indicated by broken rectangles). In D, time-course analyses show spatiotemporal changes in GFP (GFRα1)-positive spermatogonia (green) near the GDNF (upper)- and BSA (lower)-soaked beads at days 0, 3, and 5 post-transplantation. Plates D1 and D2 indicate the magnified images of the regions indicated by white arrows in “5d” (D2, the image of the area after removal of the tunica albuginea). Broken circle, bead; broken line, outline of seminiferous tubule; red arrow, Dil-marked site; white arrow, GFP/GFRα1-positive aggregate; white arrowhead, GFP/GFRα1-positive spermatogonia. Scale bar, 100 μm.

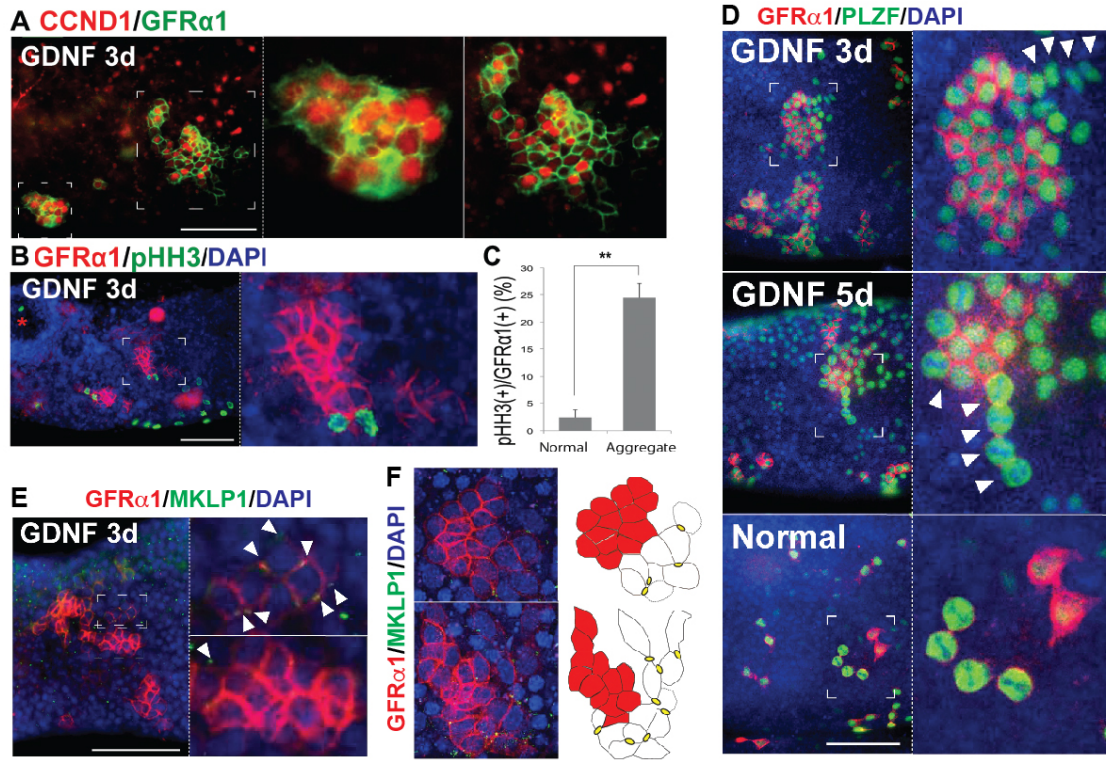


Fig. 2-4. Characterization of GFRα1-positive aggregates induced by GDNF-soaked beads. (A, B) CCND1/pHH3 (red/green) and GFRα1 (green/red) immunohistochemistry of the aggregates at day 3 post-transplantation. (C) A bar graph showing pHH3-positive indices of GFRα1-positive spermatogonia in the aggregates and in the normal healthy region of the same testes (error bars indicate standard error, ** $p < 0.01$). (D) PLZF (green) and GFRα1 (red) immunohistochemistry of the aggregates at days 3 and 5 post-transplantation. The control images in the normal healthy region of the ST are also shown in the lowest plates. PLZF-positive/GFRα1-negative cells are indicated by arrowheads. (E, F) Anti-MKLP1 (green; arrowheads) and anti-GFRα1 (red) double staining of the aggregates at day 3 post-transplantation. Plate F includes the schematic illustrations of the GFRα1-positive aggregates, showing the tightly-compacted A_{single} spermatogonia (red), intercellular bridges marked by MPLK1 (yellow), the marginal A_{paired} to A_{aligned} spermatogonia (white), and surrounding GFRα1-negative cells (broken outline). Broken rectangles in plates correspond to the insets. Scale bars, 100 μm .

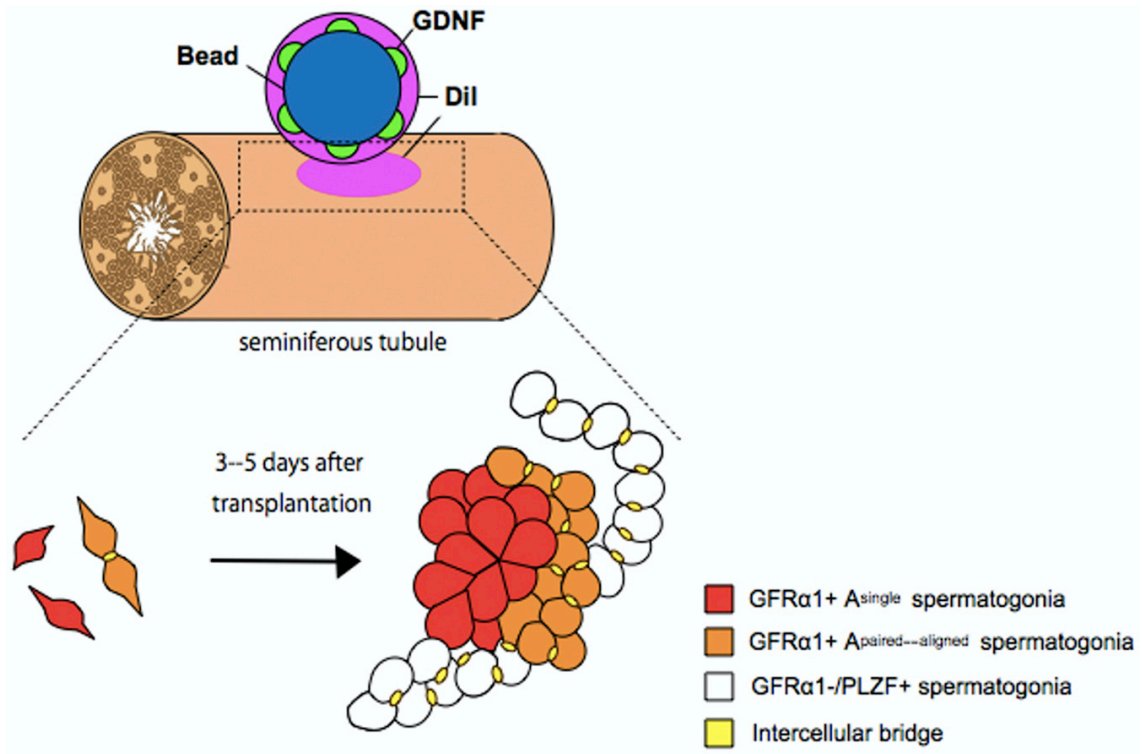


Fig. 2-5. Induction of GFRα1-positive aggregates by GDNF-soaked beads *in vivo*. Transplanted GDNF-soaked beads induced the proliferation of GFRα1-positive A_{undiff} located close to the beads, resulting in the formation of aggregates consisted of GFRα1-positive spermatogonia within 3 to 5 days post-transplantation. While most undifferentiated A_{single} remained at the core part of aggregate, A_{paired} to A_{aligned} spermatogonia appeared at the peripheral region of the aggregated. These GFRα1-positive spermatogonia in the aggregate give rise to GFRα1-negative/PLZF-positive differentiation-prone spermatogonia at the marginal part of the aggregate. This model successfully demonstrated the function of GDNF to induce proliferation of GFRα1-positive spermatogonia, while uncovered the dynamics of spermatogonia temporarily exposed to high dose of GDNF *in vivo*.

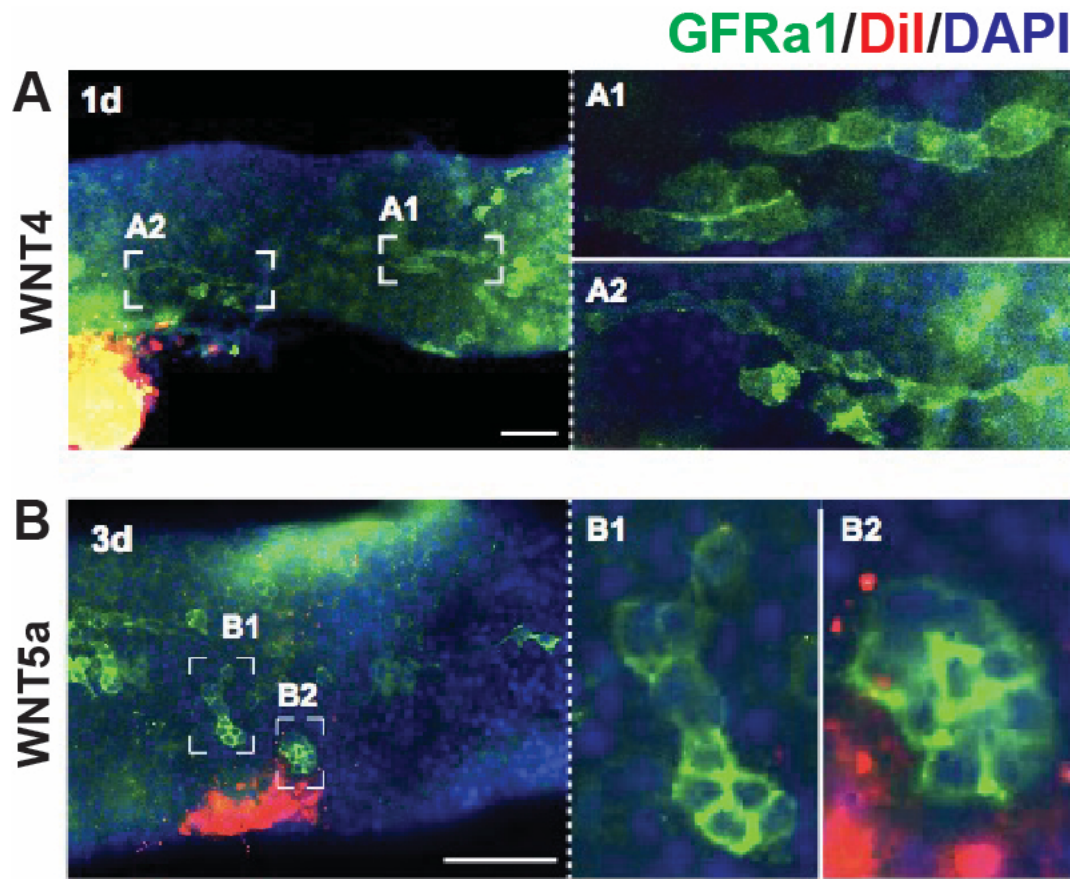


Fig. 2-6. Application of bead transplantation assay for WNT4 and WNT5a.

GFR α 1 immunohistochemistry (green) of the ST located close to the WNT4- (A) and WNT5a- (B) soaked beads. The site attached to the transplanted beads can be distinguished by DiI (red) marks. GFR α 1-positive spermatogonia around the transplanted WNT4-soaked beads were observed to be mostly $A_{aligned}$, extending the cytoplasmic process across the ST at day 1 post-transplantation (A). GFR α 1-positive spermatogonia around the transplanted WNT5a-soaked beads formed aggregates at days 3 post-transplantation (B). A1, A2 and B1, B2 represent a magnified image of the region surrounded by a broken rectangle in the left-most panels. Scale bars, 100 μ m.

Table 2-1. List of antibodies used in this study

Antigen	Dilution	Description	Company	CAT#
CCND1	1/100	Rabbit polyclonal	Thermo Fisher	RM-9104-S1
GDNF	1/100	Goat polyclonal	Santa Cruz	sc328-G
GFP	1/100	Rabbit polyclonal	MBL	M048
GFRa1	1/100	Goat polyclonal	R&D systems	AF560
pHH3	1/100	Rabbit polyclonal	Cell Signaling	9701
PLZF	1/100	Rabbit polyclonal	Santa Cruz	sc22839
MKLP1	1/100	Guinea pig polyclonal	Iwamori <i>et al.</i> , 2011	

3. CHAPTER 2

**“Paracrine signals mediate regionalization of the Sertoli
Valve epithelia”**

3.1 Abstract

A_{undiff} undergo differentiation in response to RA, while their progenitor states are maintained by a series of growth factors including FGFs. The SV serves a closed SSC niche in mammalian testis, of which epithelia constitutively express phosphorylated AKT. By taking advantage of microarray analysis, I revealed regionally distinct gene expression profiles of the RT, SV, and ST in mouse testis. Among these, I appreciated the RT-specific expression of *Fgf9*. The basement membrane of the SV is enriched with HSPG, which is an essential component for the binding of FGFs to their receptors. Exogenous administration of FGF9 in the ST induced ectopic AKT phosphorylation in Sertoli cells in the ST. These data indicate that FGF ligands secreted from the RT might modulate the unique signaling state of the SV. Furthermore, I uncovered SV-specific expression of *Cyp26a1*, which encodes an RA-degrading enzyme. Administration of excess RA at the SV disrupted its pool of SSCs by promoting their differentiation. This data indicates that high RA levels at the SV is sufficient to disrupt SSC niche in the SV. Taken together, FGF ligands secreted from the RT and low levels of RA signaling at the SV region might modulate regionalization of the SV epithelia and its local maintenance of SSCs.

3.2 Introduction

As discussed in the General Introduction, the balance between maintenance and differentiation of SSCs is coordinated by a series of paracrine factors, including FGFs, GDNF and RA in mammalian testis. The SV serves a niche for SSCs in mammalian testis; hence the SV epithelia is mainly composed of GFR α 1-positive spermatogonia and proliferative Sertoli cells with unique signaling states (Aiyama *et al.*, 2015; Nagasawa *et al.*, 2017). However, the molecular mechanism to characterize the Sertoli cells in the SV remains unclear. By using the diphtheria toxin (DT)-treated AMH-Treck Tg male mice with Sertoli cell-ablated STs, Imura-Kishi *et al.* (2021) also revealed the non-cell autonomous construction of the SV by the transplanted Sertoli cells located adjacent to the RT. This data suggests the possibility that paracrine signals derived from the RT contribute to the regionalization of SV epithelia. However, mechanism of its regional specificity and homeostasis still remain to be discovered.

Hereafter, I revealed unique molecular characteristics of the SV and RT by performing microarray analysis. By taking advantage of bead transplantation assay developed in Chapter 2, I demonstrated the ability of FGF9 to induce AKT phosphorylation in Sertoli cells. I further utilized the bead transplantation

assay to administrate RA around the SV region and discovered that low RA levels in the SV is crucial for its maintenance of SSC niche. This study provides first direct evidence that paracrine signals in the SV modulate its characteristic feature of the Sertoli cells and regulate the distribution pattern of spermatogonia therein *in vivo*.

2.3 Materials & Methods

Animals

Wild-type mice (C57BL/6 and ICR mice) and *W/W^v* mice (SLC Japan) were used in this study. All animal experiments were performed in accordance with Guidelines for Animal Use and Experimentation at the University of Tokyo, and all the experimental procedures herein performed were approved by the Institutional Animal Care and Use Committee, Graduate School of Agricultural and Life Sciences, The University of Tokyo (approval IDs, P13-762 and P13-764).

In vivo treatment of exogenous FGF9 and retinoic acid

For FGF9 treatment, FGF9 (0.1 mg/ml, R&D systems)-soaked beads (Affi-gel blue, Bio-Rad, ~50 μ m) were injected into the interstitial regions of 7-week-old *W/W^v* mouse testes as previously reported (Masaki *et al.*, 2018; Uchida *et al.*, 2016). The beads were labeled with DiI prior to the transplantation, which makes it distinguishable in the section. At 2–24 hours after the bead treatment, testes were isolated for the subsequent histology and immunohistochemical analyses. For RA treatment, wild-type male mice (ICR, 7–8 weeks old) were injected with beads (BioMag Amine) soaked in all-trans RA (40 mg/ml; Sigma-Aldrich) in 16% (vol/vol) dimethyl sulfoxide (DMSO) or DMSO (Fig. 3-5A). In this experiment, the beads were injected locally around the SV region (Fig. 3-5A) to examine the effects of locally elevated RA levels on the SV function. At 1 and 3 days after the treatment, testes were isolated for subsequent histology and immunohistochemical analyses.

Isolation of the tubular fragments from the RT, SV, and ST

To visualize the RT, SV and ST at the proximal part of the testis, trypan blue solution (0.4%; Sigma-Aldrich) was micro-injected through the efferent ducts into the testes of *W/W^v* mutant mice or wild-type ICR mice at 7 weeks of age (Fig. 3-1A). Tunica albuginea was then removed from the testes, and the RT, SV and distal convoluted ST fragments were isolated manually by using sharp forceps and 31G needles under a dissecting microscope. RT samples were collected from the main part just beneath the tunica

albuginea, and SV samples were collected as tiny, tubular fragments (< 1 mm) adjacent to the RT. ST samples were collected from the distal part of the testis far apart from the RT and SV regions. The border of the RT and SV regions were distinguishable by their distinct tubular diameters with different intensities of the trypan blue color. Of note, as a limitation of this study, it is highly likely that SV fragments contained a certain amount of the RT-derived cells due to the continuous tubular structure of the RT and SV regions. The samples were then subjected to the RNA analyses.

Immunohistochemistry and morphometry

The testes were fixed in 4% PFA and routinely embedded into paraffin or OCT compound. Cryosections (8 µm thickness) or deparaffinized sections (5 µm thickness) were subjected to immunohistochemical staining as described previously (Kishi *et al.*, 2017). The sections were incubated with primary antibodies listed in Table 3-1, and reactions were visualized by incubation with Alexa-488/594 conjugated secondary antibodies (Molecular Probes) or biotin-conjugated secondary antibodies with the Elite ABC Kit (Vector Laboratories, CA). For anti-p-AKT antibody, Alexa Fluor 488 Tyramide Signal Amplification kit (Invitrogen) was used to visualize the reaction. To verify antibody specificity for phosphorylated AKT, two serial sections were pretreated with or without alkaline phosphatase from calf intestine (ALP; #47785055; Oriental Yeast) at 34 °C for 1 hour before incubation with the primary antibody.

For whole-mount immunohistochemistry, SV and ST fragments were carefully isolated and fixed in 4% PFA. After methanol permeabilization, the fragments were incubated for 12 hours at 4 °C with anti-c-KIT (1:100 dilution; R&D Systems), anti-GFR α 1 (1:100 dilution; R&D Systems) or anti-RAR γ (1:100 dilution; Cell Signaling) antibody. After washing with PBS, samples were incubated for 2 hours at room temperature with Alexa-488/594 conjugated secondary antibodies, including DAPI. Stained whole-mount samples were photographed, and the numbers of GFR α 1-positive/RAR γ -negative, GFR α 1-positive/RAR γ -positive and c-KIT-positive cell were quantified respectively in the proximal part of SVs (*i.e.*, 0 ~ 50 µm apart from the edge of the rete testis) as previously shown (Aiyama *et al.*, 2015). Of note, in wild-type mice, a proportion of RAR γ -positive cells out of total GFR α 1-positive spermatogonia in the SV region was at $20.1 \pm 7.2\%$, similar to $21.3 \pm 7.8\%$ in the convoluted ST region. All of the stained samples were analyzed using an Olympus fluorescence microscope (BX51N-34-FL-2) and a Leica TCS SP8 (Leica Microsystems GmbH) confocal laser microscope. In addition, any non-specific signals inside the STs were detected in sections incubated with normal IgG instead of the primary antibody (data not shown).

In situ hybridization

The transcript levels in deparaffinized sections of *W/W^v* and wild-type testes were determined using the RNAscope Target Probes listed in Table 3-2 with RNAscope 2.5 HD Reagent Kit-RED system (ACDBio) according to the manufacturer's instruction.

3.4 Results

Regionally distinct gene expression profiles of the RT, SV, and ST in mouse testis

To dissect gene expression signature in the SV, RT, and ST, I first performed microarray analyses in this study. The RT, SV, and convoluted ST fragments were manually separated from adult *W/W^v* mice upon intratubular trypan blue injection (Fig. 3-1A), and then subjected to the microarray analyses (20 testes for each set of microarrays: 3 sets for RT, 4 sets for SV and ST). The transcriptomic analysis resulted in the identification of 623 and 2,304 upregulated probes in the SV and RT respectively, compared to the convoluted ST (> two-fold change with $p < 0.05$). Since 512 probes were commonly upregulated in the RT and the SV, 111 probes were identified as SV-specific probes, which are exclusively expressed in the SV region (Fig.3-1B). Gene ontology (GO) analysis of 111 SV-specific probes suggested the terms “retinoic acid metabolic process” (e.g., *Cyp26a1*, *Rbp1*; $p = 7.4E^{-02}$), “positive regulation of protein phosphorylation” (e.g., *Il34*, *Camp*, *Gpnmb*, *Ptpn5*; $p = 6.9E^{-02}$), “detection of mechanical stimulus involved in sensory perception” (e.g., *Asic2*, *Serpine2*; $p = 2.5E^{-02}$) and “positive regulation of cell proliferation” (e.g., *Il34*, *Sfrp1*, *Ctsh*; $p = 2.5E^{-02}$). On the other hand, GO analysis of 1792 RT-specific genes identified by microarray analyses yielded the terms “positive regulation of epithelial cell proliferation” (e.g., *Fgf1*, *Fgf9*, *Bmp4*, *Notch1*, *Igf1*, *Vegfa*; $p = 7.8E^{-06}$), “Wnt signaling pathway” (e.g., *Wnt7b*, *Wnt9a*; $p = 1.5E^{-02}$) and “Wound healing” (e.g., *Tgfa*, *Cx3cl1*; $p = 4.4E^{-02}$). These results suggest the secretion of various signaling factors in the RT region, which may affect the terminal end of the ST to obtain its unique phenotypes. Differentially expressed gene (DEG) analysis revealed the regionally distinct gene expression profiles between the RT, SV, and ST ($p < 0.01$, Fig. 3-1C). Among the RT-specifically upregulated genes (represented as green dots in Fig. 3-1D), I appreciated *Fgf9*, which is one of the growth factors activates AKT pathway in testicular somatic cells (Lai *et al.*, 2014; Yang *et al.*, 2021). On the other hand, among the SV-specifically upregulated genes (represented as red dots in Fig. 3-1E), I identified *Cyp26a1* as the most significantly upregulated gene with top fold

change (Fig. 3-1E). Since *Cyp26a1* encodes a cytochrome P450 enzyme which controls the metabolic inactivation of RA (Hogarth *et al.*, 2015), SV-specific expression of *Cyp26a1* implies unique RA metabolism within the SV region.

Expression profile of FGF-related genes and its potential contribution to the AKT phosphorylation in Sertoli cells.

Noting the SV-specific AKT phosphorylation (Imura-Kishi, 2019), I then asked which signaling molecule contributes to the local AKT activation. The microarray data suggested upregulation of several genes encoding growth factors in the RT, suggesting the possibility that the RT-derived signaling molecules induce the local activation of AKT in the SV region. Based on the previous study showing the SV-specific HSPG enrichment in hamsters (Aiyama *et al.*, 2015), I hypothesized that HSPG, which functions as a reservoir and co-receptor of FGF ligands (Matsuo & Kimura-Yoshida, 2013), modulates the SV-specific AKT activation through its local storage and reception of ligands produced by the RT. To test this hypothesis, I focused on FGFs as a potential upstream of AKT activation at the SV. I first confirmed the enrichment of HSPG in the basement membrane of the SV region in adult wild-type mouse testis (Fig. 3-2A), which is consistent with the previous work done in hamster (Aiyama *et al.*, 2015). HSPG was observed predominantly in the SV region, while the RT region marked by ECAD (also known as CDH1) immunoreactivity only showed little expression of HSPG (Fig. 3-2A'). I then examined the gene expression levels of FGF ligands and their receptors in RT, SV, and convoluted ST of both wild-type ICR mice and germ-cell-depleted *W/W^v* mice. qRT-PCR analyses confirmed that the expression levels of *Fgf9* and *Fgf10* were significantly higher in the RT compared to the convoluted ST in wild-type mice (Fig. 3-2B). The expression levels of *Fgf9* were significantly higher in the RT also in the *W/W^v* mutant mice, suggesting that its region-specific difference is not due to the existence of germ cells (Fig. 3-2B). Next, I examined the mRNA expression levels of two major FGF receptor genes in Sertoli cells, *Fgfr1* and *Fgfr2* (Zimmermann *et al.*, 2015). As a result, *Fgfr2* was expressed significantly higher in the RT and SV region compared to the ST region both in *W/W^v* and wild-type mice (Fig. 3-2B). *Fgfr1* expression in the SV was significantly higher in the *W/W^v* mice, but not in wild-type mice potentially due to the contamination of germ cells (Fig. 3-2B). I further performed *in situ* hybridization in wild-type mice to confirm the localization of mRNA in each gene. As a result, the expression of *Fgf9* was detected in the RT region, while hardly any *Fgf9* signals were observed in SV and ST regions (Fig. 3-2C). On the other hand, both *Fgfr1* and *Fgfr2* mRNA were detected both in the SV and RT (Fig. 3-2C). While the expression of *Fgfr1* was rather observed in Sertoli cells located at the SV, signal intensity of *Fgfr2* was

observed rather strongly at the RT epithelia (Fig. 3-2C). Such co-expression of HSPG and FGFRs in the SV region suggests the potential binding and activation of FGFs within the SV region.

AKT phosphorylation in Sertoli cells induced by exogenous application of FGF9

To investigate the correlation between FGF signaling and AKT phosphorylation at the SV region, I next examined the effect of exogenous FGF9 on the p-AKT signals in convoluted seminiferous tubules by using an *in vivo* bead transplantation assay developed in Chapter 2 (Uchida *et al.*, 2016). In this experiment, *W/W^v* mutant mice were used to exclude the effect of FGF9 on germ cells. In the absence of germ cells, p-AKT signals were observed sporadically in the convoluted seminiferous tubules of the *W/W^v* mutant mice (Fig. 3-3A), which is in consistent with the observation made in wild-type mice (Imura-Kishi, 2019; Imura-Kishi *et al.*, 2021). However, signal intensity of such p-AKT was relatively weak compared to that in the SV (Fig. 3-3B), and not all the Sertoli cells within the cross-sectioned seminiferous tubules expressed p-AKT in the *W/W^v* mutant mice (Fig. 3-3A). As described in Chapter 2, I transplanted FGF9-soaked beads into the testicular interstitium of *W/W^v* mutant mice and examined the phenotype of seminiferous tubules located close to the transplanted beads at day 1 post-transplantation (Fig.3-3C). As a result, p-AKT signals were greatly increased in the convoluted ST adjacent to the transplanted FGF9-soaked beads, but not in the ST far away from the FGF9-soaked beads nor the ST adjacent to the BSA-soaked beads (Fig. 3-3D). These findings suggest the possible contribution of FGF-FGFR signaling to the SV-specific expression of p-AKT.

Expression profile of RA-related genes and its potential contribution to the SSC niche at the SV

The microarray data suggested region-specific high expression levels of a gene encoding RA-metabolizing enzyme, *Cyp26a1*, at the SV region. It was also confirmed by qRT-PCR that the SV express *Cyp26a1* at significantly higher levels compared to the RT and the ST (Fig.3-4A). To reveal the regional expression pattern of *Cyp26a1*, I next performed *in situ* hybridization on the testis section of both wild-type and *W/W^v* mutant mice. Being consistent with the microarray data, *in situ* hybridization confirmed the region-specific expression of *Cyp26a1* in Sertoli cells located within the SV region both in *W/W^v* mice and wild-type mice (Fig.3-4B, C). These data indicate constitutively high *Cyp26a1* expression in the Sertoli cells within SV region irrespective of the presence of spermatogenic cells. On the other hand, the expression of *Cyp26b1*, which encodes another RA degradation enzyme, was expressed rather in the ST compared with the RT and the SV (Fig. 3-4A). *In situ* hybridization revealed that *Cyp26b1* signals were

mainly observed in the peritubular myoid cells outlining SV and ST as reported previously (Parekh *et al.*, 2019), as well as in Sertoli cells located within the SV region (Fig. 3-4B). Meanwhile, the expression levels of *Aldh1a1* and *Aldh1a2*, which encode RA-synthesis enzymes, did not differ markedly among the RT, SV, and ST (Fig. 3-4A). Indeed, in situ hybridization revealed the similar expression levels of *Aldh1a1* and *Aldh1a2* in the RT, SV, and ST epithelia in *W/W^v* mice (Fig.3-4E). Meanwhile, in wild-type mice, *Aldh1a2* signals were observed at high levels in germ cells located in the luminal compartment of the seminiferous tubules (Fig.3-4F). This is consistent with the qRT-PCR result shown in Fig.3-4A, in which wild-type ST with active spermatogenesis expressed *Aldh1a2* higher than *W/W^v* mice (Fig. 3-4A). These data indicate the ubiquitous RA synthesis across the RT, SV and ST, in comparison with the SV region-specific RA degradation mediated by its local *Cyp26a1* expression.

Exogenous RA disrupted SSC niche at the SV

Finally, I examined the effect of exogenous RA on the structure and function of the SV region in wild-type mouse testes (Fig. 3-5A). In this experiment, I transplanted RA-soaked microbeads locally around the SV region to temporarily increase the local RA levels (Fig. 3-5A). Being consistent with the previous report, control (DMSO-treated) mouse testes had hardly any c-KIT-positive A_{diff} within the proximal part of the SV region (0 ~ 50 μm from the edge of rete testis), where $GFR\alpha 1$ -positive/c-KIT-negative A_{undiff} were constitutively maintained (Fig. 3-5B). On the other hand, RA-treated mouse testes showed a reduced number of $GFR\alpha 1$ -positive A_{undiff} within the proximal SV region (Fig. 3-5B, C; “ $GFR\alpha 1$ +Total” in Fig. 5E), while c-KIT-positive A_{diff} were enriched within the SV region at day 1 after the RA treatment (Fig. 5B, D; “c-KIT+” in Fig. 3-5E). Since $RAR\gamma$ -positive subpopulation was previously shown to maintain the differentiation competence of $GFR\alpha 1$ -positive spermatogonia (Ikamii *et al.*, 2015; Velte *et al.*, 2019), I then quantified the $RAR\gamma$ -negative/positive subpopulation of $GFR\alpha 1$ -positive cells in the proximal SV region treated with RA and DMSO respectively. As a result, I found a drastic reduction of $RAR\gamma$ -positive subpopulation (13.0% of the control value) together with a mild reduction of a $RAR\gamma$ -negative subpopulation (51.4% of the control value) in the RA-treated group ($n=5$, two right graphs in Fig. 3-5E). These findings suggest that the c-KIT-positive spermatogonial patches observed at the proximal SV region in the RA-treated mice may have resulted directly from the A_{undiff} - A_{diff} transition of pre-existing $GFR\alpha 1$ / $RAR\gamma$ -double positive spermatogonia by the exogenous exposure to excess RA. Interestingly, in some severely affected SVs at day 3 after RA treatment, the ace-TUB-positive valve-like structures were disrupted (Fig. 3-5F). This data implies that the suppression of active spermatogenesis at the SV contribute to the maintenance of its valve-like structure. Of note, RA treatment

did not seem to affect the expression of GDNF and CCND1 in the Sertoli cells located within the SV region (Fig. 3-6), which are other characteristics of the SV region (Aiyama *et al.*, 2015). These data suggest that low RA levels in the SV region support the maintenance of its niche for A_{undiff}, as well as its valve-like structure.

3.5 Discussion

In the fetal mouse testes, FGF9 was previously shown to induce the proliferation of Sertoli cells through FGFR2 (Colvin *et al.*, 2001; Schmahl *et al.*, 2004; Kim *et al.*, 2007). FGF9, as well as FGF10, is upregulated in a testis-specific manner by 11.5 dpc and contributes to synchronous testiculogenesis of the pre-Sertoli cells in the fetal testes (Hiramatsu *et al.*, 2010). Concomitantly with the onset of *Fgf9* expression, testis-specific AKT activation also takes place in presumptive pre-Sertoli cells at 11.5 dpc (Matoba *et al.*, 2005), suggesting a potential association between FGF9 signals and p-AKT activation in the developing fetal testes. The present study demonstrated the increased p-AKT signals in Sertoli cells of the ST caused by exogenous FGF9 administration (Fig. 3-3C, D). Since FGF9 is known to activate the PI3K/AKT pathway as well as MEK/ERK pathway (Cotton *et al.*, 2008), RT-derived FGF9 can be associated with the activation of AKT signals in the Sertoli cells located within the SV region. Interestingly, the basement membrane at the SV region has the region-specific enrichment of HSPGs, which works as a reservoir for several FGF ligands (Matsuo & Kimura-Yoshida, 2013). Therefore, it might be possible that the RT-derived FGFs bind to the HSPGs at the SV region and subsequently cause signal transduction via local FGFRs. Since FGF9 is known to work over a short-range (Matsuo & Kimura-Yoshida, 2013), and the SV region is adjacent to the RT, I assume that Sertoli cells in the SV can perceive the RT-derived FGF9. Taken together, RT-derived FGF ligands and their local perception through the HSPG can be one of the causes for the activation of AKT within the SV region. Microarray analyses revealed the high expressions of various cytokine and growth factor genes in RT, including those encoding candidate ligands upstream of AKT/STAT3 signaling, such as FGF9, suggesting their potential contribution to non-cell autonomous specification and regionalization of the SV epithelia *in vivo*. Meanwhile, the microarray analysis indicated the expression of various cytokines and growth factor genes in the RT region aside from FGF9, which can also be candidate ligands upstream of AKT/STAT3 signaling. Therefore, a further study on such ligands is required to comprehensively understand the RT-derived stimuli, which play a role in the non-cell autonomous regionalization and the constitutive p-AKT/p-STAT3 activation of the SV epithelia *in vivo*.

It is traditionally known that FGFs and RA signaling acts in an opposing manner in the regionalization of various organs such as limb, neural pattern, segmentation, and somite formation (Diez del Corral *et al.*, 2003; Goldbeter *et al.*, 2007; Cunningham *et al.*, 2013). In fetal and postnatal testes, FGF9 antagonizes RA-dependent meiotic differentiation of germ cells in part by maintaining Nanos2 expression (Bowles *et al.*, 2010; Barrios *et al.*, 2010; Tassinari *et al.*, 2015). In adult testes, FGFs maintain the self-renewal of stem/progenitor spermatogonia independent of GDNF signals (Kitadate *et al.*, 2019; Takashima *et al.*, 2015), while RA deficiency supports the A_{undiff} to retain their progenitor state *in vivo* (Griswold, 2016; Busada *et al.*, 2015; Agrimson *et al.*, 2017). FGFs including FGF5 were shown to be produced by the lymphatic endothelial cells around the seminiferous tubule to support A_{undiff} (Kitadate *et al.*, 2019). Considering that lymphatic vessels from convoluted STs join together around RT and SV regions (Svingen *et al.*, 2012), the source of the FGF ligands in the RT can be its epithelial cells as well as its surrounding lymphatic tissue. Similarly, excess expression of a niche factor, GDNF, represses the differentiation of A_{undiff}, leading to inactive spermatogenesis *in vivo* (Meng *et al.*, 2000; Uchida *et al.*, 2016; Yomogida *et al.*, 2003; Savitt *et al.*, 2012). Since GDNF is also highly expressed in the SV region (Aiyama *et al.*, 2015), GDNF and FGFs may contribute to the structure of SV epithelia by suppressing the differentiation of local A_{undiff} in rodent testes.

RA has been reported to be dispensable for the meiotic initiation of the germ cells (Kumar *et al.*, 2011; Vernet *et al.*, 2020; Teletin *et al.*, 2019), whereas injection of exogenous RA promotes the differentiation of A_{undiff} *in vivo* (Endo *et al.*, 2015). Similarly, in the present study, local administration of exogenous RA promoted the ectopic appearance of c-KIT-positive A_{diff} in the SV region. Together with the SV-specific expression of *Cyp26a1*, it is reasonable to speculate that the levels of RA in the SV region are maintained low, preventing the A_{undiff} to A_{diff} transition of the local spermatogonia within the SV region. Considering that another RA metabolizing enzyme, *Cyp26b1*, expresses in the peritubular myoid cells to block the entry of interstitial RA into the seminiferous tubules (Vernet *et al.*, 2006; Parekh *et al.*, 2019), *Cyp26a1* in the SV region may also function as a local catabolic barrier insulating the A_{undiff} from RT-derived RA. Since *Cyp26a1*-null mutant mouse testes were reported to have no appreciable defects in the convoluted ST (Hogarth *et al.*, 2015), the compensational roles of *Cyp26a1* and *Cyp26b1* in the SV region cannot be neglected, yet their detailed phenotypes of the SV remain unclear. Meiotic germ cells express *Aldh1a1-3*, which make the germ cell one of the major sources of RA in the testis (Endo *et al.*, 2015), and the lack of meiotic germ cells in the SV region can also be a cause for the low-level RA within the SV region. Although RA is synthesized by both Sertoli cells and germ cells, germ cell-derived

RA has been reported to play important roles in the A_{undiff} to A_{diff} transition of spermatogonia at the initial onset of spermatogenesis (Endo *et al.*, 2015). Taken together, the lack of meiotic germ cells within the SV region contributes to its local low RA signaling state, in combination with the local degradation of RA by *Cyp26a1* expression.

In the proposed model, the specification and regionalization of the SV epithelia are non-cell autonomously mediated by the factors derived from the RT, resulting in the AKT phosphorylation in the SV Sertoli cells (Fig. 3-7). Particularly, FGFs (e.g., FGF9) may contribute to the maintenance of A_{undiff} in the SV region, through its region-specific enrichment of HSPG in the basal lamina. Moreover, the high expression of *Cyp26a1* in the SV region leads to the region-specific low-RA signaling states, which may promote the maintenance of GFR α 1-positive A_{undiff} and repress their differentiation into c-KIT-positive A_{diff} . A lack of differentiated germ cells (*i.e.*, c-KIT-positive A_{diff} and meiotic/post-meiotic germ cells) may also physically allow the formation of unique Sertoli cell morphology within the SV region, extending the cytoplasmic processes into the adluminal compartment to form the valve-like structure within the SV region. In this study, exogenous RA treatment induced the ectopic appearance of c-KIT-positive A_{diff} patches within the SV, which could be differentiated from the pre-existing GFR α 1/GFR γ 1-double positive A_{undiff} within the SV region or recruited from the proximal ST region adjacent to the SV. Such aberrant accumulation of c-KIT-positive cell patches protruding into the luminal side might have contributed to the disruption of valve-like structure of the SV. Considering the potential contribution of meiotic germ cell-derived RA for the initial A_{undiff} to A_{diff} progression of the progenitor cell population (Savitt *et al.*, 2012), the lack of advanced spermatogenic cells within the SV region may be also crucial for the physical and endocrinological maintenance of the SV epithelia.

Although the existence of the SV region has been recognized for half a century, the majority of its functionality and molecular mechanisms remain unknown. This study provided the first direct evidence of non-cell autonomous regionalization of mouse SV epithelia, as well as its unique gene expression profile. A further study on SV-specific genes may resolve the molecular mechanisms underlying the functional and biological significances of the SV region, as well as the SSC niche in mammals.

3.6 Figures & Tables

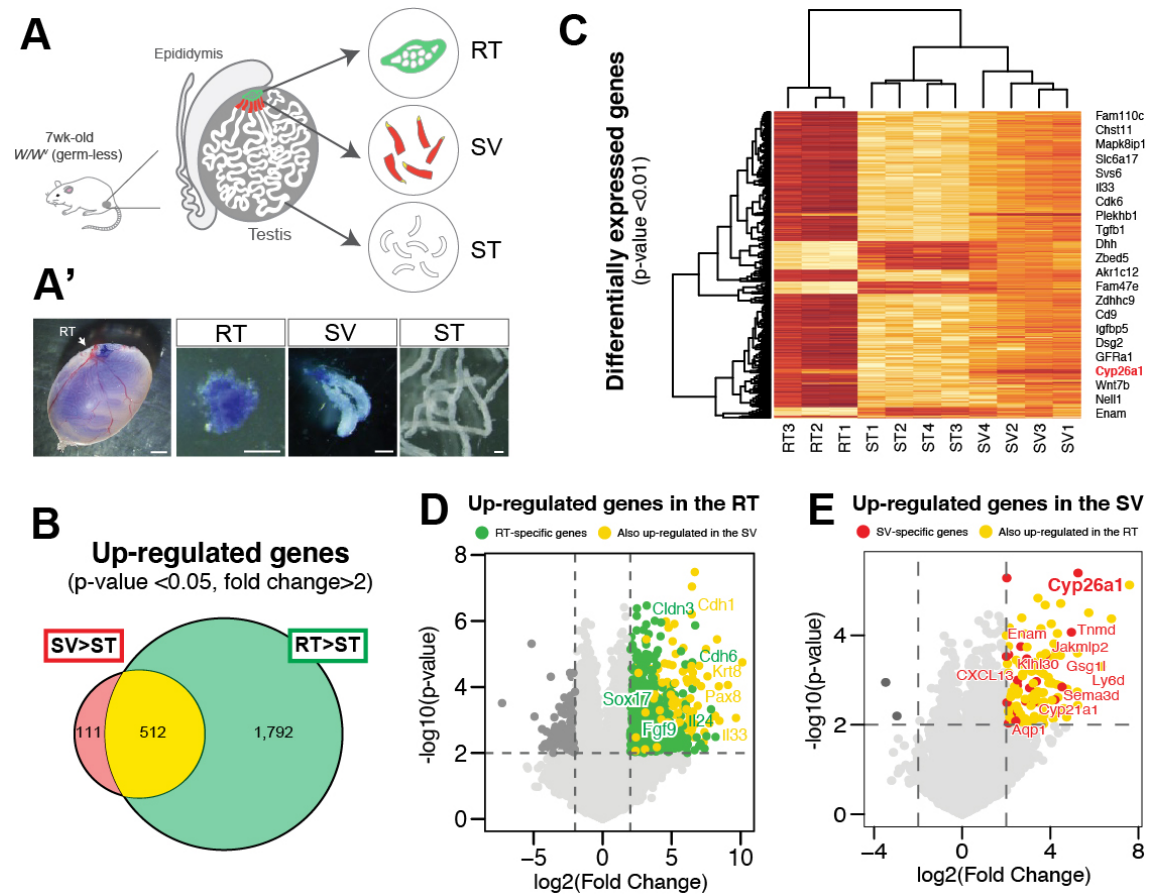


Fig. 3-1 Regionally distinct gene expression profiles of the RT, SV, and ST.

(A) Schematics illustration (A) and gross morphology (A') of the *W/W^v* mutant mouse testis injected with trypan blue dye, and the RT, SV and ST fragments isolated from the testis. 20 testes were used for each set of microarrays, and I subjected 3 sets of the RT and 4 sets of the SV and the ST for the microarray analysis. (B) Venn diagrams of the probes highly expressed in the SV (623 genes) and the RT (2,304 genes) compared to the ST (> twofold changes with p-value < 0.05). 111 probes were exclusively expressed in the SV region, which can be regarded as the SV-specific probes. (C) Heatmap representation of 862 DEGs with p-value < 0.01. (D, E) Volcano plot of log₂ Fold Change (x-axis) and -log₁₀ p-value (y-axis) of the RT (D) and the SV (E) in comparison with the ST. Red dots represent the genes exclusively expressed in the SV, while orange dots represent the genes which also express in the RT. Scale bars, 1mm (left-most panel) 200μm (right three panels) in A'.

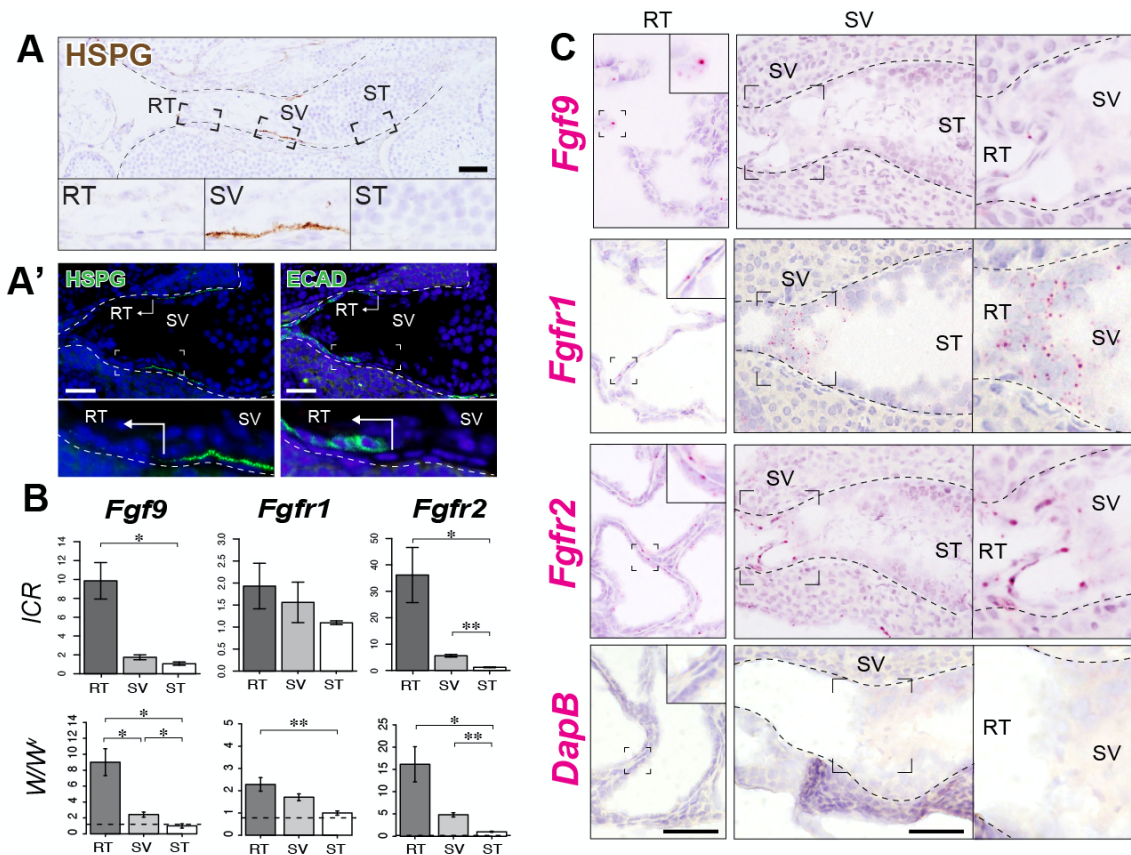


Fig. 3-2 Expression profiles of FGF-associated genes in the RT and the SV. (A) HSPG

immunohistochemistry (brown in A, green in the left plate of A'), showing high HSPG expression in the basement membrane of the SV region, compared to those in the convoluted ST and the RT marked by ECAD (E-cadherin; Cadherin-1) immunohistochemistry (green in the right plate of A'). **(B)** qRT-PCR analysis of *Fgf9*, *Fgfr1* and *Fgfr2* in the RT, SV, and convoluted ST fragments from wild-type ICR (n = 4) and *W/W^v* mice (n = 5). Analysis was performed using a two-tailed paired t-test. *p < 0.05; **p < 0.01. Broken horizontal lines in B, expression levels of each gene in the wild-type convoluted ST with active spermatogenesis. **(C)** *In situ* hybridization images of wild-type mouse testis, showing the signals of *Fgf9* in the RT, and *Fgfr1* and *Fgfr2* in both the RT and the SV. *DapB* was used as a negative control probe, showing little non-specific staining in the RT and the SV region. RT rete testis, SV Sertoli valve, ST seminiferous tubule. Scale bars represent 50 μm.

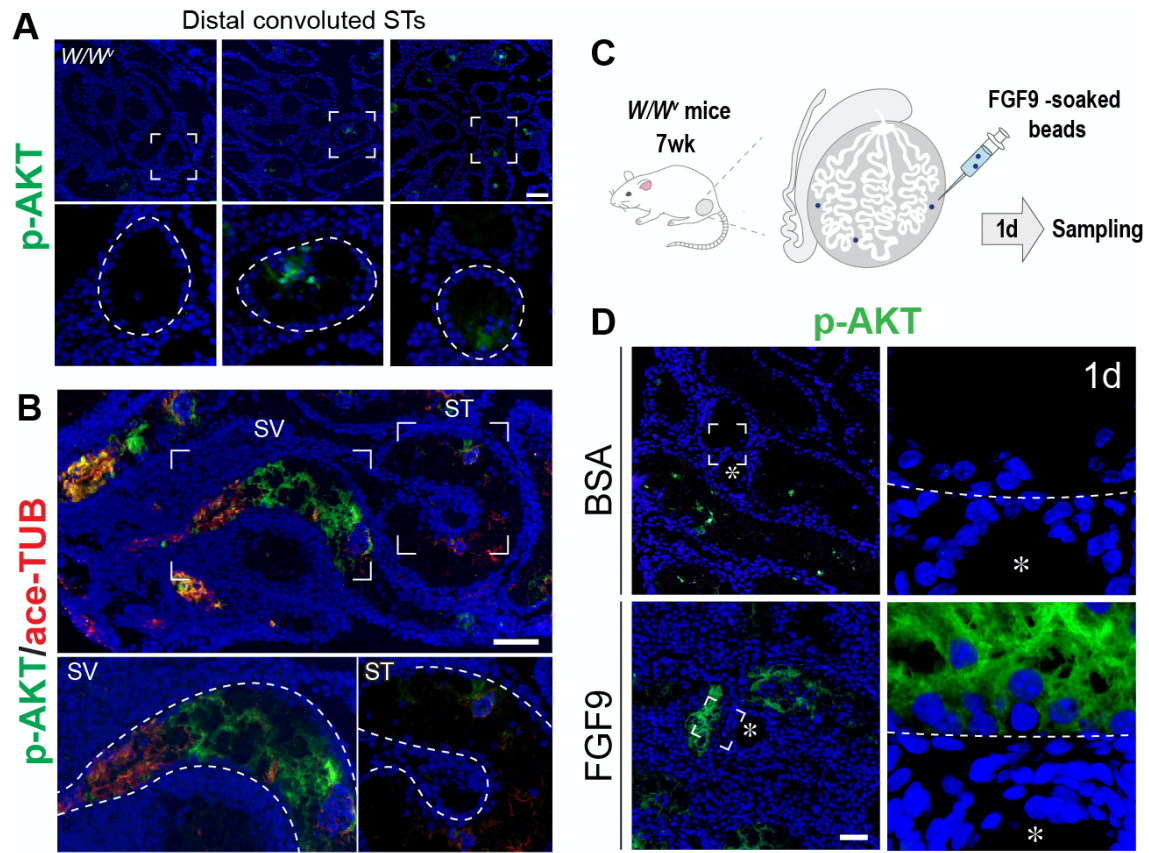


Fig. 3-3 AKT activation of Sertoli cells exposed to FGF9 in W/W^v mice

(A, B) p-AKT staining (green) and anti-ace-TUB staining (red) immunohistochemistry, showing sporadic expression patterns of p-AKT in the Sertoli cells of convoluted STs (A), in contrast to high expression levels of p-AKT around the SV region marked by ace-TUB immunohistochemistry (B). Three panels in A represent the convoluted STs from distal parts of the testis of three independent W/W^v mice. Lower panels in A and B show magnification of the region surrounded by the broken rectangle in the upper panels. (C) A schematic illustrating the experimental model. (D) p-AKT immunohistochemistry (green) of W/W^v mutant mouse testis at 24 hours after FGF9-soaked bead transplantation, showing an ectopic appearance of p-AKT signals in the ST close to the transplanted FGF9-soaked bead (asterisk), which is not observed in the tubules far away from the bead or near BSA-soaked beads (asterisk). The right-most panel in D shows the magnified image of the p-AKT-positive Sertoli cells indicated by the broken square. Asterisk, bead; Broken line, tubular wall; SV, Sertoli valve; ST, seminiferous tubule. Scale bars represent 200 μm in A–B, 50 μm in D.

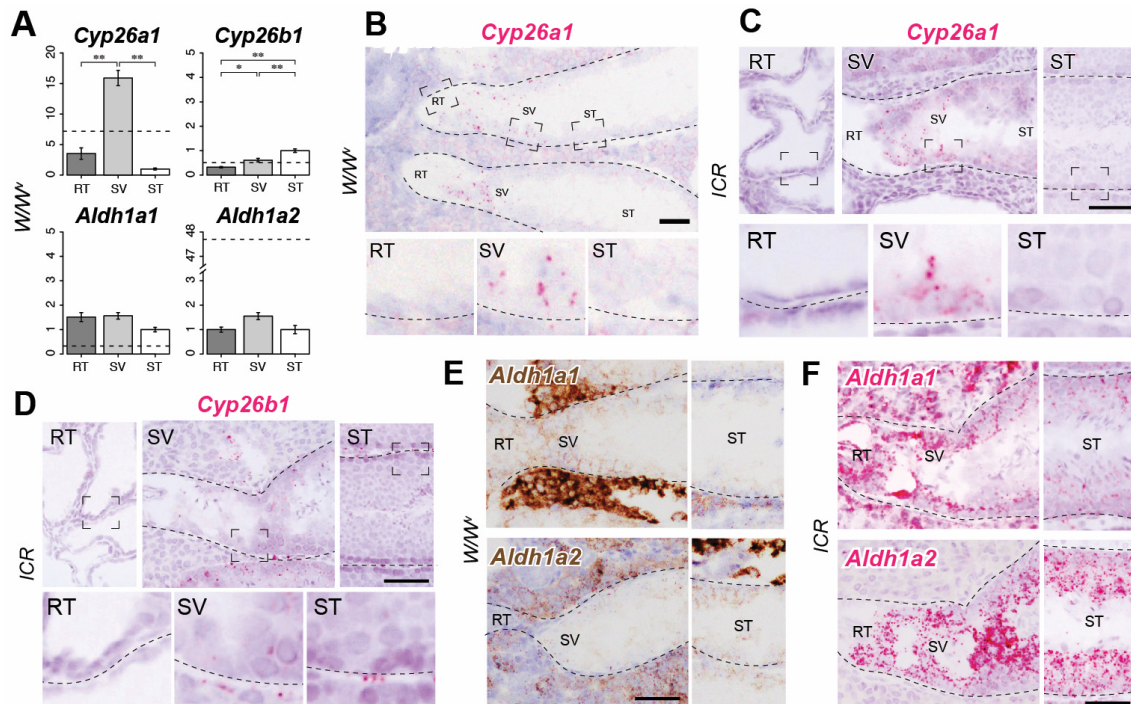


Fig. 3-4 Expression profiles of RA-associated genes in the RT and the SV.

(A) qRT-PCR analysis of *Cyp26a1*, *Cyp26b1*, *Aldh1a1* and *Aldh1a2* in the RT, SV, and convoluted ST fragments from wild-type ICR (n = 4) and *W/W^v* mice (n = 5). Data are mean \pm s.e.m. Two-tailed paired *t*-test. **p* < 0.5, ***p* < 0.01. (B–F) *In situ* hybridization of *Cyp26a1* (B–C), *Cyp26b1* (D), *Aldh1a1* and *Aldh1a2* (E, F) in *W/W^v* (B) and wild-type (C) mouse testes. In B–D, lower panels show magnification of the area indicated by broken rectangles in the upper panels. Broken line, tubular wall; RT, Rete testis; SV, Sertoli valve; ST, seminiferous tubule. Scale bars represent 50 μ m.

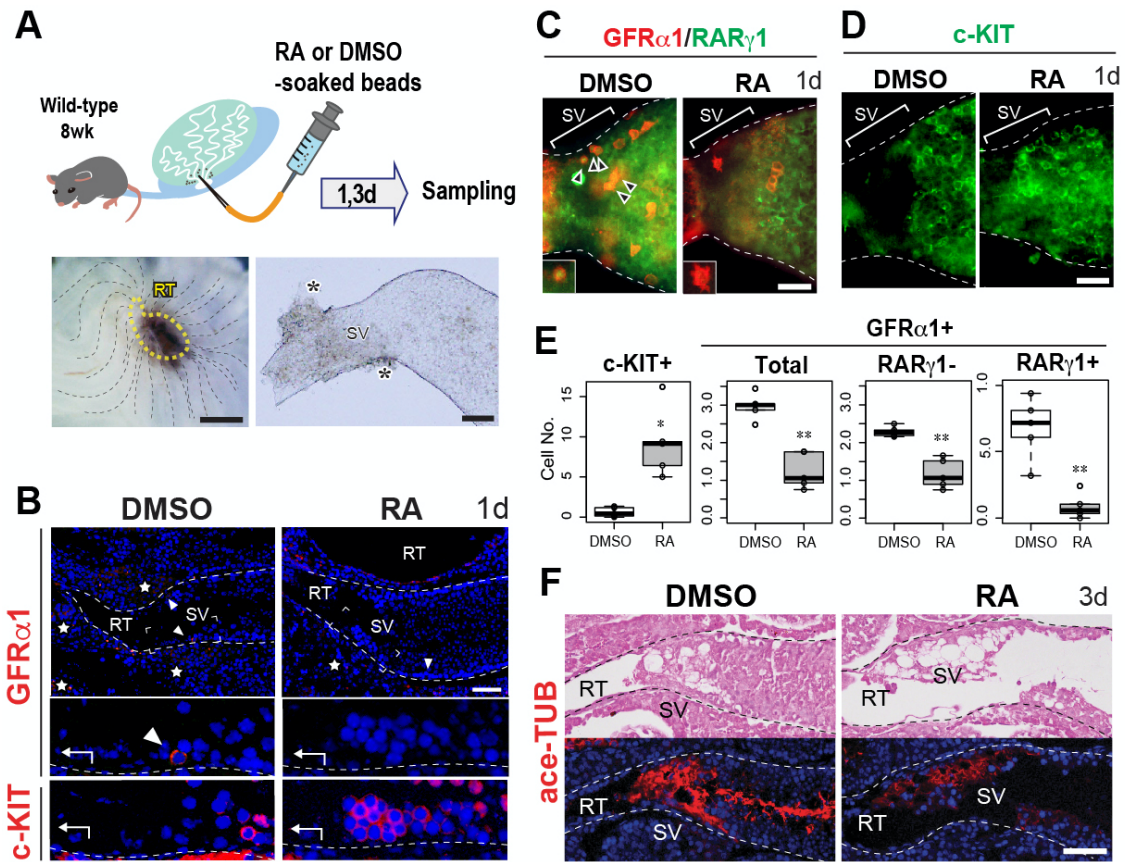


Fig. 3-5 RA-induced ectopic appearance of A_{diff} patches and the valve structure destruction in the SV. (A) Schematic representation of RA or DMSO (control)-soaked beads treatment. Left bottom panel shows the gross morphology of the testis removed of tunica albuginea, transplanted with the beads (brown) locally around the SV region, beneath the RT region indicated by the yellow broken line. Right bottom panel shows the image of an isolated SV fragment, around which the beads are attached (brown, arrows). The phenotypes of the SV epithelia were examined at day 1 (B–E) and day 3 (F) after RA treatment ($n = 4$ each). (B) Anti- $GFR\alpha1$ (red, arrowheads) and anti- $c-KIT$ (red) staining of the serial sections of the SV region, showing an ectopic appearance of a $c-KIT$ -positive A_{diff} within the SV epithelia of RA-treated testes. (C–E) Whole mount immunohistochemistry of anti- $GFR\alpha1$ (cell surface staining, red)/ $RAR\gamma1$ (nuclear staining, green) (C) and anti- $c-KIT$ (green; D) in the SV region, showing the disappearance of $GFR\alpha1/RAR\gamma1$ - double positive cells (arrowheads) and the ectopic appearance of $c-KIT$ -positive A_{diff} patches in the proximal SV region (upper left insets in c, higher magnified images of the $GFR\alpha1$ -positive cell indicated by the broken square). In (E), box plots show significant alterations of $c-KIT$ and $GFR\alpha1$ -positive (total, $RAR\gamma1$ -positive and -negative) cell number within the proximal SV region ($0 \sim 50 \mu m$ from RT; $n = 5$; $*p < 0.05$; $**p < 0.01$). Analysis was performed using unpaired Student's t-test. (F) H & E staining and ace-TUB (red) immunohistochemistry of the SV region at day 3

after RA treatment showing the disrupted ace-TUB signals in the SV region. Broken lines indicate the outlines of the ST. Images in c were taken by confocal microscopy. Insets in (a) and (c) and lower panels in (b) indicate the magnification of the region surrounded by broken rectangles in each panel. Stars in (B), non-specific signals in the interstitium. Int interstitial tissue, RT rete testis, SV Sertoli valve, ST seminiferous tubule. Scale bars represent 500 μm in the left panel of A, and 50 μm in the right panel of (B–D) and (F).

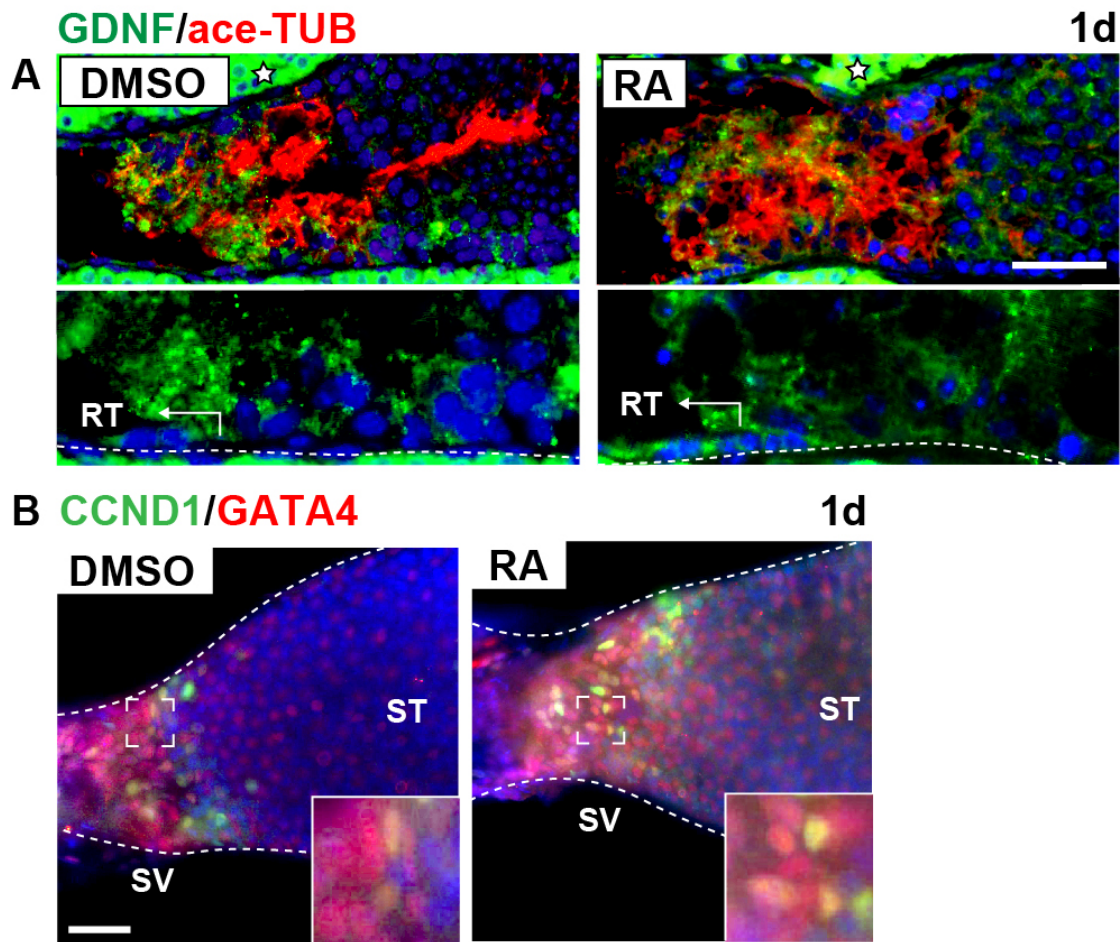


Fig. 3-6 No appreciable influences of exogenous RA treatment on the expression patterns of GDNF and CCND1 in the SV epithelia. (A) GDNF (green) and ace-TUB (red) immunohistochemistry of sagittal sections of the SV region at day 1 after the DMSO and RA treatment, showing no appreciable difference in GDNF expression in the ace-TUB-positive SV region between the DMSO- and RA-treated samples. Lower panels of green channel show the higher magnified images of the SV epithelia shown in the upper panels. (B) CCND1 (green) and GATA4 (red) immunohistochemistry of whole-mount SV samples at day 1 after the DMSO or RA treatment, showing no appreciable influences on CCND1 signals in the Sertoli cells within the SV region marked by GATA4 immunoreactivity. Insets in B show magnification of the region surrounded by the broken rectangle in each panel. Broken lines are the outlines of the ST. Star, nonspecific signals in the interstitium; RT, Rete testis; SV, Sertoli valve; ST, seminiferous tubule. Scale bars represent 50 μm.

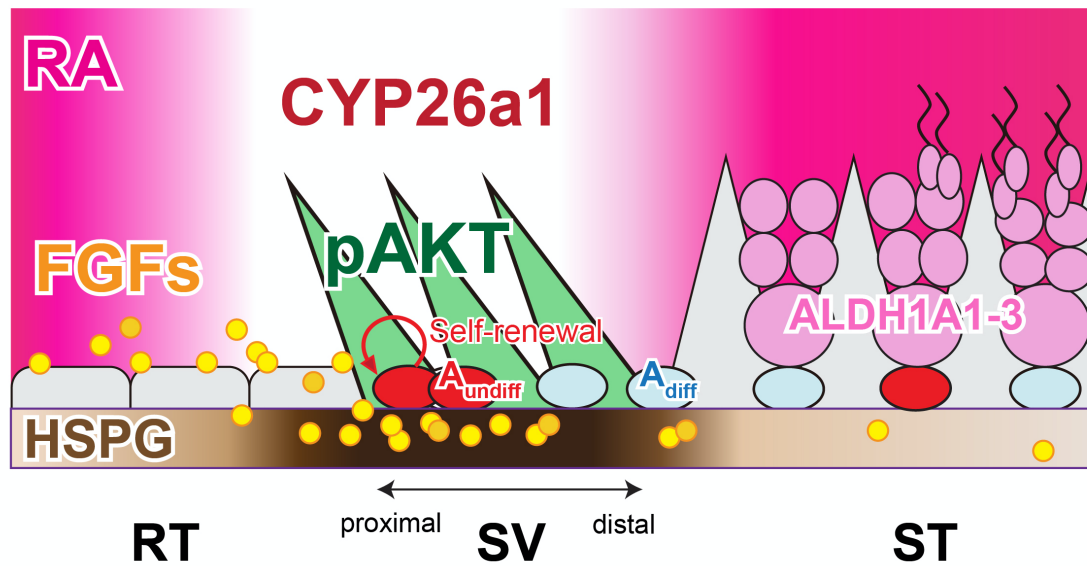


Fig. 3-7 Low RA levels and RT-derived factors may mediate the non-cell autonomous regionalization of the SV epithelia. A model schematic illustrating a potential contribution of RT-derived FGFs and local low-level RA to the regionalization of the SV epithelia. Through the region-specifically enriched HSPG in the SV region, FGFs derived from the RT (e.g., FGF9) get immobilized and perceived in the SV region, and then possibly mediate the constitutive AKT phosphorylation in the SV Sertoli cells. Such RT-derived FGF ligands can also contribute to the maintenance of stem/progenitor cell population in the SV region by promoting their self-renewal. On the other hand, SV-specific expression of CYP26A1 degrades RA within the SV region to maintain the local RA at low levels, repressing the A_{undiff} to A_{diff} transition of spermatogonia. The absence of ALDH1A1A1-3 expressing meiotic germ cells within the SV region may also contribute to the physical maintenance of the valve-like structures, as well as the low-RA levels within the SV region.

Table 3-1. List of antibodies used in this study

Antigen	Dilution	Description	Company	CAT#
ace-TUB	1/200	Mouse monoclonal	Sigma	T6793
AKT (pan)	1/300	Rabbit monoclonal	Cell Signaling	4691
CCND1	1/100	Rabbit polyclonal	Thermo Fisher	RM-9104-S1
c-KIT	1/100	Goat polyclonal	R&D Systems	AF1356
GATA4	1/75	Goat polyclonal	Santa Cruz	sc-1237
GDNF	1/100	Rabbit polyclonal	Santa Cruz	sc-328
GFR α 1	1/100	Goat polyclonal	R&D systems	AF560
HSPG (10E4)	1/100	Mouse monoclonal	Amsbio	370255-1
MVH/DDX4	1/1000	Rabbit polyclonal	Abcam	ab13840
p-AKT	1/100	Rabbit monoclonal	Cell Signaling	4060
SOX9	1/200	Rabbit polyclonal	Millipore	AB5535
RAR γ	1/100	Rabbit monoclonal	Cell Signaling	8965

Table 3-2. List of probes used for *in situ* hybridization

Gene symbol	CAT#	Accession No.
<i>Cyp26a1</i>	468,911	NM_007811.2
<i>Fgf9</i>	499,811	NM_013518.4
<i>Fgfr1</i>	443,491	NM_010206.3
<i>Fgfr2</i>	443,501	NM_010207.2
<i>PpiB</i> (positive control)	313911	NM_011149.2
<i>DapB</i> (Negative control)	310,043	EF191515

4. CHAPTER 3

**“Testicular valve formation and spermatogenesis
modulated by SOX17-positive rete testis in mammals”**

本章の内容は、雑誌掲載の形で出版する計画のため公表できない。5年以内に出版予定。

5. General Discussion

In this study, I highlighted the paracrine signaling in mammalian testis that orchestrate the dynamics of spermatogonia and the formation and/or maintenance of testicular valve at the SV. Hereafter, I discuss the significance of this study and further propose future directions and potential application of the findings obtained through this PhD thesis.

In Chapter 1, I developed a bead transplantation assay to examine the function of paracrine signaling molecules in the testis *in vivo*. The bead transplantation assay I developed in this PhD thesis is a powerful tool, which enables us to uncover function of secreted factors *in vivo* without generating a transgenic animal. Indeed, after the publication of the paper including this study (Uchida *et al.*, 2016a, 2016b), this assay was utilized in other research groups to reveal functions of growth factors. For fibroblast growth factor (FGF) family ligands, Kitadate *et al.*, (2020) demonstrated the functions of FGF5 as a mitogen for GFR α 1-positive spermatogonia by applying this bead transplantation assay (Kitadate *et al.*, 2019). By using this method, Masaki *et al.*, (2018) compared the functional differences of GDNF and FGF2 and then discovered that FGF2 supports a differentiation-prone subset of GFR α 1-positive spermatogonia, while GDNF promotes self-renewal of GFR α 1-positive spermatogonia (Masaki *et al.*, 2018). Of note, the data obtained by using the *in vivo* bead transplantation assay developed in this study could reflect both direct and indirect function of growth factors on spermatogonia. For example, growth factors derived from the bead could secondary affect functions of other somatic cells such as Sertoli cells to modulate spermatogonia. Therefore, combining both *in vivo* and *in vitro* study by considering their pros and cons will help us understand the paracrine interactions in in mammalian spermatogenesis.

In Chapter 2, I extended the bead transplantation assay developed in Chapter 1 to demonstrate the effect of FGF9 on the ST and RA on the SV. By applying the bead transplantation assay to FGF9, I successfully demonstrated the upregulation of p-AKT in Sertoli cells in the ST. The bead transplantation assay has hence proven to be useful to examine the effect of the secreted factors not only on spermatogonia, but also on Sertoli cells. The previous studies already showed the function of FGF9 to support the proliferation of spermatogonia while inhibiting meiotic differentiation of spermatogonia in the testis (Tassinari *et al.*, 2015; Yang *et al.*, 2021). FGF9 is also known to play a key role in the gonadal sex determination as a downstream target of SRY (Schmahl *et al.*, 2004; Willerton *et al.*, 2004; Li *et al.*, 2020). However, none of these studies have analyzed the effect of FGF9 on Sertoli cells in the adult testis. By taking advantage of the bead transplantation assay, this study provided the direct evidence of FGF9 action on adult Sertoli cells in the postnatal testis for the first time to my knowledge. This study paved the way for the application of bead transplantation assay to examine the function of signaling

molecules on the other testicular somatic cells, such as peritubular myoid cells, Leydig cells and macrophages.

By modifying the bead transplantation assay, I also successfully elevated the RA levels ectopically in the SV region to demonstrate that the low RA levels in the SV is indispensable for its maintenance of SSC niche. Previous studies have altered the RA levels in the testis to study its effect on spermatogenesis, either by the oral administration or by the intraperitoneal injection of RA or WIN 18,446 to increase or decrease the RA levels in the animal, respectively (reviewed in Endo et al., 2019). However, RA plays significant roles in the development and homeostasis of various organ across the body, including eyes, brains, and kidneys (Cunningham and Duester, 2015). Therefore, such a robust treatment makes it difficult to dissect the testicular phenotype from the off-target effects. The bead transplantation assay in this study let us overcome this issue, by enabling us to locally exposure the region of your interest in the testis to RA. Besides, the bead transplantation technique also saves the amount of chemical needed to conduct the experiment.

Taken together, the bead transplantation assay developed in this study is of great advantage in the research field. As demonstrated above, this technique is quite versatile. I expect that making further modification in the bead transplantation assay will not only advance the biological findings in the field, but also opening the door for its clinical application. For instance, transplantation of the beads made of magnetic material will let us assemble or disassemble the beads in the testicular interstitium after the transplantation, by bringing the magnet closer through the tunica albuginea. The beads made of bioabsorbable materials could make the assay less invasive, potentially make it available for clinical applications to restore fertility in the animals.

In Chapter 3, I delved into the detailed regulatory mechanism of the SV via RT and discovered the significant function of the RT and SV in mammalian spermatogenesis in the testis. Since these structure in the testis has been paid relatively small attention, current reproductive biotechnologies fail to benefit from the RT and SV. Therefore, I postulate that co-culture of the RT/SV and ST and/or recapitulating the unidirectional luminal fluid flow in the testicular organ culture system (Sato et al., 2011; 2015) could help enhance the efficiency of *in vitro* spermatogenesis. Indeed, a culture using a microfluidic device is known to enhance the efficiency of *in vitro* spermatogenesis compared to the conventional gas liquid interphase organ culture method (Komeya et al., 2017), emphasizing the importance of fluid flow in mammalian spermatogenesis. I also propose that xenografting of the testicular

piece (Arregui and Dobrinski, 2014; Fayomi et al., 2019) together with the RT and SV could improve its spermatogenic efficiency. In fact, preliminary data from my lab suggest that the co-transplantation of the gonad and mesonephros enhance the efficiency of spermatogenesis in the xenograft (Aiyama, 2015). Taken together, exploiting of the functional roles of the RT and SV does may help us improve the efficiency of already existing reproductive biotechnology with modifications.

Male infertility is a significant issue in a broad range of fields, including human medicine, livestock reproduction and wild-life conservation. *Ex situ* conservation of endangered animal species is of my particular interest, thus my goal as a researcher is to develop a reproductive technology that is applicable for a wide variety of species. This PhD thesis serves as a milestone for my goal, through which I could develop a novel technique to expand the SSC population (Chapter 1), artificially modulate the SSC niche (Chapter 2) and discovered the significance of the testicular valve in spermatogenesis (Chapter 3) all *in vivo*. The data obtained in the present study does not only deepen our understanding of paracrine regulation in the testis, but also may lead us overcome current limitations in the reproductive biotechnology.

6. Acknowledgement

First, I would like to express my deep gratitude to my supervisor, Dr. Yoshiakira Kanai. He always asks an impactful question in the research and never forget to enjoy science. I also thank Drs. Ryuji Hiramatsu, Masamichi Kurohmaru and Naoki Tsunekawa in Kanai's lab for guiding my research while organizing the great research environment. I am very grateful for the entire Kanai's lab for their support. Special thanks to my colleagues in Kanai's lab, Kenya Imaimatsu, Taisei Yoshigaki, Honoka Suzuki and Emi Kan for helping me in the analysis and the animal management, and Ms. Shiho Yasui, Itsuko Yagihashi, Yuki Uchiyama and Ayano Ooike for their secretary support. I also thank the former PhD students at Kanai's lab, Drs. Kasane Kishi, Yoshimi Aiyama, and Kento Miura for their support and advice.

I would like to extend my appreciation to the outstanding collaborators, Drs. Masaki Kanai-Azuma, Yoshikazu Hirate, Hinako Takase and Hitomi Suzuki in the Tokyo Medical and Dental University for the generation of transgenic mouse lines used in this thesis, and Drs. Akihiko Kudo, Yoshihiro Akimoto, Sachie Matsubara and Jyunri Hayakawa for their excellent TEM technical support. I appreciate Dr. Tokuko Iwamori at Kyushu University for providing the MPLK antibody, and Dr. Shosei Yoshida at for providing GFR α 1-GFP knock in mice. I also appreciate the researchers belong to the Grant-in Aid for Scientific Research on Innovative Area "Ensuring integrity in gametogenesis" for the constructing advice on my research. I greatly appreciate the experimental animals that devoted their life for this research.

I would like to express my deep gratitude to the Japan Society for the Promotion of Science (JSPS) for providing me a DC1 fellowship to support this journey. I would also like to thank Hitachi global research foundation for their financial support on my research project. I hope I could reward their investment to me through making exciting discoveries in science, including this research project.

Finally, I would like to thank my parents and friends, who supported my decision and encouraged me to pursue my career in research. At last, I thank my husband, Peter, who has always supported me throughout the way with all the hardship we encountered.

December 15th, 2021

Aya Uchida

7. Reference

- Abe, K., Eto, K. & Abe, S. 2008, Epidermal growth factor mediates spermatogonial proliferation in newt testis. *Reprod. Biol. Endocrinol.* vol. 6, pp. 7-7827-6-7.
- Agrimson, K.S., Oatley, M.J., Mitchell, D., Oatley, J.M., Griswold, M.D. & Hogarth, C.A. 2017, Retinoic acid deficiency leads to an increase in spermatogonial stem number in the neonatal mouse testis, but excess retinoic acid results in no change. *Dev. Biol.* vol. 432, no. 2, pp. 229-236.
- Aiyama, Y., Tsunekawa, N., Kishi, K., Kawasumi, M., Suzuki, H., Kanai-Azuma, M., Kurohmaru, M. & Kanai, Y. 2015, A Niche for GFR α 1-Positive Spermatogonia in the Terminal Segments of the Seminiferous Tubules in Hamster Testes, *Stem cells* vol. 33, no. 9, pp. 2811-2824.
- Araki, Y., Sato, T., Katagiri, K., Kubota, Y., Araki, Y. & Ogawa, T. 2010, Proliferation of mouse spermatogonial stem cells in microdrop culture, *Biol. Reprod.* vol. 83, no. 6, pp. 951-957.
- Arnold, S.L., Kent, T., Hogarth, C.A., Schlatt, S., Prasad, B., Haenisch, M., Walsh, T., Muller, C.H., Griswold, M.D., Amory, J.K. & Isoherranen, N. 2015, Importance of ALDH1A enzymes in determining human testicular retinoic acid concentrations, *J. Lipid Res.* vol. 56, no. 2, pp. 342-357.
- Arregui, L. & Dobrinski, I. 2014, Xenografting of testicular tissue pieces: 12 years of an in vivo spermatogenesis system, *Reproduction* vol. 148, no. 5, pp. R71-84.
- Artus, J., Piliszek, A. & Hadjantonakis, A.K. 2011, The primitive endoderm lineage of the mouse blastocyst: sequential transcription factor activation and regulation of differentiation by Sox17, *Dev. Biol.* vol. 350, no. 2, pp. 393-404.
- Barrios, F., Filipponi, D., Pellegrini, M., Paronetto, M.P., Di Siena, S., Geremia, R., Rossi, P., De Felici, M., Jannini, E.A. & Dolci, S. 2010, Opposing effects of retinoic acid and FGF9 on Nanos2 expression and meiotic entry of mouse germ cells, *J. Cell Sci.* vol. 123, no. 6, pp. 871-880.
- Bazigou, E. & Makinen, T. 2013, Flow control in our vessels: vascular valves make sure there is no way back, *Cell. Mol.* vol. 70, no. 6, pp. 1055-1066.
- Becht, E., McInnes, L., Healy, J., Dutertre, C.A., Kwok, I.W.H., Ng, L.G., Ginhoux, F. & Newell, E.W. 2018, Dimensionality reduction for visualizing single-cell data using UMAP, *Nat. Biotechnol.*

- Bellve, A.R., Cavicchia, J.C., Millette, C.F., O'Brien, D.A., Bhatnagar, Y.M. & Dym, M. 1977, Spermatogenic cells of the prepuberal mouse. Isolation and morphological characterization, *J. Cell Biol.* vol. 74, no. 1, pp. 68-85.
- Bhang, D.H., Kim, B.J., Kim, B.G., Schadler, K., Baek, K.H., Kim, Y.H., Hsiao, W., Ding, B.S., Rafii, S., Weiss, M.J., Chou, S.T., Kolon, T.F., Ginsberg, J.P., Ryu, B.Y. & Ryeom, S. 2018, Testicular endothelial cells are a critical population in the germline stem cell niche, *Nat. Commun.* vol. 9, no. 1, pp. 4379-018-06881-z.
- Bowles, J., Feng, C.W., Spiller, C., Davidson, T.L., Jackson, A. & Koopman, P. 2010, FGF9 suppresses meiosis and promotes male germ cell fate in mice, *Dev. Cell* vol. 19, no. 3, pp. 440-449.
- Bowles, J., Knight, D., Smith, C., Wilhelm, D., Richman, J., Mamiya, S., Yashiro, K., Chawengsaksophak, K., Wilson, M.J., Rossant, J., Hamada, H. & Koopman, P. 2006, Retinoid signaling determines germ cell fate in mice, *Science* vol. 312, no. 5773, pp. 596-600.
- Boyer, A., Yeh, J.R., Zhang, X., Paquet, M., Gaudin, A., Nagano, M.C. & Boerboom, D. 2012, CTNNB1 signaling in sertoli cells downregulates spermatogonial stem cell activity via WNT4, *PloS One*, vol. 7, no. 1, pp. e29764.
- Brinster, R.L. & Avarbock, M.R. 1994, Germline transmission of donor haplotype following spermatogonial transplantation, *Proc. Natl. Acad. Sci. U. S. A.*, vol. 91, no. 24, pp. 11303-11307.
- Brinster, R.L. & Zimmermann, J.W. 1994, Spermatogenesis following male germ-cell transplantation, *Proc. Natl. Acad. Sci. U. S. A.* vol. 91, no. 24, pp. 11298-11302.
- Brucato, S., Fagnen, G., Villers, C., Bonnamy, P.J., Langris, M. & Bocquet, J. 2001, Biochemical characterization of integral membrane heparan sulfate proteoglycans in Sertoli cells from immature rat testis, *Biochimica et biophysica acta*, vol. 1510, no. 1-2, pp. 474-487.
- Busada, J.T., Chappell, V.A., Niedenberger, B.A., Kaye, E.P., Keiper, B.D., Hogarth, C.A. & Geyer, C.B. 2015, Retinoic acid regulates Kit translation during spermatogonial differentiation in the mouse, *Dev. Biol.* vol. 397, no. 1, pp. 140-149.
- Cadigan, K.M. 2008, Wnt-beta-catenin signaling, *Curr. Biol.* vol. 18, no. 20, pp. R943-7.

- Carrieri, C., Comazzetto, S., Grover, A., Morgan, M., Bunes, A., Nerlov, C. & O'Carroll, D. 2017, A transit-amplifying population underpins the efficient regenerative capacity of the testis, *J. Exp. Med.* vol. 214, no. 6, pp. 1631-1641.
- Chassot, A.A., Gillot, I. & Chaboissier, M.C. 2014, R-spondin1, WNT4, and the CTNNB1 signaling pathway: strict control over ovarian differentiation. *Reproduction* vol. 148, no. 6, pp. R97-110.
- Chen, L.Y., Brown, P.R., Willis, W.B. & Eddy, E.M. 2014, Peritubular myoid cells participate in male mouse spermatogonial stem cell maintenance. *Endocrinology*, vol. 155, no. 12, pp. 4964-4974.
- Chen, L.Y., Willis, W.D. & Eddy, E.M. 2016, Targeting the Gdnf Gene in peritubular myoid cells disrupts undifferentiated spermatogonial cell development. *Proc. Natl. Acad. Sci. U. S. A.* vol. 113, no. 7, pp. 1829-1834.
- Chen, S.R., Tang, J.X., Cheng, J.M., Hao, X.X., Wang, Y.Q., Wang, X.X. & Liu, Y.X. 2016, Does murine spermatogenesis require WNT signalling? A lesson from Gpr177 conditional knockout mouse models. *Cell death & disease*, vol. 7, no. 6, pp. e2281.
- Chen, Y., Zhu, J.Y., Hong, K.H., Mikles, D.C., Georg, G.I., Goldstein, A.S., Amory, J.K. & Schonbrunn, E. 2018, Structural Basis of ALDH1A2 Inhibition by Irreversible and Reversible Small Molecule Inhibitors, *ACS Chem. Biol.* vol. 13, no. 3, pp. 582-590.
- Cheng, C.Y. & Mruk, D.D. 2012, The blood-testis barrier and its implications for male contraception, *Pharmacol. Rev.* vol. 64, no. 1, pp. 16-64.
- Chihara, M., Ikebuchi, R., Otsuka, S., Ichii, O., Hashimoto, Y., Suzuki, A., Saga, Y. & Kon, Y. 2013, Mice stage-specific claudin 3 expression regulates progression of meiosis in early stage spermatocytes, *Biol. Reprod.*, vol. 89, no. 1, pp. 3.
- Chihara, M., Otsuka, S., Ichii, O. & Kon, Y. 2013, Vitamin A deprivation affects the progression of the spermatogenic wave and initial formation of the blood-testis barrier, resulting in irreversible testicular degeneration in mice, *J. Reprod. Dev.* vol. 59, no. 6, pp. 525-535.
- Cotton, L.M., O'Bryan, M.K. & Hinton, B.T. 2008, Cellular signaling by fibroblast growth factors (FGFs) and their receptors (FGFRs) in male reproduction, *Endocr. Rev.* vol. 29, no. 2, pp. 193-216.

- Creemers, L.B., Meng, X., den Ouden, K., van Pelt, A.M., Izadyar, F., Santoro, M., Sariola, H. & de Rooij, D.G. 2002, Transplantation of germ cells from glial cell line-derived neurotrophic factor-overexpressing mice to host testes depleted of endogenous spermatogenesis by fractionated irradiation, *Biol. Reprod.* vol. 66, no. 6, pp. 1579-1584.
- Cunningham, T.J. & Duester, G. 2015, Mechanisms of retinoic acid signalling and its roles in organ and limb development. *Nat. Rev.* vol. 16, no. 2, pp. 110-123.
- Cunningham, T.J., Zhao, X., Sandell, L.L., Evans, S.M., Trainor, P.A. & Duester, G. 2013, "Antagonism between retinoic acid and fibroblast growth factor signaling during limb development", *Cell Rep.* vol. 3, no. 5, pp. 1503-1511.
- de Rooij, D.G. & Russell, L.D. 2000, All you wanted to know about spermatogonia but were afraid to ask. *J. Androl.* vol. 21, no. 6, pp. 776-798.
- DeFalco, T., Potter, S.J., Williams, A.V., Waller, B., Kan, M.J. & Capel, B. 2015, Macrophages Contribute to the Spermatogonial Niche in the Adult Testis. *Cell Rep.* vol. 12, no. 7, pp. 1107-1119.
- Deltour, L., Haselbeck, R.J., Ang, H.L. & Duester, G. 1997, Localization of class I and class IV alcohol dehydrogenases in mouse testis and epididymis: potential retinol dehydrogenases for endogenous retinoic acid synthesis, *Biol. Reprod.* vol. 56, no. 1, pp. 102-109.
- Deng, C.Y., Lv, M., Luo, B.H., Zhao, S.Z., Mo, Z.C. & Xie, Y.J. 2021, The Role of the PI3K/AKT/mTOR Signalling Pathway in Male Reproduction. *Curr. Mol. Med.* vol. 21, no. 7, pp. 539-548.
- Dhillon, H., Zigman, J.M., Ye, C., Lee, C.E., McGovern, R.A., Tang, V., Kenny, C.D., Christiansen, L.M., White, R.D., Edelstein, E.A., Coppari, R., Balthasar, N., Cowley, M.A., Chua, S., Jr, Elmquist, J.K. & Lowell, B.B. 2006, Leptin directly activates SF1 neurons in the VMH, and this action by leptin is required for normal body-weight homeostasis, *Neuron*, vol. 49, no. 2, pp. 191-203.
- Diez del Corral, R., Olivera-Martinez, I., Goriely, A., Gale, E., Maden, M. & Storey, K. 2003, Opposing FGF and retinoid pathways control ventral neural pattern, neuronal differentiation, and segmentation during body axis extension, *Neuron*, vol. 40, no. 1, pp. 65-79.

- Diez-Torre, A., Silvan, U., Moreno, P., Gumucio, J. & Arechaga, J. 2011, Peritubular myoid cell-derived factors and its potential role in the progression of testicular germ cell tumours. *Int. J. Androl.* vol. 34, no. 4 Pt 2, pp. e252-65.
- Dovere, L., Fera, S., Grasso, M., Lamberti, D., Gargioli, C., Muciaccia, B., Lustri, A.M., Stefanini, M. & Vicini, E. 2013, The niche-derived glial cell line-derived neurotrophic factor (GDNF) induces migration of mouse spermatogonial stem/progenitor cells. *PLoS One*, vol. 8, no. 4, pp. e59431.
- Dym, M. 1994, Basement membrane regulation of Sertoli cells, *Endocr. Rev.* vol. 15, no. 1, pp. 102-115.
- Dym, M. 1974, The fine structure of monkey Sertoli cells in the transitional zone at the junction of the seminiferous tubules with the tubuli recti, *Am. j. anat.*, vol. 140, no. 1, pp. 1-25.
- Endo, T., Freinkman, E., de Rooij, D.G. & Page, D.C. 2017, Periodic production of retinoic acid by meiotic and somatic cells coordinates four transitions in mouse spermatogenesis. *Proc. Natl. Acad. Sci. U. S. A.* vol. 114, no. 47, pp. E10132-E10141.
- Endo, T., Mikedis, M.M., Nicholls, P.K., Page, D.C. & de Rooij, D.G. 2019, Retinoic Acid and Germ Cell Development in the Ovary and Testis, *Biomolecules*, vol. 9, no. 12, pp. 10.3390/biom9120775.
- Endo, T., Romer, K.A., Anderson, E.L., Baltus, A.E., de Rooij, D.G. & Page, D.C. 2015, Periodic retinoic acid-STRA8 signaling intersects with periodic germ-cell competencies to regulate spermatogenesis, *Proc. Natl. Acad. Sci. U. S. A.* vol. 112, no. 18, pp. E2347-56.
- Fawcett, D.W. & Dym, M. 1974, A glycogen-rich segment of the tubuli recti and proximal portion of the rete testis in the guinea-pig. *J. reprod. fertil.*, vol. 38, no. 2, pp. 401-409.
- Fayomi, A.P., Peters, K., Sukhwani, M., Valli-Pulaski, H., Shetty, G., Meistrich, M.L., Houser, L., Robertson, N., Roberts, V., Ramsey, C., Hanna, C., Hennebold, J.D., Dobrinski, I. & Orwig, K.E. 2019, Autologous grafting of cryopreserved prepubertal rhesus testis produces sperm and offspring. *Science* vol. 363, no. 6433, pp. 1314-1319.
- Figueiredo, A.F.A., Hess, R.A., Batlouni, S.R., Wnuk, N.T., Tavares, A.O., Abarikwu, S.O., Costa, G.M.J. & Franca, L.R. 2021, Insights into differentiation and function of the transition region between the seminiferous tubule and rete testis. *Differentiation*, vol. 120, pp. 36-47.

- Fisher, D. 2002, New light shed on fluid formation in the seminiferous tubules of the rat. *J. Physiol.* vol. 542, no. Pt 2, pp. 445-452.
- Fleck, D., Kenzler, L., Mundt, N., Strauch, M., Uesaka, N., Moosmann, R., Bruentgens, F., Missel, A., Mayerhofer, A., Merhof, D., Spehr, J. & Spehr, M. 2021, ATP activation of peritubular cells drives testicular sperm transport. *eLife*, vol. 10, pp. 10.7554/eLife.62885.
- Free, M.J., Jaffe, R.A. & Morford, D.E. 1980, Sperm transport through the rete testis in anesthetized rats: role of the testicular capsule and effect of gonadotropins and prostaglandins. *Biol. Reprod.* vol. 22, no. 5, pp. 1073-1078.
- Garbuzov, A., Pech, M.F., Hasegawa, K., Sukhwani, M., Zhang, R.J., Orwig, K.E. & Artandi, S.E. 2018, Purification of GFRalpha1+ and GFRalpha1- Spermatogonial Stem Cells Reveals a Niche-Dependent Mechanism for Fate Determination. *Stem Cell Rep.* vol. 10, no. 2, pp. 553-567.
- Gely-Pernot, A., Raverdeau, M., Teletin, M., Vernet, N., Feret, B., Klopfenstein, M., Dennefeld, C., Davidson, I., Benoit, G., Mark, M. & Ghyselinck, N.B. 2015, Retinoic Acid Receptors Control Spermatogonia Cell-Fate and Induce Expression of the SALL4A Transcription Factor. *PLoS Genet.* vol. 11, no. 10, pp. e1005501.
- Geng, X., Cha, B., Mahamud, M.R. & Srinivasan, R.S. 2017, Intraluminal valves: development, function and disease. *Dis. Model. Mech.* vol. 10, no. 11, pp. 1273-1287.
- Gewiss, R.L., Schleif, M.C. & Griswold, M.D. 2021, The role of retinoic acid in the commitment to meiosis. *Asian J. Androl.* vol. 23, no. 6, pp. 549-554.
- Goetz, R. & Mohammadi, M. 2013, Exploring mechanisms of FGF signalling through the lens of structural biology. *Nat. Rev.* vol. 14, no. 3, pp. 166-180.
- Goldbeter, A., Gonze, D. & Pourquie, O. 2007, Sharp developmental thresholds defined through bistability by antagonistic gradients of retinoic acid and FGF signaling. *Dev. Dyn.* vol. 236, no. 6, pp. 1495-1508.

- Golestaneh, N., Beauchamp, E., Fallen, S., Kokkinaki, M., Uren, A. & Dym, M. 2009, Wnt signaling promotes proliferation and stemness regulation of spermatogonial stem/progenitor cells. *Reproduction* vol. 138, no. 1, pp. 151-162.
- Gong, J., Zeng, Q., Yu, D. & Duan, Y.G. 2020, T Lymphocytes and Testicular Immunity: A New Insight into Immune Regulation in Testes. *Int. J. Mol.* vol. 22, no. 1, pp. 10.3390/ijms22010057.
- Gow, A., Southwood, C.M., Li, J.S., Pariali, M., Riordan, G.P., Brodie, S.E., Danias, J., Bronstein, J.M., Kachar, B. & Lazzarini, R.A. 1999, CNS myelin and sertoli cell tight junction strands are absent in *Osp/claudin-11* null mice. *Cell*, vol. 99, no. 6, pp. 649-659.
- Grasso, M., Fusco, A., Dove, L., de Rooij, D.G., Stefanini, M., Boitani, C. & Vicini, E. 2012, Distribution of GFRA1-expressing spermatogonia in adult mouse testis. *Reproduction*, vol. 143, no. 3, pp. 325-332.
- Griswold, M.D. 2016, Spermatogenesis: The Commitment to Meiosis, *Physiol. Rev.* vol. 96, no. 1, pp. 1-17.
- Hadley, M.A. & Dym, M. 1987, Immunocytochemistry of extracellular matrix in the lamina propria of the rat testis: electron microscopic localization, *Biol. Reprod.*, vol. 37, no. 5, pp. 1283-1289.
- Hao, Y., Hao, S., Andersen-Nissen, E., Mauck, W.M., 3rd, Zheng, S., Butler, A., Lee, M.J., Wilk, A.J., Darby, C., Zager, M., Hoffman, P., Stoeckius, M., Papalexi, E., Mimitou, E.P., Jain, J., Srivastava, A., Stuart, T., Fleming, L.M., Yeung, B., Rogers, A.J., McElrath, J.M., Blish, C.A., Gottardo, R., Smibert, P. & Satija, R. 2021, Integrated analysis of multimodal single-cell data. *Cell*, vol. 184, no. 13, pp. 3573-3587.e29.
- Hara, K., Nakagawa, T., Enomoto, H., Suzuki, M., Yamamoto, M., Simons, B.D. & Yoshida, S. 2014, Mouse spermatogenic stem cells continually interconvert between equipotent singly isolated and syncytial states. *Cell Stem Cell*, vol. 14, no. 5, pp. 658-672.
- Hasegawa, K. & Saga, Y. 2014, FGF8-FGFR1 signaling acts as a niche factor for maintaining undifferentiated spermatogonia in the mouse. *Biol. Reprod.* vol. 91, no. 6, pp. 145.

- Hess, R.A., Sharpe, R.M. & Hinton, B.T. 2021, Estrogens and development of the rete testis, efferent ductules, epididymis and vas deferens. *Differentiation*, vol. 118, pp. 41-71.
- Higashiyama, H., Ozawa, A., Sumitomo, H., Uemura, M., Fujino, K., Igarashi, H., Imaimatsu, K., Tsunekawa, N., Hirate, Y., Kurohmaru, M., Saijoh, Y., Kanai-Azuma, M. & Kanai, Y. 2017, Embryonic cholecystitis and defective gallbladder contraction in the Sox17-haploinsufficient mouse model of biliary atresia. *Development*, vol. 144, no. 10, pp. 1906-1917.
- Hiramatsu, R., Harikae, K., Tsunekawa, N., Kurohmaru, M., Matsuo, I. & Kanai, Y. 2010, FGF signaling directs a center-to-pole expansion of tubulogenesis in mouse testis differentiation. *Development*, vol. 137, no. 2, pp. 303-312.
- Hirate, Y., Hayakawa, K., Nakano, Y., Kumazawa, S., Miura, K., Kanai, Y. & Kanai-Azuma, M. 2020, Early Crypt Formation Defects in the Uterine Epithelia of Sox17 Heterozygous Mice. *Sex. Dev.*, vol. 14, no. 1-6, pp. 40-50.
- Hirate, Y., Suzuki, H., Kawasumi, M., Takase, H.M., Igarashi, H., Naquet, P., Kanai, Y. & Kanai-Azuma, M. 2016, Mouse Sox17 haploinsufficiency leads to female subfertility due to impaired implantation, *Sci. Rep.* vol. 6, pp. 24171.
- Hogarth, C.A., Evans, E., Onken, J., Kent, T., Mitchell, D., Petkovich, M. & Griswold, M.D. 2015, CYP26 Enzymes Are Necessary Within the Postnatal Seminiferous Epithelium for Normal Murine Spermatogenesis. *Biol. Reprod.* vol. 93, no. 1, pp. 19.
- Huckins, C. 1978, Behavior of stem cell spermatogonia in the adult rat irradiated testis. *Biol. Reprod.* vol. 19, no. 4, pp. 747-760.
- Huleihel, M., Fadlon, E., Abuelhija, A., Piltcher Haber, E. & Lunenfeld, E. 2013, Glial cell line-derived neurotrophic factor (GDNF) induced migration of spermatogonial cells in vitro via MEK and NF-kB pathways. *Differentiation* vol. 86, no. 1-2, pp. 38-47.
- Ibtisham, F. & Honaramooz, A. 2020, Spermatogonial Stem Cells for In Vitro Spermatogenesis and In Vivo Restoration of Fertility. *Cells*, vol. 9, no. 3, pp. 10.3390/cells9030745.

- Igarashi, H., Uemura, M., Hiramatsu, R., Hiramatsu, R., Segami, S., Pattarapanawan, M., Hirate, Y., Yoshimura, Y., Hashimoto, H., Higashiyama, H., Sumitomo, H., Kurohmaru, M., Saijoh, Y., Suemizu, H., Kanai-Azuma, M. & Kanai, Y. 2018, Sox17 is essential for proper formation of the marginal zone of extraembryonic endoderm adjacent to a developing mouse placental disk. *Biol. Reprod.* vol. 99, no. 3, pp. 578-589.
- Ikami, K., Tokue, M., Sugimoto, R., Noda, C., Kobayashi, S., Hara, K. & Yoshida, S. 2015, Hierarchical differentiation competence in response to retinoic acid ensures stem cell maintenance during mouse spermatogenesis. *Development*, vol. 142, no. 9, pp. 1582-1592.
- Imura-Kishi, K., Uchida, A., Tsunekawa, N., Suzuki, H., Takase, H.M., Hirate, Y., Kanai-Azuma, M., Hiramatsu, R., Kurohmaru, M. & Kanai, Y. 2021, Low retinoic acid levels mediate regionalization of the Sertoli valve in the terminal segment of mouse seminiferous tubules. *Sci. Rep.* vol. 11, no. 1, pp. 1110-020-79987-4.
- Ishiguro, K.I., Matsuura, K., Tani, N., Takeda, N., Usuki, S., Yamane, M., Sugimoto, M., Fujimura, S., Hosokawa, M., Chuma, S., Ko, M.S.H., Araki, K. & Niwa, H. 2020, MEIOSIN Directs the Switch from Mitosis to Meiosis in Mammalian Germ Cells. *Dev. Cell*, vol. 52, no. 4, pp. 429-445.e10.
- Ishii, K., Kanatsu-Shinohara, M., Toyokuni, S. & Shinohara, T. 2012, FGF2 mediates mouse spermatogonial stem cell self-renewal via upregulation of Etv5 and Bcl6b through MAP2K1 activation. *Development*, vol. 139, no. 10, pp. 1734-1743.
- Itoh, N., Nakayama, Y. & Konishi, M. 2016, Roles of FGFs As Paracrine or Endocrine Signals in Liver Development, Health, and Disease. *Front. Cell Dev. Biol.* vol. 4, pp. 30.
- Iwamori, T., Lin, Y.N., Ma, L., Iwamori, N. & Matzuk, M.M. 2011, Identification and characterization of RBM44 as a novel intercellular bridge protein. *PloS One*, vol. 6, no. 2, pp. e17066.
- Jeays-Ward, K., Dandonneau, M. & Swain, A. 2004, Wnt4 is required for proper male as well as female sexual development. *Dev. Biol.*, vol. 276, no. 2, pp. 431-440.
- Jonte, G. & Holstein, A.F. 1987, On the morphology of the transitional zones from the rete testis into the ductuli efferentes and from the ductuli efferentes into the ductus epididymidis. Investigations on the human testis and epididymis. *Andrologia*, vol. 19, no. 3, pp. 398-412.

- Jostes, S.V., Fellermeier, M., Arevalo, L., Merges, G.E., Kristiansen, G., Nettersheim, D. & Schorle, H. 2020, Unique and redundant roles of SOX2 and SOX17 in regulating the germ cell tumor fate. *Int. J. Cancer Res.* vol. 146, no. 6, pp. 1592-1605.
- Kam, R.K., Deng, Y., Chen, Y. & Zhao, H. 2012, Retinoic acid synthesis and functions in early embryonic development. *Cell Biosci.* vol. 2, no. 1, pp. 11-3701-2-11.
- Kanai-Azuma, M., Kanai, Y., Gad, J.M., Tajima, Y., Taya, C., Kurohmaru, M., Sanai, Y., Yonekawa, H., Yazaki, K., Tam, P.P. & Hayashi, Y. 2002, Depletion of definitive gut endoderm in Sox17-null mutant mice. *Development*, vol. 129, no. 10, pp. 2367-2379.
- Kanatsu-Shinohara, M., Inoue, K., Ogonuki, N., Morimoto, H., Ogura, A. & Shinohara, T. 2011, Serum- and feeder-free culture of mouse germline stem cells. *Biol. Reprod.* vol. 84, no. 1, pp. 97-105.
- Kanatsu-Shinohara, M., Inoue, K., Takashima, S., Takehashi, M., Ogonuki, N., Morimoto, H., Nagasawa, T., Ogura, A. & Shinohara, T. 2012, Reconstitution of mouse spermatogonial stem cell niches in culture. *Cell Stem Cell*, vol. 11, no. 4, pp. 567-578.
- Kanatsu-Shinohara, M., Miki, H., Inoue, K., Ogonuki, N., Toyokuni, S., Ogura, A. & Shinohara, T. 2005, Long-term culture of mouse male germline stem cells under serum-or feeder-free conditions. *Biol.Reprod.* vol. 72, no. 4, pp. 985-991.
- Kanatsu-Shinohara, M., Morimoto, H. & Shinohara, T. 2016, Fertility of Male Germline Stem Cells Following Spermatogonial Transplantation in Infertile Mouse Models. *Biol. Reprod.* vol. 94, no. 5, pp. 112.
- Kanatsu-Shinohara, M., Ogonuki, N., Inoue, K., Miki, H., Ogura, A., Toyokuni, S. & Shinohara, T. 2003, Long-term proliferation in culture and germline transmission of mouse male germline stem cells. *Biol. Reprod.*, vol. 69, no. 2, pp. 612-616.
- Kanatsu-Shinohara, M., Ogonuki, N., Iwano, T., Lee, J., Kazuki, Y., Inoue, K., Miki, H., Takehashi, M., Toyokuni, S., Shinkai, Y., Oshimura, M., Ishino, F., Ogura, A. & Shinohara, T. 2005, Genetic and epigenetic properties of mouse male germline stem cells during long-term culture. *Development*, vol. 132, no. 18, pp. 4155-4163.

- Kanatsu-Shinohara, M., Ogonuki, N., Matoba, S., Ogura, A. & Shinohara, T. 2020, Autologous transplantation of spermatogonial stem cells restores fertility in congenitally infertile mice. *Proc. Natl. Acad. Sci. U. S. A.* vol. 117, no. 14, pp. 7837-7844.
- Kanatsu-Shinohara, M. & Shinohara, T. 2013, Spermatogonial stem cell self-renewal and development. *Annu. Rev. Cell Dev. Biol.* vol. 29, pp. 163-187.
- Kim, I., Saunders, T.L. & Morrison, S.J. 2007, Sox17 dependence distinguishes the transcriptional regulation of fetal from adult hematopoietic stem cells. *Cell*, vol. 130, no. 3, pp. 470-483.
- Kim, Y., Bingham, N., Sekido, R., Parker, K.L., Lovell-Badge, R. & Capel, B. 2007, Fibroblast growth factor receptor 2 regulates proliferation and Sertoli differentiation during male sex determination. *Proc. Natl. Acad. Sci. U. S. A.* vol. 104, no. 42, pp. 16558-16563.
- Kim, Y., Kobayashi, A., Sekido, R., DiNapoli, L., Brennan, J., Chaboissier, M.C., Poulat, F., Behringer, R.R., Lovell-Badge, R. & Capel, B. 2006, "Fgf9 and Wnt4 act as antagonistic signals to regulate mammalian sex determination", *PLoS biology*, vol. 4, no. 6, pp. e187.
- Kinoshita, M., Shimosato, D., Yamane, M. & Niwa, H. 2015, "Sox7 is dispensable for primitive endoderm differentiation from mouse ES cells", *BMC Dev. Biol.* vol. 15, pp. 37-015-0079-4.
- Kishi, K., Uchida, A., Takase, H.M., Suzuki, H., Kurohmaru, M., Tsunekawa, N., Kanai-Azuma, M., Wood, S.A. & Kanai, Y. 2017, "Spermatogonial deubiquitinase USP9X is essential for proper spermatogenesis in mice", *Reproduction*, vol. 154, no. 2, pp. 135-143.
- Kitadate, Y., Jorg, D.J., Tokue, M., Maruyama, A., Ichikawa, R., Tsuchiya, S., Segi-Nishida, E., Nakagawa, T., Uchida, A., Kimura-Yoshida, C., Mizuno, S., Sugiyama, F., Azami, T., Ema, M., Noda, C., Kobayashi, S., Matsuo, I., Kanai, Y., Nagasawa, T., Sugimoto, Y., Takahashi, S., Simons, B.D. & Yoshida, S. 2019, Competition for Mitogens Regulates Spermatogenic Stem Cell Homeostasis in an Open Niche. *Cell Stem Cell*, vol. 24, no. 1, pp. 79-92.e6.
- Kleinman, H.K. & Schnaper, H.W. 1993, Basement membrane matrices in tissue development. *J. Respir.* vol. 8, no. 3, pp. 238-239.

- Komeya, M., Hayashi, K., Nakamura, H., Yamanaka, H., Sanjo, H., Kojima, K., Sato, T., Yao, M., Kimura, H., Fujii, T. & Ogawa, T. 2017, Pumpless microfluidic system driven by hydrostatic pressure induces and maintains mouse spermatogenesis in vitro. *Sci. Rep.* vol. 7, no. 1, pp. 15459-017-15799-3.
- Kubota, H., Avarbock, M.R. & Brinster, R.L. 2004, Growth factors essential for self-renewal and expansion of mouse spermatogonial stem cells. *Proc. Natl. Acad. Sci. U. S. A.* vol. 101, no. 47, pp. 16489-16494.
- Kulibin, A.Y. & Malolina, E.A. 2020, Formation of the rete testis during mouse embryonic development. *Dev. Dyn.* vol. 249, no. 12, pp. 1486-1499.
- Kulibin, A.Y. & Malolina, E.A. 2016, Only a small population of adult Sertoli cells actively proliferates in culture. *Reproduction*, vol. 152, no. 4, pp. 271-281.
- Kumar, S., Chatzi, C., Brade, T., Cunningham, T.J., Zhao, X. & Duester, G. 2011, Sex-specific timing of meiotic initiation is regulated by Cyp26b1 independent of retinoic acid signalling. *Nat. Commun.* vol. 2, pp. 151.
- Li, N., Tang, E.I. & Cheng, C.Y. 2016, Regulation of blood-testis barrier by actin binding proteins and protein kinases. *Reproduction* vol. 151, no. 3, pp. R29-41.
- Lian, G., Miller, K.A. & Enders, G.C. 1992, Localization and synthesis of entactin in seminiferous tubules of the mouse. *Biol. Reprod.* vol. 47, no. 3, pp. 316-325.
- Lindner, S.G. 1982, On the morphology of the transitional zone of the seminiferous tubule and the rete testis in man. *Andrologia*, vol. 14, no. 4, pp. 352-362.
- Lopez-Fernandez, L.A. & del Mazo, J. 1997, The cytosolic aldehyde dehydrogenase gene (Aldh1) is developmentally expressed in Leydig cells. *FEBS letters*, vol. 407, no. 2, pp. 225-229.
- Lord, T., Oatley, M.J. & Oatley, J.M. 2018, Testicular Architecture Is Critical for Mediation of Retinoic Acid Responsiveness by Undifferentiated Spermatogonial Subtypes in the Mouse. *Stem Cell Rep.* vol. 10, no. 2, pp. 538-552.

- Lovelace, D.L., Gao, Z., Mutoji, K., Song, Y.C., Ruan, J. & Hermann, B.P. 2016, The regulatory repertoire of PLZF and SALL4 in undifferentiated spermatogonia. *Development* vol. 143, no. 11, pp. 1893-1906.
- MacGregor, G.R., Russell, L.D., Van Beek, M.E., Hanten, G.R., Kovac, M.J., Kozak, C.A., Meistrich, M.L. & Overbeek, P.A. 1990, Symplastic spermatids (sys): a recessive insertional mutation in mice causing a defect in spermatogenesis. *Proc. Natl. Acad. Sci. U. S. A.* vol. 87, no. 13, pp. 5016-5020.
- Maekawa, M., Kamimura, K. & Nagano, T. 1996, Peritubular myoid cells in the testis: their structure and function. *Arch. Histol. Cytol.* vol. 59, no. 1, pp. 1-13.
- Major, A.T., Estermann, M.A. & Smith, C.A. 2021, Anatomy, Endocrine Regulation, and Embryonic Development of the Rete Testis. *Endocrinology*, vol. 162, no. 6, pp. 10.1210/endocr/bqab046.
- Malolina, E.A. & Kulibin, A.Y. 2019, The rete testis harbors Sertoli-like cells capable of expressing DMRT1. *Reproduction* vol. 158, no. 5, pp. 399-413.
- Masaki, K., Sakai, M., Kuroki, S., Jo, J.I., Hoshina, K., Fujimori, Y., Oka, K., Amano, T., Yamanaka, T., Tachibana, M., Tabata, Y., Shiozawa, T., Ishizuka, O., Hochi, S. & Takashima, S. 2018, FGF2 Has Distinct Molecular Functions from GDNF in the Mouse Germline Niche. *Stem Cell Rep.* vol. 10, no. 6, pp. 1782-1792.
- Matoba, S., Kanai, Y., Kidokoro, T., Kanai-Azuma, M., Kawakami, H., Hayashi, Y. & Kurohmaru, M. 2005, A novel Sry-downstream cellular event which preserves the readily available energy source of glycogen in mouse sex differentiation. *J. Cell Sci.* vol. 118, no. Pt 7, pp. 1449-1459.
- Matsui, T., Kanai-Azuma, M., Hara, K., Matoba, S., Hiramatsu, R., Kawakami, H., Kurohmaru, M., Koopman, P. & Kanai, Y. 2006, Redundant roles of Sox17 and Sox18 in postnatal angiogenesis in mice. *J. Cell Sci.* vol. 119, no. Pt 17, pp. 3513-3526.
- Matsuo, I. & Kimura-Yoshida, C. 2013, Extracellular modulation of Fibroblast Growth Factor signaling through heparan sulfate proteoglycans in mammalian development. *Curr. Opin. Genet. Dev.* vol. 23, no. 4, pp. 399-407.

- Meng, X., Lindahl, M., Hyvonen, M.E., Parvinen, M., de Rooij, D.G., Hess, M.W., Raatikainen-Ahokas, A., Sainio, K., Rauvala, H., Lakso, M., Pichel, J.G., Westphal, H., Saarma, M. & Sariola, H. 2000, Regulation of cell fate decision of undifferentiated spermatogonia by GDNF. *Science* vol. 287, no. 5457, pp. 1489-1493.
- Molotkov, A., Fan, X., Deltour, L., Foglio, M.H., Martras, S., Farres, J., Pares, X. & Duester, G. 2002, Stimulation of retinoic acid production and growth by ubiquitously expressed alcohol dehydrogenase Adh3. *Proc. Natl. Acad. Sci. U. S. A.* vol. 99, no. 8, pp. 5337-5342.
- Morimoto, H., Iwata, K., Ogonuki, N., Inoue, K., Atsuo, O., Kanatsu-Shinohara, M., Morimoto, T., Yabe-Nishimura, C. & Shinohara, T. 2013, "ROS are required for mouse spermatogonial stem cell self-renewal", *Cell Stem Cell*, vol. 12, no. 6, pp. 774-786.
- Morimoto, H., Kanatsu-Shinohara, M., Takashima, S., Chuma, S., Nakatsuji, N., Takehashi, M. & Shinohara, T. 2009, "Phenotypic plasticity of mouse spermatogonial stem cells", *PloS one*, vol. 4, no. 11, pp. e7909.
- Morrison, S.J. & Spradling, A.C. 2008, "Stem cells and niches: mechanisms that promote stem cell maintenance throughout life", *Cell*, vol. 132, no. 4, pp. 598-611.
- Mruk, D.D. & Cheng, C.Y. 2015, The Mammalian Blood-Testis Barrier: Its Biology and Regulation. *Endocr. Rev.* vol. 36, no. 5, pp. 564-591.
- Nagai, R., Shinomura, M., Kishi, K., Aiyama, Y., Harikae, K., Sato, T., Kanai-Azuma, M., Kurohmaru, M., Tsunekawa, N. & Kanai, Y. 2012, "Dynamics of GFRalpha1-positive spermatogonia at the early stages of colonization in the recipient testes of W/Wnu male mice", *Dev. Dyn.* vol. 241, no. 8, pp. 1374-1384.
- Nagano, M., Ryu, B.Y., Brinster, C.J., Avarbock, M.R. & Brinster, R.L. 2003, Maintenance of mouse male germ line stem cells in vitro. *Biol. Reprod.* vol. 68, no. 6, pp. 2207-2214.
- Nagasawa, K., Imura-Kishi, K., Uchida, A., Hiramatsu, R., Kurohmaru, M. & Kanai, Y. 2018, "Regionally distinct patterns of STAT3 phosphorylation in the seminiferous epithelia of mouse testes", *Mol. Reprod. Dev.* vol. 85, no. 3, pp. 262-270.

- Nakagawa, T., Jorg, D.J., Watanabe, H., Mizuno, S., Han, S., Ikeda, T., Omatsu, Y., Nishimura, K., Fujita, M., Takahashi, S., Kondoh, G., Simons, B.D., Yoshida, S. & Nagasawa, T. 2021, A multistate stem cell dynamics maintains homeostasis in mouse spermatogenesis. *Cell Rep.*, vol. 37, no. 3, pp. 109875.
- Nakagawa, T., Nabeshima, Y. & Yoshida, S. 2007, Functional identification of the actual and potential stem cell compartments in mouse spermatogenesis. *Dev. Cell*, vol. 12, no. 2, pp. 195-206.
- Nakagawa, T., Sharma, M., Nabeshima, Y., Braun, R.E. & Yoshida, S. 2010, Functional hierarchy and reversibility within the murine spermatogenic stem cell compartment. *Science*, vol. 328, no. 5974, pp. 62-67.
- Nakamura, Y., Jorg, D.J., Kon, Y., Simons, B.D. & Yoshida, S. 2021, Transient suppression of transplanted spermatogonial stem cell differentiation restores fertility in mice. *Cell Stem Cell*, vol. 28, no. 8, pp. 1443-1456.e7.
- Oakberg, E.F. 1971, Spermatogonial stem-cell renewal in the mouse. *Anat. Rec.* vol. 169, no. 3, pp. 515-531.
- Oatley, J.M. & Griswold, M.D. 2020, MEIOSIN: A New Watchman of Meiotic Initiation in Mammalian Germ Cells. *Dev. Cell*, vol. 52, no. 4, pp. 397-398.
- Oatley, J.M., Oatley, M.J., Avarbock, M.R., Tobias, J.W. & Brinster, R.L. 2009, Colony stimulating factor 1 is an extrinsic stimulator of mouse spermatogonial stem cell self-renewal. *Development*, vol. 136, no. 7, pp. 1191-1199.
- O'Donnell, L. 2015, Mechanisms of spermiogenesis and spermiation and how they are disturbed. *Spermatogenesis*, vol. 4, no. 2, pp. e979623.
- Ogawa, T., Dobrinski, I., Avarbock, M.R. & Brinster, R.L. 2000, Transplantation of male germ line stem cells restores fertility in infertile mice. *Nat. Med.* vol. 6, no. 1, pp. 29-34.
- Ohbo, K., Yoshida, S., Ohmura, M., Ohneda, O., Ogawa, T., Tsuchiya, H., Kuwana, T., Kehler, J., Abe, K., Scholer, H.R. & Suda, T. 2003, Identification and characterization of stem cells in prepubertal spermatogenesis in mice. *Dev. Biol.* vol. 258, no. 1, pp. 209-225.

- Omotehara, T., Wu, X., Kuramasu, M. & Itoh, M. 2020, Connection between seminiferous tubules and epididymal duct is originally induced before sex differentiation in a sex-independent manner. *Dev. Dyn.* vol. 249, no. 6, pp. 754-764.
- Ornitz, D.M. & Itoh, N. 2015, The Fibroblast Growth Factor signaling pathway. *Dev. Biol.* vol. 4, no. 3, pp. 215-266.
- Osman, D.I. 1978, On the ultrastructure of modified Sertoli cells in the terminal segment of seminiferous tubules in the boar. *J. Anatomy*, vol. 127, no. Pt 3, pp. 603-613.
- Osman, D.I. & Ploen, L. 1978, The mammalian tubuli recti: ultrastructural study. *Anat. Rec.* vol. 192, no. 1, pp. 1-17.
- Ozpolat, B., Mehta, K. & Lopez-Berestein, G. 2005, Regulation of a highly specific retinoic acid-4-hydroxylase (CYP26A1) enzyme and all-trans-retinoic acid metabolism in human intestinal, liver, endothelial, and acute promyelocytic leukemia cells. *Leuk. Lymphoma*, vol. 46, no. 10, pp. 1497-1506.
- Parekh, P.A., Garcia, T.X., Waheeb, R., Jain, V., Gandhi, P., Meistrich, M.L., Shetty, G. & Hofmann, M.C. 2019, Undifferentiated spermatogonia regulate Cyp26b1 expression through NOTCH signaling and drive germ cell differentiation. *FASEB* vol. 33, no. 7, pp. 8423-8435.
- Pellegrini, M., Grimaldi, P., Rossi, P., Geremia, R. & Dolci, S. 2003, Developmental expression of BMP4/ALK3/SMAD5 signaling pathway in the mouse testis: a potential role of BMP4 in spermatogonia differentiation. *J. Cell Sci.* vol. 116, no. Pt 16, pp. 3363-3372.
- Persico, V., Callaini, G. & Riparbelli, M.G. 2019, The male stem cell niche of *Drosophila melanogaster*: Interactions between the germline stem cells and the hub. *Exp. Cell Res.* vol. 383, no. 1, pp. 111489.
- Pichel, J.G., Shen, L., Sheng, H.Z., Granholm, A.C., Drago, J., Grinberg, A., Lee, E.J., Huang, S.P., Saarma, M., Hoffer, B.J., Sariola, H. & Westphal, H. 1996, Defects in enteric innervation and kidney development in mice lacking GDNF. *Nature*, vol. 382, no. 6586, pp. 73-76.
- Rao, T.P. & Kuhl, M. 2010, An updated overview on Wnt signaling pathways: a prelude for more. *Circ. Res.* vol. 106, no. 12, pp. 1798-1806.

- Rato, L., Socorro, S., Cavaco, J.E. & Oliveira, P.F. 2010, Tubular fluid secretion in the seminiferous epithelium: ion transporters and aquaporins in Sertoli cells. *J. Membr. Biol.* vol. 236, no. 2, pp. 215-224.
- ROOSEN-RUNGE, E.C. 1961, The rete testis in the albino rat: its structure, development and morphological significance. *Acta Anatomica*, vol. 45, pp. 1-30.
- Ross, A.C., Cifelli, C.J., Zolfaghari, R. & Li, N.Q. 2011, Multiple cytochrome P-450 genes are concomitantly regulated by vitamin A under steady-state conditions and by retinoic acid during hepatic first-pass metabolism. *Physiol. Genomics*. vol. 43, no. 1, pp. 57-67.
- Russell, L.D., Ren, H.P., Sinha Hikim, I., Schulze, W. & Sinha Hikim, A.P. 1990, A comparative study in twelve mammalian species of volume densities, volumes, and numerical densities of selected testis components, emphasizing those related to the Sertoli cell. *J. Anat.* vol. 188, no. 1, pp. 21-30.
- Safian, D., Ryane, N., Bogerd, J. & Schulz, R.W. 2018, Fsh stimulates Leydig cell Wnt5a production, enriching zebrafish type A spermatogonia. *J. Endocrinol.* vol. 239, no. 3, pp. 351-363.
- Sakamoto, Y., Hara, K., Kanai-Azuma, M., Matsui, T., Miura, Y., Tsunekawa, N., Kurohmaru, M., Saijoh, Y., Koopman, P. & Kanai, Y. 2007, Redundant roles of Sox17 and Sox18 in early cardiovascular development of mouse embryos. *Biochem. Biophys. Res. Commun.* vol. 360, no. 3, pp. 539-544.
- Sato, T., Aiyama, Y., Ishii-Inagaki, M., Hara, K., Tsunekawa, N., Harikae, K., Uemura-Kamata, M., Shinomura, M., Zhu, X.B., Maeda, S., Kuwahara-Otani, S., Kudo, A., Kawakami, H., Kanai-Azuma, M., Fujiwara, M., Miyamae, Y., Yoshida, S., Seki, M., Kurohmaru, M. & Kanai, Y. 2011, Cyclical and patch-like GDNF distribution along the basal surface of Sertoli cells in mouse and hamster testes. *PloS One*, vol. 6, no. 12, pp. e28367.
- Sato, T., Katagiri, K., Gohbara, A., Inoue, K., Ogonuki, N., Ogura, A., Kubota, Y. & Ogawa, T. 2011, In vitro production of functional sperm in cultured neonatal mouse testes. *Nature*, vol. 471, no. 7339, pp. 504-507.
- Sato, T., Katagiri, K., Kojima, K., Komeya, M., Yao, M. & Ogawa, T. 2015, In Vitro Spermatogenesis in Explanted Adult Mouse Testis Tissues. *PloS One*, vol. 10, no. 6, pp. e0130171.

- Savitt, J., Singh, D., Zhang, C., Chen, L.C., Folmer, J., Shokat, K.M. & Wright, W.W. 2012, The in vivo response of stem and other undifferentiated spermatogonia to the reversible inhibition of glial cell line-derived neurotrophic factor signaling in the adult. *Stem Cells*, vol. 30, no. 4, pp. 732-740.
- Schmahl, J., Kim, Y., Colvin, J.S., Ornitz, D.M. & Capel, B. 2004, Fgf9 induces proliferation and nuclear localization of FGFR2 in Sertoli precursors during male sex determination. *Development*, vol. 131, no. 15, pp. 3627-3636.
- Setchell, B.P. 2008, Blood-testis barrier, junctional and transport proteins and spermatogenesis. *Adv. Exp. Med.* vol. 636, pp. 212-233.
- Setchell, B.P., Ploen, L. & Ritzen, E.M. 1998, Reduction in fluid secretion by rat testis by drugs that block potassium channels. *J. Reprod. Fertil.* vol. 112, no. 1, pp. 87-94.
- Sharma, M. & Braun, R.E. 2018, Cyclical expression of GDNF is required for spermatogonial stem cell homeostasis. *Development*, vol. 145, no. 5, pp. 10.1242/dev.151555.
- Shimoda, M., Kanai-Azuma, M., Hara, K., Miyazaki, S., Kanai, Y., Monden, M. & Miyazaki, J. 2007, Sox17 plays a substantial role in late-stage differentiation of the extraembryonic endoderm in vitro. *J. Cell Sci.* vol. 120, no. Pt 21, pp. 3859-3869.
- Shinomura, M., Kishi, K., Tomita, A., Kawasumi, M., Kanezashi, H., Kuroda, Y., Tsunekawa, N., Ozawa, A., Aiyama, Y., Yoneda, A., Suzuki, H., Saito, M., Picard, J.Y., Kohno, K., Kurohmaru, M., Kanai-Azuma, M. & Kanai, Y. 2014, A novel Amh-Treck transgenic mouse line allows toxin-dependent loss of supporting cells in gonads. *Reproduction*, vol. 148, no. 6, pp. H1-9.
- Spence, J.R., Lange, A.W., Lin, S.C., Kaestner, K.H., Lowy, A.M., Kim, I., Whitsett, J.A. & Wells, J.M. 2009, Sox17 regulates organ lineage segregation of ventral foregut progenitor cells. *Dev. Cell*, vol. 17, no. 1, pp. 62-74.
- Stuart, T., Butler, A., Hoffman, P., Hafemeister, C., Papalexi, E., Mauck, W.M., 3rd, Hao, Y., Stoeckius, M., Smibert, P. & Satija, R. 2019, Comprehensive Integration of Single-Cell Data. *Cell*, vol. 177, no. 7, pp. 1888-1902.e21.

- Subash, S.K. & Kumar, P.G. 2021, Spermatogonial stem cells: A story of self-renewal and differentiation. *Front. Biosci.* vol. 26, pp. 163-205.
- Suzuki, H., Sada, A., Yoshida, S. & Saga, Y. 2009, The heterogeneity of spermatogonia is revealed by their topology and expression of marker proteins including the germ cell-specific proteins Nanos2 and Nanos3. *Dev. Biol.*, vol. 336, no. 2, pp. 222-231.
- Svingen, T., Francois, M., Wilhelm, D. & Koopman, P. 2012, Three-dimensional imaging of Prox1-EGFP transgenic mouse gonads reveals divergent modes of lymphangiogenesis in the testis and ovary. *PloS One*, vol. 7, no. 12, pp. e52620.
- Tadokoro, Y., Yomogida, K., Ohta, H., Tohda, A. & Nishimune, Y. 2002, Homeostatic regulation of germinal stem cell proliferation by the GDNF/FSH pathway. *Mech. Dev.* vol. 113, no. 1, pp. 29-39.
- Tainosho, S., Naito, M., Hirai, S., Terayama, H., Qu, N. & Itoh, M. 2011, Multilayered structure of the basal lamina of the tubuli recti in normal mice. *Med. Mol. Morphol.* vol. 44, no. 1, pp. 34-38.
- Takahashi, K., Naito, M., Terayama, H., Qu, N., Cheng, L., Tainosho, S. & Itoh, M. 2007, Immunomorphological aspects of the tubuli recti and the surrounding interstitium in normal mice. *Int. J. Androl.* vol. 30, no. 1, pp. 21-27.
- Takase, H.M. & Nusse, R. 2016, Paracrine Wnt/beta-catenin signaling mediates proliferation of undifferentiated spermatogonia in the adult mouse testis. *Proc. Natl. Acad. Sci. U. S. A.* vol. 113, no. 11, pp. E1489-97.
- Takase, Y., Tadokoro, R. & Takahashi, Y. 2013, "Low cost labeling with highlighter ink efficiently visualizes developing blood vessels in avian and mouse embryos", *Dev. Growth Differ.* vol. 55, no. 9, pp. 792-801.
- Takashima, S., Kanatsu-Shinohara, M., Tanaka, T., Morimoto, H., Inoue, K., Ogonuki, N., Jijiwa, M., Takahashi, M., Ogura, A. & Shinohara, T. 2015, Functional differences between GDNF-dependent and FGF2-dependent mouse spermatogonial stem cell self-renewal. *Stem Cell Rep.* vol. 4, no. 3, pp. 489-502.

- Tassinari, V., Campolo, F., Cesarini, V., Todaro, F., Dolci, S. & Rossi, P. 2015, Fgf9 inhibition of meiotic differentiation in spermatogonia is mediated by Erk-dependent activation of Nodal-Smad2/3 signaling and is antagonized by Kit Ligand. *Cell Death Dis.* vol. 6, pp. e1688.
- Teletin, M., Vernet, N., Yu, J., Klopfenstein, M., Jones, J.W., Feret, B., Kane, M.A., Ghyselinck, N.B. & Mark, M. 2019, Two functionally redundant sources of retinoic acid secure spermatogonia differentiation in the seminiferous epithelium. *Development*, vol. 146, no. 1, pp. 10.1242/dev.170225.
- THOMPSON, J.N., HOWELL, J.M. & PITT, G.A. 1964, Vitamin a and Reproduction in Rats. *Proc. Royal Soc. B.* vol. 159, pp. 510-535.
- Tian, R., Yao, C., Yang, C., Zhu, Z., Li, C., Zhi, E., Wang, J., Li, P., Chen, H., Yuan, Q., He, Z. & Li, Z. 2019, Fibroblast growth factor-5 promotes spermatogonial stem cell proliferation via ERK and AKT activation. *Stem Cell Res. Ther.* vol. 10, no. 1, pp. 40-019-1139-7.
- Timpl, R. 1993, Proteoglycans of basement membranes. *Experientia*, vol. 49, no. 5, pp. 417-428.
- Tripiciano, A., Filippini, A., Ballarini, F. & Palombi, F. 1998, Contractile response of peritubular myoid cells to prostaglandin F2alpha. *Mol. Cell. Endocrinol.* vol. 138, no. 1-2, pp. 143-150.
- Tuck, R.R., Setchell, B.P., Waites, G.M. & Young, J.A. 1970, The composition of fluid collected by micropuncture and catheterization from the seminiferous tubules and rete testis of rats. *Pflugers Arch.* vol. 318, no. 3, pp. 225-243.
- Uchida, A. & Kanai, Y. 2016, Data on in vivo phenotypes of GFRalpha1-positive spermatogonia stimulated by interstitial GDNF signals in mouse testes. *Data in brief*, vol. 8, pp. 1255-1258.
- Uchida, A., Kishi, K., Aiyama, Y., Miura, K., Takase, H.M., Suzuki, H., Kanai-Azuma, M., Iwamori, T., Kurohmaru, M., Tsunekawa, N. & Kanai, Y. 2016, In vivo dynamics of GFRalpha1-positive spermatogonia stimulated by GDNF signals using a bead transplantation assay. *Biochem. Biophys. Res. Commun.* vol. 476, no. 4, pp. 546-552.

- Uchida, A., Sakib, S., Labit, E., Abbasi, S., Scott, R.W., Underhill, T.M., Biernaskie, J. & Dobrinski, I. 2020, Development and function of smooth muscle cells is modulated by Hic1 in mouse testis. *Development*, vol. 147, no. 13, pp. 10.1242/dev.185884.
- Velte, E.K., Niedenberger, B.A., Serra, N.D., Singh, A., Roa-DeLaCruz, L., Hermann, B.P. & Geyer, C.B. 2019, Differential RA responsiveness directs formation of functionally distinct spermatogonial populations at the initiation of spermatogenesis in the mouse. *Development*, vol. 146, no. 12, pp. 10.1242/dev.173088.
- Vernet, N., Condrea, D., Mayere, C., Feret, B., Klopfenstein, M., Magnant, W., Alunni, V., Teletin, M., Souali-Crespo, S., Nef, S., Mark, M. & Ghyselinck, N.B. 2020, Meiosis occurs normally in the fetal ovary of mice lacking all retinoic acid receptors. *Scii Adv.*, vol. 6, no. 21, pp. 10.1126/sciadv.aaz1139.
- Wang, X., Penzes, P. & Napoli, J.L. 1996, Cloning of a cDNA encoding an aldehyde dehydrogenase and its expression in Escherichia coli. Recognition of retinal as substrate. *J. Biol. Chem.* vol. 271, no. 27, pp. 16288-16293.
- Wen, Q., Tang, E.I., Li, N., Mruk, D.D., Lee, W.M., Silvestrini, B. & Cheng, C.Y. 2018, Regulation of Blood-Testis Barrier (BTB) Dynamics, Role of Actin-, and Microtubule-Based Cytoskeletons. *Methods Mol. Biol.* vol. 1748, pp. 229-243.
- Wolbach, S.B. & Howe, P.R. 1925, Tissue Changes Following Deprivation of Fat-Soluble a Vitamin. *J. Exp. Med.*, vol. 42, no. 6, pp. 753-777.
- Wrobel, K.H., Sinowatz, F. & Mademann, R. 1982, The fine structure of the terminal segment of the bovine seminiferous tubule. *Cell Tissue Res.* vol. 225, no. 1, pp. 29-44.
- Wu, F.J., Lin, T.Y., Sung, L.Y., Chang, W.F., Wu, P.C. & Luo, C.W. 2017, BMP8A sustains spermatogenesis by activating both SMAD1/5/8 and SMAD2/3 in spermatogonia. *Sci. Signal.* vol. 10, no. 477, pp. 10.1126/scisignal.aal1910.
- Xie, Y., Su, N., Yang, J., Tan, Q., Huang, S., Jin, M., Ni, Z., Zhang, B., Zhang, D., Luo, F., Chen, H., Sun, X., Feng, J.Q., Qi, H. & Chen, L. 2020, FGF/FGFR signaling in health and disease. *Signal Transduct. Target. Ther.* vol. 5, no. 1, pp. 181.

- Yamada, R., Oguri, A., Fujiki, K., Shirahige, K., Hirate, Y., Kanai-Azuma, M., Takezoe, H., Akimoto, Y., Takahashi, N. & Kanai, Y. 2021, MAB21L1 modulates gene expression and DNA metabolic processes in the lens placode. *Dis. Models Mech.*
- Yan, H.H., Mruk, D.D., Lee, W.M. & Cheng, C.Y. 2007, Ectoplasmic specialization: a friend or a foe of spermatogenesis?", *BioEssays : news and reviews in molecular, cellular and developmental biology*, vol. 29, no. 1, pp. 36-48.
- Yang, F., Whelan, E.C., Guan, X., Deng, B., Wang, S., Sun, J., Avarbock, M.R., Wu, X. & Brinster, R.L. 2021, FGF9 promotes mouse spermatogonial stem cell proliferation mediated by p38 MAPK signalling. *Cell Prolif.* vol. 54, no. 1, pp. e12933.
- Yeh, J.R., Zhang, X. & Nagano, M.C. 2012, Indirect effects of Wnt3a/beta-catenin signalling support mouse spermatogonial stem cells in vitro. *PLoS One*, vol. 7, no. 6, pp. e40002.
- Yeh, J.R., Zhang, X. & Nagano, M.C. 2011, Wnt5a is a cell-extrinsic factor that supports self-renewal of mouse spermatogonial stem cells. *J. Cell Sci.* vol. 124, no. Pt 14, pp. 2357-2366.
- Yomogida, K., Yagura, Y., Tadokoro, Y. & Nishimune, Y. 2003, Dramatic expansion of germinal stem cells by ectopically expressed human glial cell line-derived neurotrophic factor in mouse Sertoli cells. *Biol. Reprod.* vol. 69, no. 4, pp. 1303-1307.
- Yoshida, S. 2018, Open niche regulation of mouse spermatogenic stem cells. *Dev. Growth Differ.* vol. 60, no. 9, pp. 542-552.
- Yoshida, S., Sukeno, M. & Nabeshima, Y. 2007, A vasculature-associated niche for undifferentiated spermatogonia in the mouse testis. *Science*, vol. 317, no. 5845, pp. 1722-1726.
- Zhai, Y., Sperkova, Z. & Napoli, J.L. 2001, Cellular expression of retinal dehydrogenase types 1 and 2: effects of vitamin A status on testis mRNA. *J. Cell. Physiol.* vol. 186, no. 2, pp. 220-232.
- Zimmermann, C., Stevant, I., Borel, C., Conne, B., Pitetti, J.L., Calvel, P., Kaessmann, H., Jegou, B., Chalmel, F. & Nef, S. 2015, Research resource: the dynamic transcriptional profile of sertoli cells during the progression of spermatogenesis. *J. Mol. Endocrinol.* vol. 29, no. 4, pp. 627-642.